The Analysis of $^{81}Kr^{m}$ Equilibrium Inhalation Data.

by

David Hamilton B.Sc., M.Sc.

A thesis submitted for the degree of Doctor of Philosophy of the Department of Engineering, at the University of Warwick.

June 1983

Abstract. Two methods of analysing the data available from routine $^{81}Kr^{m}$ equilibrium inhalation investigations were developed. The data were acquired from a gamma camera in the form of a sequential series of images from which multiple breath activity-time curves were generated for a number of regions in the lung. The first method developed was based on a description of the behaviour of the radioactive gas in the lung using a mathematical model. Values of specific mean expiratory gas flow, that is mean expiratory gas flow per unit lung volume, were calculated from the application of the model to the expiratory phase only of a single breath activity-time curve which was created from the multiple breath activity-time curve using post-acquisition gating. This method overcame the problem of the non-uniform inspiratory concentration of the tracer gas experienced in previously reported techniques of analysing inhalation data obtained using poorly soluble radioactive gases. The second method developed calculated phase differences between lung regions by cross-correlating the multiple breath activity-time curve obtained from one lung region with that obtained from another lung region. Such phase differences have not previously been measured using the inhalation of poorly soluble radioactive tracer gases.

Contents.

Tables.

Figures.

Photographs.

Acknowledgements.

My sincere thanks are extended to Dr. K.R. Godfrey, Professor J.L. Douce, Mr. J.A. McIntosh, Dr. D.A. Causer, Dr. G. Jones, Dr. D. Taylor, the technical and nursing staff of the Radioisotope Department at Walsgrave Hospital, the Coventry Area Health Authority and the Coventry and Warwickshire Hospital Saturday Fund for their help and encouragement in this project.

CHAPTER 1 **Introduction.**

To investigate regional function of the airways of the lung, techniques are available which complement anatomical tests, such as radiography. Those which are non-invasive are based on the measurement of gas flow, inert tracer gas dilution or radioactive tracer gas distribution.

Methods which utilise radioactive tracer gases provide an estimate of flow to a region by measuring the fractional exchange of gas. They are influenced, however, by the inspiratory concentration of the radioactive tracer gas.

Presently there are no reports in the literature of the measurement of phase differences in the flow of gas between different regions of the lung using inhalation techniques.

The work described in this thesis had two objectives, to provide an estimate of gas flow to a region which was not influenced by the inspiratory concentration of the radioactive tracer gas and to provide an estimate of phase differences in the flow of gas to different regions of the lung.

1.1 **Anatomy.**

There are three mass transport systems involved in the function of the lung, two contain blood and one contains gas. Of the blood transport systems one, the bronchial circulation, supplies the tissues of the lung with their metabolic needs

and the other, the pulmonary circulation, perfuses the lung tissue or the parenchyma, which forms the periphery of the gas transport system.

The gas transport system comprises a non-respiratory section where gas exchange with the pulmonary circulation does not occur and a respiratory section where it does. The non-respiratory section, or the dead space, includes the nose, pharynx, larynx, trachea and the main bronchi. The respiratory section includes the bronchioles and alveoli. Both the non-respiratory and the respiratory sections are shown in figures (1.1), (1.2) and (1.3). The airways decrease in diameter at each of 23 bifurcations from the trachea to the alveoli, those produced at each bifurcation belong to one generation, numbered from 1 to 23. (Secker-Walker R.H., 1978 and Alderson P.O., and Line B.R., 1980).

Figure 1.1. The Anatomy of the Lungs, shown in the antero-posterior orientation.

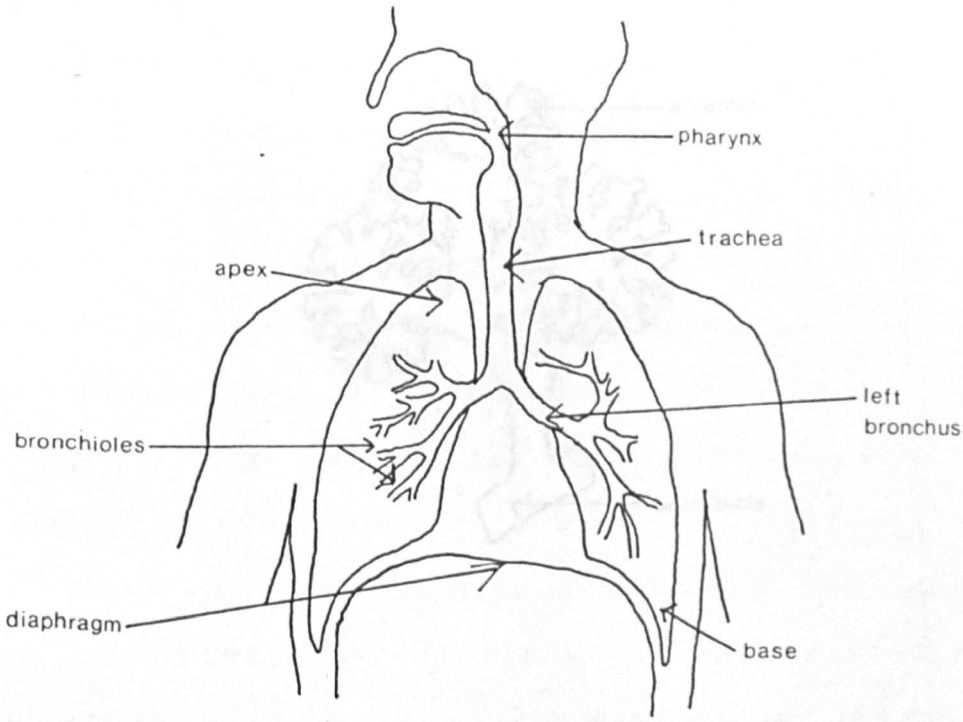

Figure 1.2. The Anatomy of the Trachea, Bronchi and Bronchioles, shown in the antero-posterior orientation.

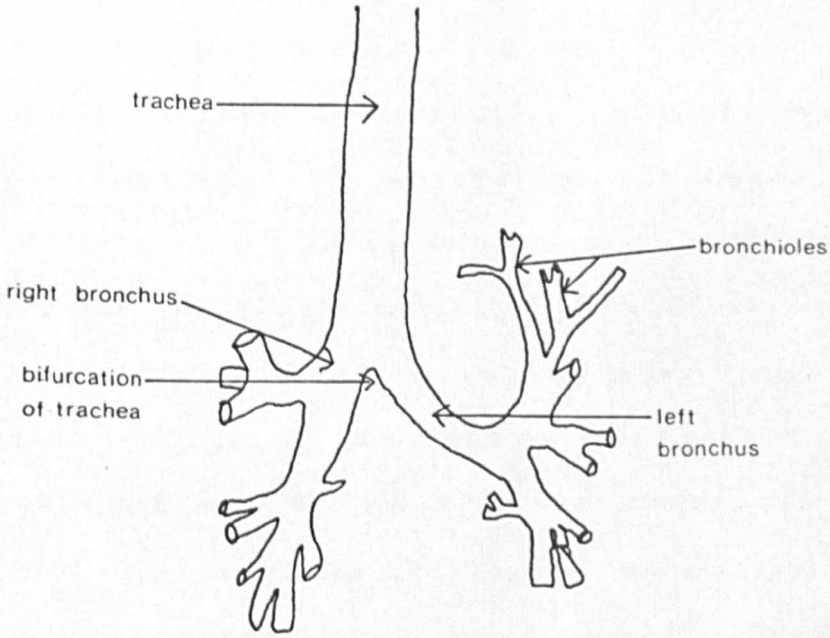

Figure 1.3. The Anatomy of the Bronchioles and Alveoli.

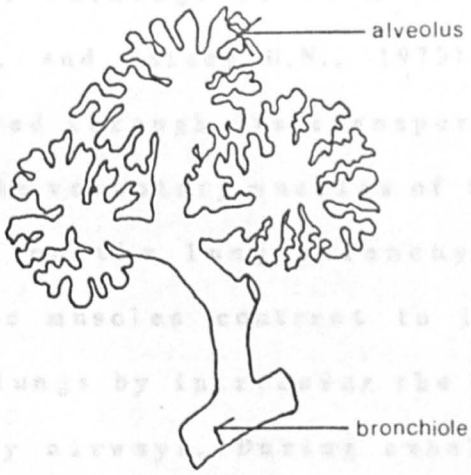

1.2 Physiology.

The intimate contact of the pulmonary circulation and the gas transport system facilitates gas exchange between blood and air. (Higenbottam T., and Maisey M.N., 1979).

Gas is moved through its transport system by the action of the voluntary muscles of the rib cage and diaphragm on the lung parenchyma. During inhalation these muscles contract to increase the volume of the lungs by increasing the diameter of the respiratory airways. During exhalation they relax to allow the lungs to shrink under the action of the natural elasticity of the parenchyma by reducing the diameter of the respiratory airways. Expiration during a tidal breath is, therefore, a passive process, the energy coming from the elastic recoil forces within the lung. (Secker-Walker R.H., 1978 and Alderson P.O., and Line B.R., 1980).

Gas is transported from the mouth to the respiratory airways by convection and diffusion. In the proximal regions, convection dominates, the flow is driven by a pressure gradient and the whole body of gas may be ascribed a flow velocity. In the distal regions diffusion is the more important mechanism and each gas species moves at a rate largely determined by its own concentration gradient. The diffusion distance is of the order of only a millimetre, however, so that bulk flow is

the rate limiting process. (Winlove C.P., et. al., 1976).

During an expiration gas in the dead space is expelled from the body. It is followed by gas from the respiratory airways, some of which remains in the dead space and mixes with gas from other regions. During an inspiration, gas in the dead space is re-inspired to the different regions of the lung and is followed by clean air from the atmosphere (Fowler W.S., 1952). Upto the first one third of a tidal volume, that is the volume change during a normal relaxed breath, comprises dead space gas. (Grant B.J.B., et. al., 1974, Ciofetta G., et. al., 1980).

Compliance is the change in lung volume for a given pressure gradient between the outside of the lung and the alveoli. (Higenbottam T., and Maisey M.N., 1979, Secker-Walker R.H., 1978). Alveoli with low compliance have small volumes and exchange a large fraction of their volume with each respiration. Alveoli with increased compliance are larger than normal for a given pressure and exchange a smaller fraction of their volume during respiration. (Alderson P.O., and Line B.R., 1980).

Airway resistance is the ratio of the driving pressure to the airflow rate. (Secker-Walker R.H., 1978). Airflow rates, pressure differences and

airway resistance are very low in the alveoli because of the very large cross-sectional area caused by the divisions. (Fowler W.S., 1952). Only 10%-20% of resistance is accounted for by the small airways. (Secker-Walker R.H., 1978, Alderson P.O., and Line B.R., 1980).

Functional Residual Capacity, or FRC, is the volume of air in the lungs at the end of each expiration during normal tidal breathing. (Secker-Walker R.H., 1978). Its value is determined by the balance between the elastic recoil forces of the lung and the elastic recoil forces of the chest wall. (Secker-Walker R.H., 1978 and Alderson P.O., and Line B.R., 1980). Residual Volume, or RV, is the volume of air in the lungs at the end of a maximal expiration. It is the minimum volume of air that can be contained by the lungs. Total Lung Capacity, or TLC, is the volume of air in the lungs at the end of a maximal inspiration. It is the maximum volume of air that can be contained by the lungs.

At low lung volumes, the apical alveoli are distorted by the weight of the lung below them. At higher volumes the lung stiffens and the apical distortion due to the weight of the lung lessens. (Fowler W.S., 1952, Grant B.J.B., et. al., 1974, Alpert N.M., et. al., 1975, Arnot R.N., et. al., 1981, Secker-Walker R.H., 1978 and Alderson P.O.,

and Line B.R., 1980). From RV to FRC, the upper zones expand more rapidly than the lower zones, at FRC, both zones expand at the same rate and from FRC to TLC, the lower zones expand more rapidly. (West J.B., 1966). During a slow inspiration the distribution will depend more on compliance and during a rapid inspiration it will depend more on airway resistance. (Secker-Walker R.H., 1978 and Alderson P.O., and Line B.R., 1980). At low flow rates (0.1 litre/second) there is greater ventilation to the base and at high flow rates (1.0 litre/second) there is greater ventilation to the apex. (Grant B.J.B., et. al., 1974).

In addition to those diseases, such as pneumonia, in which the distal air spaces are filled with fluid, other primarily ventilatory lung diseases result in disturbances of regional ventilation. (Higenbottam T., and Maisey M.N., 1979). Inflammatory, oedematous or fibrotic disease processes are all associated with decreased compliance. Such regions will shrink in volume and also receive less air than surrounding normal lung during each breath. Emphysema is associated with an increase in compliance. Airway resistance is increased in any condition associated with narrowing of the airways, such as bronchospasm, oedema of the bronchial walls, excess mucus,

tumours, strictures or foreign bodies. Emphysema is also associated with increased airway resistance because it weakens support of the airways and allows them to become distorted. A further mechanism for reduced airflow rates in emphysema is the loss of elastic recoil. Compliance is reduced diffusely in diffuse fibrosing alveolitis, pulmonary oedema and locally in pneumonia and atelectasis. Resistance is diffusely increased in asthma, chronic bronchitis, emphysema and locally in obstruction due to a foreign body or a large endobronchial tumour. In the context of ventilation imaging, restrictive lung disease refers to idiopathic pulmonary fibrosis or radiation fibrosis, where lung stiffness predominates over airway obstruction. (Secker-Walker R.H., 1978, Alderson P.O., and Line B.R., 1980).

Airways disease begins in the small airways, those less than 2mm in diameter (Secker-Walker R.H., 1978), and develops to involve larger airways. While it is confined to the small airways it is reversible but this is not the case once it has progressed to the large airways. Because the small airways contribute little to the total airway resistance, standard tests are relatively insensitive to changes in these airways. (Alderson P.O., and Line B.R., 1980).

An index of airways function is the efficiency

with which gas from outside the body is exchanged with gas in the respiratory airways. A measurement of this efficiency is ventilation which is the fractional exchange of air per unit time or flow per unit time. (Secker-Walker R.H., 1978, Alderson P.O., and Line B.R., 1980, Secker-Walker R.H., et. al., 1973, Hughes J.M.B., 1979, Ciofetta G., et. al., 1980). In the upright position, at FRC, ventilation per unit lung volume increases approximately linearly by 1.5-2.0 from upper to lower zones. (Secker-Walker R.H., 1978, Alderson P.O., and Line B.R., 1980 and West J.B., 1966). There is probably no redistribution of regional flow with changes in minute ventilation (ventilation per minute) in normal individuals, but this is unlikely in patients with lung disease, however. (Alderson P.O., and Line B.R., 1980).

1.3 Tests of Airways Function.

Precise knowledge of regional function is required for the assessment of patients with chronic lung disease but most tests of pulmonary function are incapable of describing separately the behaviour of different parts of the lung. The ventilation of each lung or individual lobes can be measured by bronchospirometry but considerable skill is required and it is measured under conditions which are very different from normal

relaxed breathing. It is also unpleasant and hazardous. (Ball W.C., et. al., 1962).

Non-invasive tests are possible using measurements of gas movement. Certain respiratory manoeuvres are performed by the patient and the volume of gas moved in a certain time is measured. This requires co-operation from the patient and produces indices only for the lung as a whole.

Non-invasive tests are also possible using poorly soluble tracer gases. Those gases are chosen which are non-toxic and poorly soluble. A known quantity of gas is introduced into the lungs and its dilution is measured at the mouth. This again produces indices only for the lung as a whole.

Non-invasive tests of regional function are possible using radioactive tracer gases and may be divided into those using very soluble gases and those using poorly soluble gases. (West J.B., 1966, West J.B., 1977).Gases available for use as radioactive tracers must have the same characteristics as non-radioactive tracer gases and must also emit enough gamma radiation to be detectable by external monitoring equipment.

1.4 Equipment.

Information on the regional distribution of radioactive gas in the lungs is obtained using equipment designed for the external detection of gamma radiation. This is based on the scintillation counter developed in 1947 by Kallman and shown in figure (1.4). Incident gamma photons are detected by the scintillations they produce in the sodium iodide crystal. These are recorded as current pulses in the photomultiplier tube and, depending on the adjustments of the electronic stages in the photomultiplier assembly, gamma photons of a certain energy only are recorded. This enables rejection of scattered radiation and radiation from different radioisotopes

External monitoring equipment is used either in the form of a multiple probe device or a gamma camera. The signal is a measurement of the concentration of the radioactive gas in different lung regions multiplied by the volume of the lung region. For inhalation studies, the detectors are normally positioned against the back of the subject and so view data from the back to the front of the subject, that is in the postero-anterior (PA) position.

The gamma camera, developed by Anger in 1958 (Anger H.O., 1958, Anger H.O., 1963, Anger H.O., et. al., 1965 and Anger H.O., 1967) and shown in

figure (1.5), incorporates a matrix of scintillation counters which are connected to a single large sodium iodide crystal by a light guide. The outputs from the photomultiplier assemblies are fed into an analogue computer which is capable of determining at which point, on the crystal, scintillation occurs.

Before they impinge on the crystal the gamma photons are collimated by a parallel hole lead collimator so that the image projected onto the crystal is a spatial representation of the source of the radiation.

The gamma camera has the advantage over other forms of external radiation monitoring equipment that information from the whole lung is available at each measurement. They provide rapid, simultaneous assessment of radioactivity within small regions over the entire chest, and permit both a pictorial and a quantitative display of changes in distribution of a tracer gas in the lungs. (Grant B.J.B., et. al., 1974, Nosil J., et. al., 1976).

Figure 1.4. The Scintillation Counter (Wagner H.N. Jr., 1975).

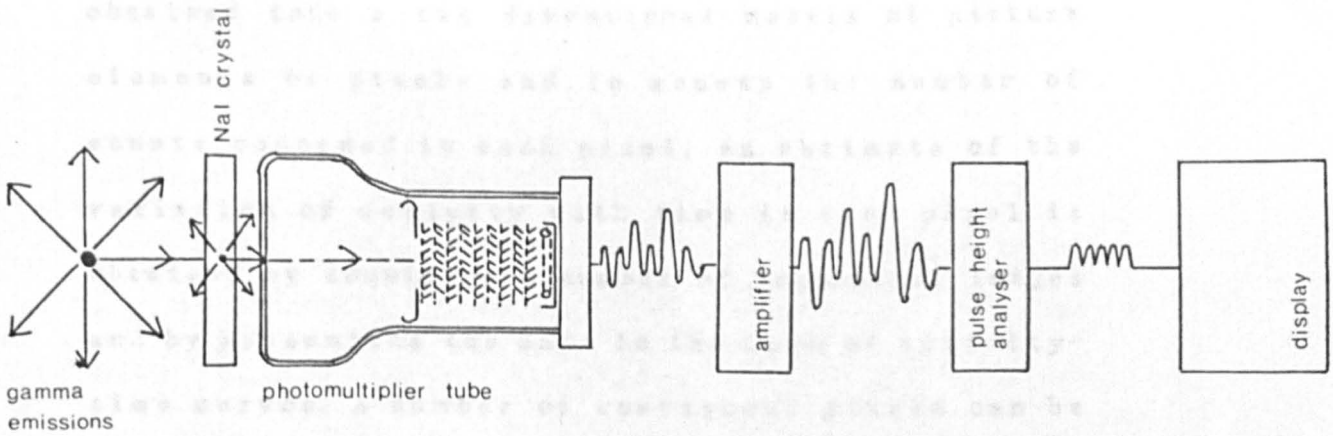

Figure 1.5. The Gamma Camera with parallel hole lead Collimator (Wagner H.N. Jr., 1975).

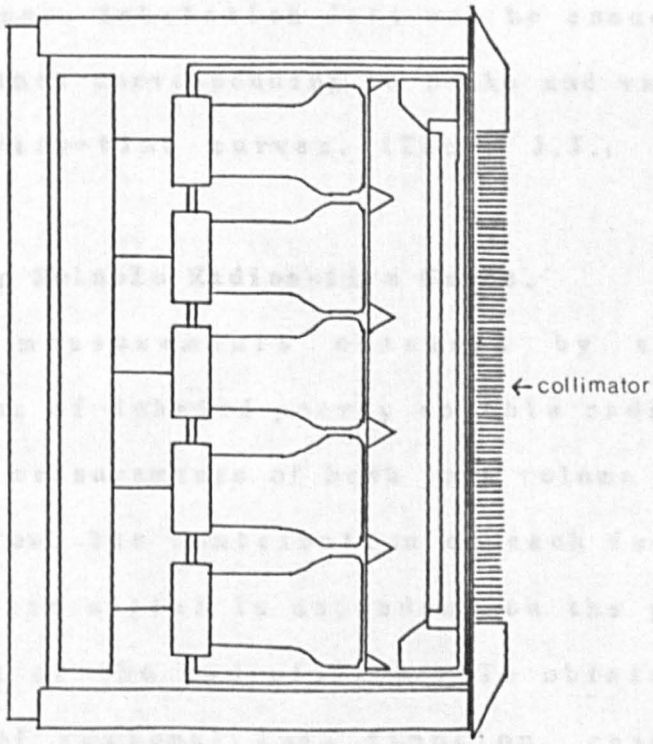

1.5 Data.

It is possible, by interfacing the gamma camera to a digital computer, to divide the image obtained into a two dimensional matrix of picture elements or pixels and to access the number of counts recorded in each pixel. An estimate of the variation of activity with time in each pixel is obtained by acquiring a number of sequential images and by presenting the data in the form of activity-time curves. A number of contiguous pixels can be concatenated to define a region on the image, within which individual pixel counts are summed.

Functional or parametric imaging enables time varying functions to be condensed into a simple index suitable for display in real space. (Nosil J., et. al., 1976, Ullman V., and Kuba J., 1978). For instance, inhalation data can be condensed by adding frames corresponding to peaks and valleys on the activity-time curves. (Touya J.J., et. al., 1979).

1.6 Poorly Soluble Radioactive Gases.

The measurements obtained by external monitoring of inhaled poorly soluble radioactive gases are measurements of both lung volume and lung ventilation. The contribution of each factor to the detected signal is dependent on the physical half-life of the radioisotope. To obtain useful indices of regional lung function, respiratory

manoeuvres by the patient or mathematical manipulations of data obtained during relaxed, that is tidal, breathing are required.

It has been shown that a single lung can be ventilated unevenly (Fowler W.S., 1952) but it suffices in pulmonary function studies to resolve each lung into only a few regions. (Overton T.R., et. al., 1973). The amplitude of movement of the lung regions is at the most of the order of 1 cm for tidal breathing. This together with statistical considerations of the number of lung counts determine the size of the lung region. (Bajzer Z., and Nosil J., 1980). Frequently an upper, mid and lower region are considered in each lung. (Alderson P.O., and Line B.R., 1980). Four regions in each lung were considered in the work described in this thesis.

The gas is normally introduced by a face mask or via a mouthpiece from a reservoir. As the lungs expand, radioactive gas is drawn in through the upper respiratory tract and the trachea and into the peripheral airways. Because the radioactive gas is poorly soluble, very little gets absorbed into the blood at the alveolar-capillary membrane and most remains in the gas phase. During an expiration a little of the radioactive gas, now reduced in concentration, is expelled from the lungs to the

atmosphere. Thus, during a sequence of inspirations and expirations the activity in the lungs builds up because less is removed during expiration than is introduced during inspiration. An equilibrium state is reached when the maximum concentration is achieved in the lungs. At this point as much activity is removed from the lungs during an expiration as is introduced during an inspiration. When the supply of radioactive gas is stopped and only clean air is taken into the lungs during an inspiration, there is a gradual reduction in activity because the exhaled concentration is now greater than the inspired concentration. The gradual increase in concentration from zero to equilibrium is called washin and the gradual decrease in activity from equilibrium to zero is called washout.

There are three ways of measuring regional ventilation using poorly soluble radioactive gases. The original method, was to record the gradual washin or washout of radioactivity. A number of different mathematical techniques have been used to analyse these curves. The most recently proposed method, however, has been to measure the distribution of a radioisotope with a very short half-life at equilibrium.

The most usual gas for inhalation ivestigations has been ^{133}Xe. This suffers from a

number of disadvantages which include its relatively high solubility. Because of this some gas will dissolve in the blood at the alveolar-capillary boundary and be transported from the lungs to the tissues of the chest. This complicates the interpretation of washin and washout curves because components of tissue content are added to the curves observed by external monitoring equipment.

One of the most recently introduced gases is $^{81}Kr^{m}$. It is a very insoluble gas and this together with its very short physical half-life of 13 seconds means that it has the advantage over ^{133}Xe that the externally detected signal, can be assumed to originate from atoms in the gas phase of the lung and not from atoms in the tissues of the thorax (Bajzer Z., and Nosil J., 1980).

It was this gas which was used to measure the regional distribution at equilibrium in the recently proposed analysis technique (Fazio F., and Jones T., 1975). It has been shown, however, that assumptions made in this paper are not justified under all conditions and attention has focussed on methods of analysing the data obtained using this radioisotope to overcome these problems.

One technique has been to apply a mathematical model of the behaviour of gas in the lung to the

data obtained during a washout procedure. The models proposed, to date, take into account both the radioactive decay of the radioisotope and the periodicity of the respiration. They assume, however, a continuous flow of gas through the lung during the breathing cycle and also a constant concentration of radioactive gas during the inspiratory phase.

In this thesis, a mathematical model was developed which described the behaviour of radioactive gas in the lung over a single breath. It was based on the same assumptions as the previous continuous flow models and included a consideration of radioactive decay. The previous models were extended to reflect the fact that gas changes direction during the breathing cycle. Thus, both the periodicity and direction of respiration were considered.

The model was applied only to the expiratory phase of the activity-time curve to avoid the problems associated with inspiration of a non-uniform concentration of radioactive tracer gas. Values of specific mean expiratory gas flow, that is mean expiratory gas flow per unit lung volume, were obtained.

Data was acquired on a gamma camera from $^{81}Kr^{m}$ at equilibrium in the lungs. The problem of low counting rates during a single breath was overcome

by producing an average respiratory cycle from serially collected images using post-acquisition analysis based on the detected activity in the lung.

An alternative method, of improving the counting statistics, considered was to gate the study at equilibrium. This involved determining the beginning and end of a breathing cycle using a physiological trigger, dividing the cycle into a number of time intervals and adding the data from a number of breathing cycles to these intervals (Touya J.J., et. al., 1981).

It was difficult to envisage a physiological trigger which would not interfere with the breathing pattern of the patient by constraining his motion. Other factors which influenced the choice was the inconvenience associated with extra patient connected equipment and the possibility of variation in the breathing cycle duration during data acquisition. The latter could be accommodated more readily by the post-acquisition analysis.

An attempt was made to measure the phase difference of gas flow between lung regions. Consideration was given to using Fourier analysis of single breath data. This was rejected in favour of cross-correlation which made use of all the data available in the multiple breath activity-time

curve.

The adequacy of the mathematical model was assessed using simulated noise-free activity-time curves which were used to investigate the relationship between specific mean expiratory gas flow and specific ventilation.

The susceptibility of the model analysis to Poisson noise was assessed using equilibrium activity-time curves which were simulated at various activity levels. Poisson noise was superimposed and the simulation parameters were extracted using the analysis suggested.

The reliability of the technique in clinical practice was assessed using two sequential studies on a number of patients with a variety of respiratory diseases.

A further clinical study, involving one study on both normal subjects and patients with a variety of respiratory diseases, was undertaken to compare the values of specific mean expiratory gas flow obtained from the model analysis with the values of specific ventilation published in the literature.

The susceptibility of the phase analysis to Poisson noise was assessed using equilibrium activity-time curves which were simulated at various activity levels. Poisson noise was superimposed and the simulated phase differences were extracted using the analysis suggested.

CHAPTER 2 **Review of Past Work.**

A variety of mathematical techniques have been used to calculate physiological indices from data acquired during inhalation investigations using poorly soluble radioactive gases. The techniques vary according to whether the data was acquired during the washin, equilibrium or washout phases of a study. The accuracy of the results obtained from these analyses are affected by the physical properties of the radioactive tracer gases.

If ^{133}Xe is used, signal attenuation and scatter occurs, even though the lung is an ineffective photon attenuator. The gamma rays of ^{133}Xe undergo an approximate 45% attenuation through 10 cm of inflated lung. (Alderson P.O., and Line B.R., 1980 and Harf A., et. al., 1978). Gamma rays from positron emitters such as ^{13}N undergo only a 28% attenuation, however, (Hughes J.M.B., 1979) but they penetrate the septa of even a high energy collimator, causing considerable loss in resolution, whereas those from $^{81}Kr^{m}$ are not high enough to penetrate such a collimator. (Nosil J., et. al., 1977).

2.1 **Analysis of Washin Data.**

The simplest method used to analyse data acquired during the washin phase is to express the changes in count rate in terms of the time required to reach 50% or 90% of the equilibrium count rate.

Another method makes use of the assumption that the washin activity-time curve is monoexponential in normal lung regions. (Alderson P.O., and Line B.R., 1980). In this method, the area under the washin curve is determined for each region and is expressed as a percentage of the total area under this part of the washin curve for both lungs. The distribution at the end of washin is normalised in a similar fashion and the ratio obtained is a measure of the relative ventilation in each region. (Secker-Walker R.H., 1978).

Van de Mark Th. W., et. al., 1980 warned, however, that since xenon is soluble in blood, this would give rise to multi-exponential washin curves.

A consideration of the kinetics of a poorly soluble radioactive gas in terms of a continuous model for lung ventilation is sufficient to explain the limitations of the washin type study. During the washin phase the tracer is mixed with inhaled air at a constant concentration and the increase of activity in the lung per unit of time is equal to the difference between the flow to the lungs multiplied by the concentration of the tracer in the inhaled air and the loss of activity due to expiration or decay. Of two regions of equal volume, the lesser ventilated region will have a slower rise in activity but both regions will

eventually reach the same level of activity. Hence there is only a short time during which the difference between well and poorly ventilated regions will be reflected by the tracer distribution. This time is smaller for smaller differences.

To overcome this short observation time, breath-holding during a single-breath inhalation is used. This, however, is un-physiological and is difficult to perform. (Goris M., and Daspit S., 1978 and Alpert N.M., et. al., 1975). It was a very popular technique before computers became readily available and was based on the observation that after an inhalation, the maximum counting rate demonstrated a general relationship to the regional fraction of the tidal volume. (Jones R.H., et. al., 1974). When this was compared to the counting rate obtained during a subsequent equilibrium phase it provided a reliable method of calculating relative ventilation per unit volume. (Fowler W.S., 1952, Ball W.C., et. al., 1962, Khalil Ali M., et. al., 1975 and Overton T.R., et. al., 1973).

The breath-holding technique made four assumptions that: 1. the radioactive tracer was evenly mixed with the air during the inspiration, 2. the concentration of radioactive tracer in the lung came to equilibrium with the reservoir concentration, 3. corrections could be made for any

systemically absorbed tracer and 4. the single breath distribution corresponded to the distribution of air exchange. Assumptions 2 and 4 are unlikely to be satisfied in patients with obstructive airways disease. (Alderson P.O., and Line B.R., 1980).

A problem with the washin technique was that the distribution of the bolus was greatly influenced by the lung volume at which the inspiration of tracer began and the flow rate at which it proceeded. (Jones R.H., et. al., 1974). For example, in patients with localised emphysema the relative ventilation of the most severely affected areas was greatly reduced during quiet breathing but those areas received a much larger fraction of the inspired air on deep inspiration. (Ball W.C., et. al., 1962). Another problem was that the counts over the lungs following a single inhalation included tracer within the large conducting airways as well as within the respiratory airways. (Jones R.H., et. al., 1974).

2.2 Analysis of Equilibrium Data.

Equilibrium is the condition most similar to normal relaxed tidal breathing and is the best condition under which to study lung physiology. At equilibrium, the activity distribution of radioactive gases is related to lung volumes and

not to ventilation, however. (Goris M., and Daspit S., 1978).

Although the most popular, ^{133}Xe is not the ideal tracer gas. There is a small but appreciable solubility of xenon in blood. In normal subjects, the chest wall contributes about 5% to the counting rate after 2 minutes of rebreathing (West J.B., 1977) whereas, for example, the blood-gas partition coefficient fot nitrogen is a lot lower and only 2-3% of ^{13}N could be detected in arterial blood. (Nosil J., et. al., 1976).

Regional lung volume is under-estimated by measuring the count rate over the lung region after rebreathing ^{133}Xe for a few minutes because removal of radioactivity by the blood prevents a complete equilibrium, with an alveolar ^{133}Xe concentration equal to the inspired one. (Matthews C.M.E., and Dollery C.T., 1965). Ronchetti R., et. al., 1974 reported that after 10 minutes of washin, a normal adult attained a concentration of only 81% of the inspired ^{133}Xe concentration. West J.B., 1977 reported that in one normal subject, the concentration of xenon reached 89% of the spirometer concentration in the upper zone, but only 74% in the lower zone.

2.2.1 $^{81}Kr^{m}$.

Because ^{13}N is not readily available, the most ideal radioisotope to use is $^{81}Kr^{m}$. It is less soluble than other readily available radioactive tracer gases and does not dissolve to an appreciable extent in the blood (Bajzer Z., and Nosil J., 1980). The radiation detected by a gamma camera can therefore be safely assumed to originate from radioactive atoms in the gas phase of the lung. The use of $^{81}Kr^{m}$ is, however, limited by the present analysis techniques as to the information obtainable.

It has been suggested that, because of its very short half-life, continuous tidal breathing of $^{81}Kr^{m}$ produced the same information as a sum of a series of separate single-breaths of a radioactive gas with a longer half-life. Fazio F., and Jones T., 1975 developed the following argument. At equilibrium, during continuous inhalation of $^{81}Kr^{m}$, the arrival of the gas in the alveolar compartment equals the removal by ventilatory washout and radioactive decay. The rapid radioactive decay relative to the ventilatory turnover rate per unit volume results in an alveolar concentration at equilibrium much less than that in the inspired air. Hence the contribution of the $^{81}Kr^{m}$ washout to this process is small. Equilibration of the radioisotope in the lung therefore depends on the

balance between the arrival of $^{81}Kr^{m}$ and radioactive decay. $^{81}Kr^{m}$ lung counts, N, are proportional to:

$$N = \frac{\dot{V}}{\frac{\dot{V}}{V} + \lambda} \qquad (2.1)$$

where, $\dot{V}$ is the total ventilation, $\dot{V}/V$ the ventilation per unit of lung volume and λ the radioactive decay constant of $^{81}Kr^{m}$ which is 0.05 per second.

This equation involves two assumptions: that the ventilation is continuous and that inspired and expired alveolar ventilations are equal. (Harf A., et. al., 1978). The relationship is independent of the combination of tidal volume and frequency used to achieve a given ventilation. For example, it is not altered by the inspiratory time varying from from 30% to 70% of the respiratory cycle. (Modell H.I., and Graham M.M., 1982).

The demominator is dominated by the high value of λ, hence the lung signal is more dependent on ventilation than on ventilatory washout. This results in an almost linear relation between radioactivity and regional ventilation for both normal and reduced ventilation rates in adults and the equilibrium concentration is linearly related to the fractional ventilation rate ($\dot{V}/V$).

Since activities are concentrations multiplied by volumes, the activity distribution is proportional to the ventilation distribution, (Fazio F., and Jones T., 1975, Harf A., et. al., 1976, Goris M., and Daspit S., 1978, Jones T., 1978b and Arnot R.N., et. al., 1981) but when regional ventilation per unit alveolar volume is high, ie., greater than the half-life of $^{81}Kr^{m}$, the distribution at equilibrium tends to reflect the distribution of lung volume rather than ventilation. (Ciofetta G., et. al., 1980, Harf A., et. al., 1978, Ham H.R., et al., 1981, Arnot R.N., et. al., 1978 and Alderson P.O., and Line B.R., 1980).

Usually both volume and concentration are variable and unknown, the volume distribution being subject to both anatomical and projectional variables. Jones T., 1978a reported that the initial blush of indiscriminate use of $^{81}Kr^{m}$ by continuous inhalation to produce images of ventilation was already waning and ways of analysing equilibrium images to provide quantitative measurements of flow were being sought.

2.2.2 Problems of Use of $^{81}Kr^{m}$.

It was recognised that the information contained in a single $^{81}Kr^{m}$ inhalation image was a fairly crude representation of regional ventilation ($\dot{V}$) and not at all representative of ventilatory turnover ($\dot{V}/V$) which is the basic quantitative measure of ventilation and of which absolute values are required. (Jones T., 1978b, and Hughes J.M.B., 1979).

When specific ventilation ranges from well below normal to normal, the difference between changes in activity ratios and changes in ventilation ratios in two regions can be of the order of 10%, while if specific ventilation ranges from normal values to those found after exercise then such differences can be more than 25%. The use of $^{81}Kr^{m}$ alone for accurate measurements is therefore very limited. Each activity ratio gives a correct qualitative indication of relative ventilation but an incorrect indication of the relation between the two ventilation ratios. Without correction $^{81}Kr^{m}$ count ratios can give a qualitative indication of the relative regional ventilation in a single image, but when comparing different images, changes in relative regional ventilation may be accompanied by no change in the $^{81}Kr^{m}$ count ratios or by a change in the opposite direction, depending on the values of specific

ventilation involved. Similarly changes in $^{81}Kr^{m}$ count ratios may occur when there is no change in ventilation ratio. (Arnot R.N., et. al., 1981).

Some workers stated that the continuous inhalation image is useful clinically, however. Fazio F., et. al., 1979 reported that it proved adequate for the assessment of bronchial asthma. Miller T.R., et. al., 1981 reported that there was excellent correlation between $^{81}Kr^{m}$ equilibrium images and washout data for the assessment of suspected pulmonary embolism.

Other workers reported that there were disadvantages to the continuous inhalation technique. McKenzie S.A., and Fitzpatrick M.L., 1981 stated that the quantitative information about the distribution of ventilation obtainable by inhalation of radioactive gases was not helpful in the monitoring of the progress of a generalised disorder such as cystic fibrosis where the distribution of ventilation may appear to remain uniform. They suggested that for the proper evaluation of function using tracer techniques, the measurement of the clearance rate of the gas as an index of ventilatory turnover would be desirable.

An example given by Hughes J.M.B., 1979 of the situation in chronic bronchitis clarifies the point. A patchy ventilation image was observed as

if normal areas existed alongside abnormal ones. But when regional ventilation was expressed in absolute units by performing a washout, all areas were grossly abnormal, the difference in the $^{81}Kr^{m}$ image being one of degree. Ciofetta G., et. al., 1980 reported a case of a small alveolar volume in one lung causing that lung to seem relatively poorly ventilated but which, on washout analysis, revealed similar values of $\dot{V}/V$ to the other lung.

Both Schor R.A., et. al., 1978 and Alderson P.O., and Line B.R., 1980 reported that washout data were considerably more sensitive than $^{81}Kr^{m}$ equilibrium images in the detection of regional ventilatory abnormalities, especially when mild in degree. The latter authors also suggested that the diffuse nature of restrictive disease contributed to a relatively normal appearance of $^{81}Kr^{m}$ images.

The short half-life of $^{81}Kr^{m}$ itself has serious disadvantages when imaging for obstructive lung disease. (Simpson A.E., et. al., 1980). Although the short half-life precludes the performance of washout studies it is long enough to allow a degree of redistribution of activity by diffusion from well ventilated areas of the lung to more poorly ventilated areas. (Simpson A.E., et al., 1980, Alderson P.O., and Line B.R., 1980 and Yano Y., et. al., 1970). Also because of the length of the transit time to peripheral parts of the

lung, $^{81}Kr^{m}$ may not have access to the entire volume of any lung region. (Amis T.C., 1979) and the distribution volume of $^{81}Kr^{m}$ was reported as being substantially less than the end-inspiratory volume. (Modell H.I., and Graham M.M., 1982).

2.2.3 Problems of Administration of $^{81}Kr^{m}$.

Another disadvantage of continuous inhalation of $^{81}Kr^{m}$ is similar to that experienced in washin studies but is exagerated because of its rapid decay. If an ordinary face mask is used, it provides a small reservoir for radioactive gas. Activity builds up towards the end of expiration, giving a sharp burst of activity at the beginning of the next inspiration. As inspiratory flow builds up, so the level of activity in the inspired gas falls, (Hughes J.M.B., 1979 and Amis T.C., 1979) and if the inhaled $^{81}Kr^{m}$ is not of constant concentration, artefacts in the count density distribution can occur. (Arnot R.N., et. al., 1978).

Reservoirs may be used to improve the activity utilisation (Mostafa A.B., et. al., 1983) but when it comes to improving the concentration pattern reservoirs are impractical without high activity generators because of the low count rates that result. (Alderson P.O., and Line B.R., 1980).

Lamb J.F., et. al., 1978 stated, however,

that almost any delivery system which can quickly transfer radioactive $^{81}Kr^{m}$ to a patient's inspired breath may be used because even if a constant concentration was applied at the mouth the concentration of $^{81}Kr^{m}$ at the lower end of the trachea could not be kept constant because of the dead space gas present from the previous breath. This argument was extended by Arnot R.N., et. al., 1978 who stated that some radioactive decay will occur during inspiration causing a variation in any constant concentration applied at the mouth but that this is of less consequence than the inhalation during the first part of the breath of dead space gas in which $^{81}Kr^{m}$ concentration may only be 50% of that in the remainder of the tidal volume.

The effect of the dead space is also exagerated because $^{81}Kr^{m}$ is not well mixed with resident lung gas during inspiration. This results in gas relatively rich in tracer leaving the system during expiration. (Modell H.I., and Graham M.M., 1982). Hence, at low tidal volumes the concentration of radioactivity in dead space gas is about 40% of the inspired concentration but at high tidal volumes it can be 70% of the inspired concentration. Therefore regional radioactivity will depend on the proportion of dead space gas in the alveolar inspirate, as well as on regional $\dot{V}/V$.

Arnot R.N., et. al., 1981, however, noted that a high proportion of dead space low concentration $^{81}Kr^{m}$ distributed to a region reflects less effective ventilation in that region, therefore the effect is in the correct direction but difficult to assess.

Another problem associated with the continuous administration of $^{81}Kr^{m}$ is the identification of the lung volume under investigation. During a breathing cycle lung volume varies between FRC and end-inspiratory volume. $\dot{V}/V$ obtained from washout curves refers to a lung volume equal to (FRC+TV-dead space) but the $\dot{V}/V$ in the equilibrium equation for $^{81}Kr^{m}$ may be close to FRC alone if counts are accumulated during the entire breathing period when expiration time is longer than inspiration time. (Arnot R.N., et. al., 1978). It is difficult to determine what volume is most appropriate when calculating $^{81}Kr^{m}$ concentration within the lung. Calculating concentration using FRC will yield an over-estimate and using end-inspiratory volume will yield an under-estimate. (Modell H.I., and Graham M.M., 1982).

2.3 Analysis of Washout Data.

Washout studies are more popular than washin studies because the clearance rate of the tracer gas during air breathing can be obtained in patients more easily than the accumulation rate. (Jones R.H., et. al., 1974).

The washout study has another distinct advantage. If all the counts are collected during that phase, the lesser ventilated regions yield higher counts. When the ventilation rate is half normal the integrated count rate is twice normal, for equal volumes. (Goris M., and Daspit S., 1978 and Ball W.C., et. al., 1962). A number of different mathematical techniques have been used to analyse washout curves.

The simplest method is to express the changes in count rate in terms of the time required to reach the 50% or the 10% of the peak level during washout. These methods, however, depend only on analysis of time changes which can vary greatly with the rate of minute ventilation. They are heavily weighted by the contribution of normal airways during early phases of washout. Also, because they are insensitive to changes of shape of the curve, undue weight is given to either well ventilated or poorly ventilated regions. (Alderson P.O., and Line B.R., 1980 and Nosil J., et. al., 1976).

A second method is to calculate the regional clearance rates by fitting a straight line to the first 50%-60% of a semi-logarithmic plot of the clearance curve to obtain a measure of the mean regional specific ventilation. This method uses the whole washout curve and so does not ignore the contributions of poorly ventilated regions. (Amis T.C., 1979 and Alderson P.O., and Line B.R., 1980). Another advantage of working with the initial slope is that it is dominated by the clearance of tracer from the lung and little influenced by clearance of activity dissolved in the chest wall tissues or returning to the lung by recirculation of dissolved tracer. (Amis T.C., 1979).

A third method determines the ventilation as the flow of air per unit lung volume or the fractional exchange of air per unit time by using the ratio of the height of the washin curve at equilibrium to the area under the whole clearance curve (the Height/Area technique). This method is based on the Stewart-Hamilton equation which was developed for cardiac measurements. It assumes that the quantity of radioactive tracer gas in the lungs at the end of washin can be considered as a bolus injection for the washout that follows. Again, this method uses the whole washout curve and so does not ignore the contribution of poorly ventilated

regions. (Secker-Walker R.H., et. al., 1975 and Alderson P.O., and Line B.R., 1980). The method is, however, sensitive to errors in estimating the height used for the calculation (Secker-Walker R.H., et. al., 1975 and McKenzie S.A., and Fitzpatrick M.L., 1981) and for this reason it is very sensitive to tissue background. (West J.B., 1977).

A number of authors vouch for the accuracy of the washout technique. Secker-Walker R.H., et. al., 1973 state that there was a highly significant correlation between the tidal volume and the fractional exchange of air per breath calculated from washout curves. Jones R.H., et. al., 1974 stated that there was a close correlation of the slope of a washout curve with the actual minute volume in each lung and it provided an accurate index of the distribution of alveolar ventilation.

As for the washin technique, the washout analysis can be described by a continuous flow model. While the patient rebreathes fresh air the loss of activity from the lungs is equal to the concentration of the tracer in the lungs, multiplied by the average flow to the outside plus the amount disappearing by decay. This should result in a single exponential curve. (Goris M., and Daspit S., 1978, Jones R.H., et. al., 1974, Alpert N.M., et. al., 1975, Simpson A.E., et. al.,

1980 and Parkin A., et. al., 1982).

The washouts after single breath inhalation and after rebreathing of radioactive tracer gas are not identical. (Devos P., et. al., 1978). The disappearance rate of a single inhalation provides the least accurate description of regional ventilation. Lack of uniform mixing of a single breath within aerated lung probably represents the greatest source of error by this approach. The residual lung volume dilutes the concentration of radioactive tracer gas in inspired air leaving a lower concentration of gas in the alveoli than in the conducting airways. Therefore, the initial washout rate appears more rapidly than the rate of alveolar clearance of tracer gas. The error resulting from removal of tracer from conducting airways is minimised following rebreathing of tracer gas which produces a more even distribution within the conducting airways and alveoli. (Jones R.H., et. al., 1974).

2.3.1 **Tissue Background.**

A number of problems arise in the analysis of washout curves mainly to do with the absorption of the radioactive tracer gas into the blood resulting in a tissue background count. To obtain the true pulmonary curve, the contribution of blood and chest wall activity must be removed. (Alderson

P.O., and Line B.R., 1980). ^{13}N, however, has the advantage of low solubility in the tissues. (Alpert N.M., et. al., 1975 and Arnot R.N., et. al., 1981) and there is reasonable agreement between the elimination of ^{13}N in the expired air, where the chest wall is excluded, compared with that recorded over the lung. (Nosil J., et. al., 1976 and Arnot R.N., et. al., 1978).

Although some authors state that the activity-time curve of the washout is nearly mono-exponential in normal regions (Alderson P.O., and Line B.R., 1980), others state that washout curves do not follow a mono-exponential course, even in normals. (Henriksen O., et. al., 1980, Winlove C.P., et. al., 1976 and Van de Mark Th. W., et. al., 1980). The washout curve is definitely not a single exponential in lung disease. (Nosil J., et. al., 1976 and Amis T.C., 1979).

During washout the tissues act as a source of tracer, returning gas to the alveolar airspace. (Arnot R.N., et. al., 1978 and Van de Mark Th. W., et. al., 1980). This slows the washout rate by approximately 5% when recorded by a gamma camera. (Arnot R.N., et. al., 1981). Quantitative analysis of washout curves is made difficult because the later part is influenced by this return of dissolved gas. Counting rates from these tissues rise roughly in linear fashion but do not exceed 2%

of the simultaneous counts from normally ventilated lung even after as much as 10 minutes of rebreathing. (Fowler W.S., 1952, Secker-Walker R.H., et. al., 1973 and Van de Mark Th. W., et. al., 1980). Secker-Walker R.H., et. al., 1973 gave an example of the fractional exchange of air calculated without background correction from the washout curves. It averaged 65% of that determined from the washin curves, where tissue background had little effect. With the tissue background correction, however, the difference was only 8%, and this could be explained because it was comparable to the difference in tidal volumes between the washin and washout parts of the procedure. These authors recommended that both the height of the curve at the end of washin and the area under the washout curve be corrected for tissue content.

A physical model of the background compartments would be quite complex and usually, as an approximation, a constant background is considered. (Bunow B., et. al., 1979).

Van de Mark Th. W., et. al., 1980, however, recently proposed a method to improve on this by taking into account the climbing background. They proposed that a xenon washin or washout curve should be described as a five-exponential function

in which the component with the largest exponent was directly related to gas clearance of the lung. The claimed improvement over the previously described methods was criticized by Williams L.E., 1981 who attributed it to the increased number of parameters used. This was disputed by the original authors, however.

2.3.2 **Dead Space.**

Another source of error in the washout analysis, is the regional variations in the distribution of the dead space gas, which affects regional washout curves because the proportions of dead space gas and fresh air entering the alveoli varies. (West J.B., 1977 and Arnot R.N., et. al., 1981).

At the end of expiration, the dead space is filled with gas from the alveoli. The composition of this gas varies throughout the lung depending on regional $\dot{V}/V$, but in the major airways the gas contains mixed contributions from all lung regions. During inspiration, this gas may be distributed in a non-uniform fashion, so altering the fraction of radioactivity re-inhaled by each region of the lung. This would distort the relationship between the regional washout curves. For example, if the whole of the dead space gas were delivered to one particular region while the rest of the lungs received only fresh inactive gas during

inspiration, then the washout from that region would be slowed down. However, it can be argued that if all the dead space gas is redistributed to a particular region, then the effective ventilation to that region is decreased, and it is proper for this to be reflected in a slower washout measurement. Thus the effect of the re-inspiration of radioactive dead space gas on radioactive measurements is in the correct direction though it cannot be assessed quantitatively. (Arnot R.N., et. al., 1981).

Another factor which may lead to an error is the determination of specific ventilation by equating it directly to the washout rates defined by smooth curves fitted to ventilation data since ventilation is a discontinuous process and which should be taken into account when calculating specific ventilation from the parameters of smooth washout curves. (Arnot R.N., et. al., 1981).

2.3.3 **Mean Transit Time.**

A method of analysing washin and washout curves which is independent of the shape of the curve is mean transit time. It was originally proposed to describe the mean time of transit of radioactive tracer particles injected into an artery of an organ and monitored at the outflow of that organ. (Kety S.S., 1949 and Meier P., and

Zierler K.L., 1954). Zierler K.L., 1965 extended the argument to include the administration of poorly soluble radioactive gases by inhalation and demonstrated that mean transit time is the reciprocal of the rate constant obtained from the slope of the semi-logarithmic replot of washout data.

Bassingthwaighte J.B., et. al., 1970 pointed out that the assumption of a steady state is not realized due to the pulsatile nature of the respiratory cycle but that this does not invalidate the calculation if an adequate number of full cycles are used in the calculation.

Nosil J., et. al., 1976 introduced the idea of calculating the mean transit time as the ratio of the first to the zeroth moment of the washout curve.

Orr J.S., et. al., 1978, later qualified by Tofts P.S., and Linney A.D., 1978, criticised the assumptions made by Secker-Walker R.H., et. al., 1973 and Nosil J., et. al., 1976. They argued that the results of Nosil J., et. al., 1976 were valid only for a bolus administration and a monoexponential curve and not, as stated, for washout from rebreathing equilibrium. Henriksen O., et. al., 1981 also made these criticisms. Nosil J., still maintains that his assumptions are correct, however (personal discussion). The authors stated

that the method of Secker-Walker R.H., et. al., 1973 is applicable only when the washout curve is monoexponential.

Leeman S., and Orr J.S., 1979 developed these arguments and suggested that the mean transit time when calculated as the ratio of the first to the zeroth moment, not of the washout curve, but of its second derivative will be independent of the shape of the washout curve.

Zadro M., et. al., 1981 extended these arguments further to make the method independent of the assumption of initial radioisotope uniformity of distribution.

Orr J.S., 1979 proposed the development of a more realistic model of the system using the analogy between the procedure of continuous administration of short-lived tracer and the Laplace transform. Chackett K.F., 1980 proposed the fitting of Laguerre functions to the data to directly determine the second time-differentials.

2.3.4 Radioactive Decay.

Because of its rapid decay it is not possible to follow washout patterns using $^{81}Kr^{m}$. (Yano Y., et. al., 1970). The very low count rates with poor statistics which occur towards the tail of the curve are exagerated in low ventilation regions where the initial count rate is low. (Amis T.C.,

1979). An alternative approach to achieve absolute values of flow turnover rates, is to repeat the $^{81}Kr^{m}$ procedure using $^{85}Kr^{m}$, which has a longer half-life at 4.4 hours. (Jones T., 1978b). Because of its long half-life, the concentration of the $^{85}Kr^{m}$ builds up to reach that of the concentration in the inspired gas and can be used to calibrate the $^{81}Kr^{m}$ data. (Jones T., et al., 1978, Alderson P.O., and Line B.R., 1980 and Amis T.C., et. al., 1978).

Parkin A., et. al, 1982 stated that washout is possible using $^{81}Kr^{m}$ if a lower limit of acceptability for V/V is set arbitrarily at 0.7 per minute to accomodate the rapid radioactive decay. They reported that most of their subjects were within the range 1.0-2.0 per minute which is the range quoted as normal.

2.4 Mathematical Models.

In order to describe the behaviour of poorly soluble radioactive gases in the lung mathematical models have been developed. The behaviour of the tracer gas in a homogeneous lung unit was initially described and the inhomogeneity of the real lung was then represented by arraying a number of these units in parallel.

Winlove C.P., et. al., 1976 took as the model lung unit a homogeneous compartment of volume V, which contains N(t) tracer molecules at time t.

The external air was considered as a reservoir of volume V_o which contained $N_o(t)$ tracer molecules at time t. Gas was assumed to flow continuously from the reservoir to the lung and back into the reservoir at a rate λ. The periodicity of respiration was neglected.

In the time interval $t-(t+\Delta t)$, $\lambda N_o(t)\Delta t/V_o$ tracer molecules entered the lung unit from the external reservoir whilst $\lambda N(t)\Delta t/V$ passed in the opposite direction.

The net change in the number of tracer molecules in the time interval Δt, $\Delta N(t)$ was therefore:

$$\Delta N(t)=\left[\frac{\lambda N_o(t)}{V_o}-\frac{\lambda N(t)}{V}\right]\Delta t \qquad (2.2)$$

$$\frac{dN(t)}{dt}+\frac{\lambda N(t)}{V}=\frac{\lambda N_o(t)}{V_o} \qquad (2.3)$$

$$N(t)=e^{-\lambda t/V}\left[\int_0^t \frac{\lambda N_o(t)e^{\lambda t/V}}{V_o}dt+N(0)\right] \qquad (2.4)$$

where N(0) was the number of tracer molecules in the lung unit at time t=0.

It was assumed that the radioactive gas was inhaled at a constant concentration h_2 for a period τ_2 and that thereafter the concentration in the external reservoir, $N_o(t)/V_o$ was negligible.

Under these conditions equation (2.4) showed the number of tracer molecules in the lung unit during washin was:

$$N(t)=h_2V\left[1-e^{-\lambda t/V}\right] \qquad t<\tau_2 \quad (2.5)$$

and during clearance:

$$N(t)=h_2V\left[e^{\lambda\tau_2/V}-1\right]e^{-\lambda t/V} \qquad t>\tau_2 \quad (2.6)$$

If, however, inhalation was prolonged then $e^{-\lambda\tau_2/V}$ became negligible. This corresponded to the attainment of an equilibrium level of $N(t)=h_2V$ molecules and the subsequent clearance satisfied:

$$N(t)=h_2Ve^{-\lambda t'/V} \qquad t'>0 \quad (2.7)$$

Bajzer Z., and Nosil J., 1977 and Bajzer Z., et. al., 1977 constructed a model based on the previous assumptions but also took into account that the tracer concentration in lung decreased by radioactive decay.

The number ΔN_d of radioactive tracer atoms in the lung unit, LU, which have decayed in the time interval $[t, t+\Delta t]$ was

$$\Delta N_d=\lambda N(t)\Delta t \qquad (2.8)$$

where λ was the decay constant, and the number ΔN_e of radioactive tracer atoms removed from LU was

$$\Delta N_e=\frac{\emptyset N(t)}{V}\Delta t \qquad (2.9)$$

The number of radioactive tracer atoms which arrive at LU in the same time interval is

$$\Delta N_i = \emptyset \frac{N_o}{V_o} \Delta t = \emptyset C \Delta t \qquad (2.10)$$

They obtained the number of radioactive tracer atoms at any time during or after inhalation as the number of counts obtained in some time interval $[t-\tau, t]$ as a function of time t. Thus the theoretical expression to be compared with the measured data was the following:

$$M(t) = E\int_{t-\tau}^{t} \lambda N(s)ds \qquad (2.11)$$

$$= \frac{E\lambda\emptyset C}{D}\left[\tau + \frac{e^{-Dt}(1-e^{Dt})}{D}\right] \qquad \tau \leqslant t \leqslant T$$

$$= \frac{E\lambda\emptyset C}{D}\left[T - t + \tau + \left[\frac{1-e^{-Dt}(e^{DT}+e^{D\tau}-1)}{D}\right]\right] \qquad T \leqslant t \leqslant T+\tau$$

$$= \frac{E\lambda\emptyset C}{D^2}(e^{DT}-1)(e^{D\tau}-1)e^{-Dt} \qquad t \geqslant T+\tau$$

$$D = \lambda + \frac{\emptyset}{V}$$

Fitting the expression (2.11) to the data, they obtained specific ventilation, $\emptyset/V$.

Spaventi S., et. al., 1978 and Ciofetta G., et. al., 1980 develop the work of Bajzer Z., and Nosil J., 1977 to make the fitting a simpler operation.

Bajzer Z., and Nosil J., 1980 developed the model to take into account the periodicity of breathing by describing the time dependence of lung volume by a general periodic function.

To describe the complex variation of lung volume with time they chose the general periodic functions to be represented by a Fourier series, the coefficients of which determined the shape of the corresponding periodic curves. For the ith lung unit:

$$V_i(t)=v_i+\frac{1}{2}w_i f_i(t) \qquad (2.12)$$

$$f_i(t)=\sum_{l=0}^{\alpha} a_l^{(i)} \cos\frac{2\pi l}{T}t \qquad (2.13)$$

where, T was the breathing period, w_i was the tidal volume of the LU and v_i was the functional residual capacity of the LU. The solution for the number, N(t), of radioactive tracer atoms in the LU was,

$$N(t)=N_o\left[\frac{v}{v+w}\right]^n e^{-\lambda t} \qquad nT\leqslant t\leqslant nT+T_{in} \qquad (2.14)$$

$$N(t)=N_o\left[\frac{v}{v+w}\right]^n e^{-\lambda t}\left[\frac{V(t)}{v+w}\right] \qquad nT+T_{in}\leqslant t\leqslant (n+1)T$$

$n=0,1,2,\ldots\ldots$

2.5 Phase Analysis.

Bossuyt A., et. al., 1981 described the application, to a gamma-ray transmission ventilation investigation, of data processing techniques which were developed for the study of regional cardiac function. Functional images, based on a Fourier transform (Vos P.H., 1981 and Wendt R.E., et. al., 1982), were applied to a series of images that represented an average respiratory cycle. (Wainwright R.J., and Maisey M.N., 1978).

They reported that during slow breathing using preferentially the thoracic musculature, inspiration started at the apices while expiration began at the bases. During slow breathing using preferentially the abdominal musculature, expiration still began at the bases but inspiration occurred simultaneously at the apices and bases. During fast breathing, inspiration and expiration of the apices preceded that of the bases.

Phase shifts in young healthy erect adults were minimal during slow breathing using preferentially the thoracic musculature but became more evident during slow breathing using preferentially the abdominal musculature. During fast breathing, phase shifts were markedly accentuated.

Compared to healthy subjects, patients with lung disease showed larger phase shifts.

2.6 Clinical Results.

Healthy subjects show a gentle gradient of increasing ventilation from apex to base, with the left lung having slightly greater values than the right. The smaller gradient in the right lung may be related to the smaller diaphragmatic movement that takes place on this side. (Secker-Walker R.H., et. al., 1973, Secker-Walker R.H., et. al., 1975 and Miller J.M., et. al., 1970). Amis T.C., 1979 reported that there was no difference between individual right and left lungs. Regional values from six papers are summarised in table (2.1).

In patients with chronic obstructive lung disease the gradient, from apex to base, is reversed (Secker-Walker R.H., et. al., 1975) and a decrease from one zone to one below indicates the presence of a ventilatory defect. (Miller J.M., et. al, 1970).

The mean value for each region in patients with chronic obstructive lung disease is less than the mean value for each comparable region in normal subjects. In patients with obstructive lung disease, the mean value for the apical zone in the left lung is greater than that of the healthy volunteers, while the mean value for both basal zones is lower. (Secker-Walker R.H., et. al., 1975). Regional values from four papers are summarised in table (2.2).

Absolute values of specific ventilation [per second] for the lung as a whole were reported as 0.025 by Rosenzweig D.Y., et. al., 1969 and Amis T.C., 1979 and as 0.015-0.030 by Ciofetta G., et. al., 1980 Amis T.C., 1979 reported values for the upper regions as 0.014 and for the lower as 0.018 while those reported by Rosenzweig D.Y., et. al., 1969 for the upper regions were 0.021 and for the lower regions were 0.023.

Bajzer Z., and Nosil J., 1977 obtained a value for the lung as a whole of 0.0182±0.0004 for a healthy subject. Bajzer Z., and Nosil J., 1980 obtained a value of 0.033±0.002 for the lung as a whole by fitting their model to 18 breathing periods of the data shown in figure (2.1) for a normal subject. They also performed this study on seven normal subjects and obtained a specific ventilation varying between 0.028 and 0.039 with a mean value and standard deviation 0.033±0.003 for the lung as a whole. Spaventi S., et. al., 1978 obtained values from seven healthy subjects for the right (0.023±0.003), left (0.021±0.002) and both lungs taken together (0.022±0.002). Nosil J., et. al., 1977 and Bajzer Z., et. al., 1977 obtained values in four regions: left upper zone (0.016), right upper zone (0.016), left lower zone (0.025) and right lower zone (0.020).

Figure 2.1. Washout data published by Bajzer Z., and Nosil J., 1980.

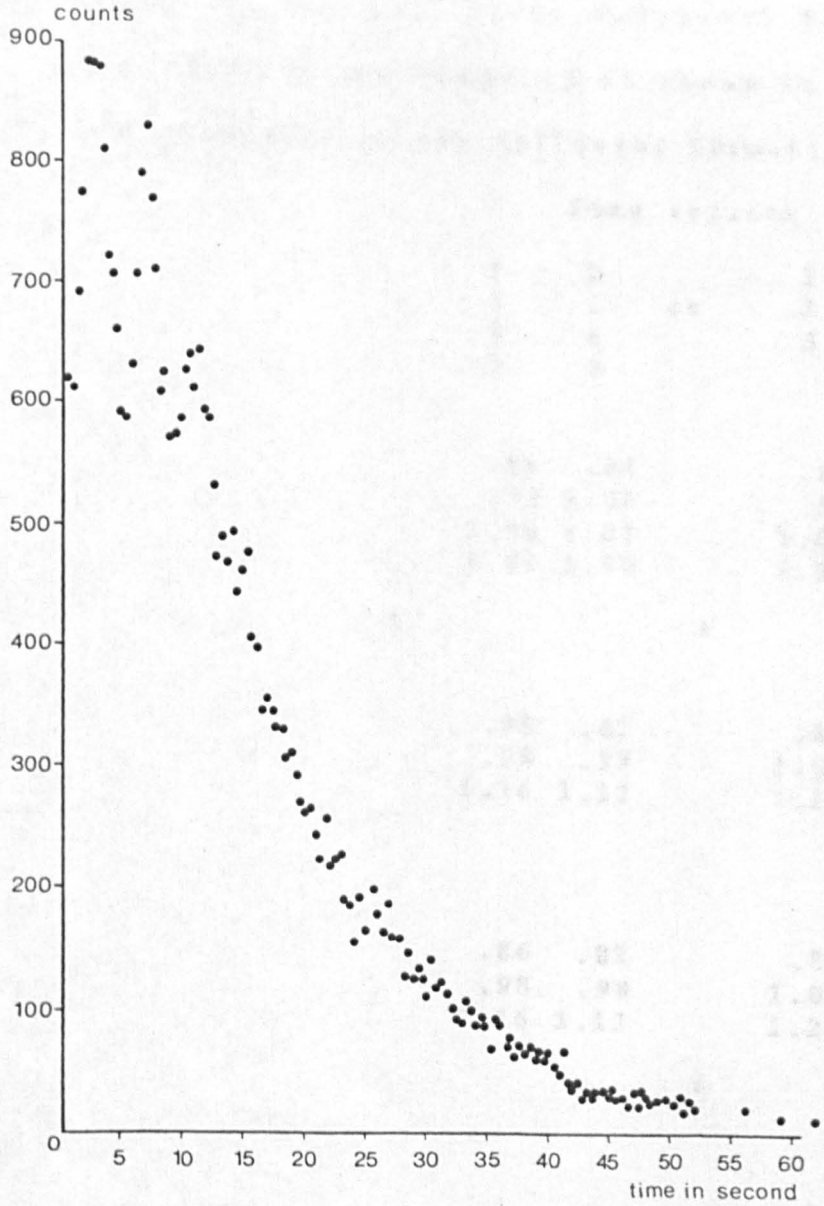

Table 2.1. Published values of regional specific ventilation, displayed as relative indices, for normal subjects from 1:Overton T.R., et. al., 1973, 2:Miller J.M., et. al., 1970, 3:Secker-Walker R.H., et. al., 1975, 4:Loken M.K., et. al., 1969, 5:Konietzko N., et. al., 1970, 6:Mannell T.J., et. al., 1966. Results are numbered as shown in figure (2.2) and displayed in the following format:

Lung regions

1	2		1	2
3	4	or	3	4
5	6		5	6
7	8			

.84	.84		.87	.78
.99	1.00		.96	.89
1.04	1.07		1.06	.98
1.43	1.30		1.29	1.23
1			2	
.83	.82		.80	.79
.98	.98		1.02	1.06
1.16	1.12		1.10	1.15
3			4	
.86	.82		.84	.81
.98	.98		1.05	.90
1.16	1.12		1.23	1.11
5			6	

Table 2.2. Published values of regional specific ventilation, displayed as relative indices, for patients with respiratory disease from 1: Secker-Walker R.H., et. al., 1975 (COAD), 2:Loken M.K., et. al., 1969 (Cystic Fibrosis), 3:Loken M.K., et. al., 1969 (Chronic Bronchitis), 4:Mannell T.J., et. al. 1966 (Not specified). Results are numbered as shown in figure (2.2) and displayed in the following format:

Lung regions

1	2
3	4
5	6

.97	.95		1.06	.78
1.01	.96		1.10	.85
1.03	.91		.94	1.28
1			2	

.88	.87		1.23	1.30
1.05	1.05		1.14	1.02
.83	1.11		.75	.59
3			4	

Figure 2.2. The numbering and position of eight and six lung regions, shown in the postero-anterior orientation.

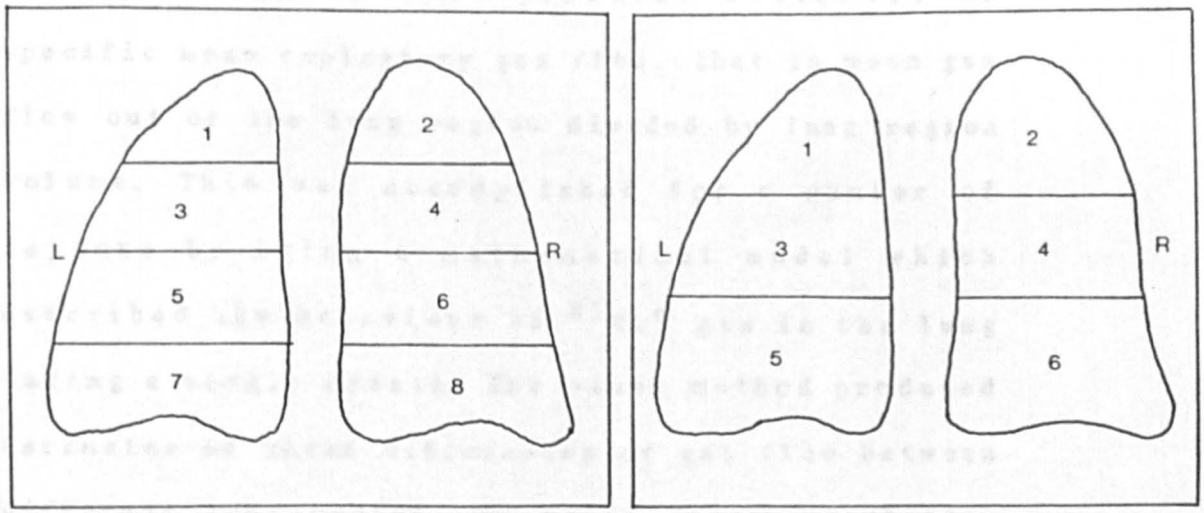

CHAPTER 3 Analysis Techniques.

Two methods of analysing the data available from routine $^{81}Kr^{m}$ inhalation investigations to provide indices of regional lung function were developed. One method produced estimates of specific mean expiratory gas flow, that is mean gas flow out of the lung region divided by lung region volume. This was accomplished for a number of regions by using a mathematical model which described the behaviour of $^{81}Kr^{m}$ gas in the lung during a single breath. The other method produced estimates of phase differences of gas flow between different lung regions by using cross-correlation techniques.

A major consideration during the development of the techniques was that all the information required by the analyses should be available using the protocol normally employed for $^{81}Kr^{m}$ inhalation imaging. This involved imaging during continuous administration of radioactive gas to a subject who was breathing quietly at tidal volumes. It was important that the technique should not require any extra cooperation or any more equipment connected to the patient, because a major reason for the popularity of the routine test has been the simplicity with which a complete study can be undertaken. The information necessary for the calculation of the indices had to be obtained,

therefore, by mathematical manipulation of the available data.

3.1 Mathematical Model.

The behaviour of $^{81}Kr^{m}$ gas in the lung during a single breath was modelled using separate equations to describe the variation in the number of radioactive atoms present in the lung during inspiration and expiration. To derive these equations the same assumptions were made concerning the initial conditions and the composition of the lung as in a previous model which was reported by Winlove C.P., et. al., 1975 for ^{13}N washout data, extended by Bajzer Z., and Nosil J., 1977 for use with $^{81}Kr^{m}$ washout data, by incorporation of a consideration of radioactive decay, and extended further by Bajzer Z., and Nosil J., 1980 to include the periodicity of respiration. The assumptions were that:

1. the lung is represented by a number of lung units in parallel array,
2. a lung unit is a homogeneous compartment of volume V(t) containing N(t) radioactive tracer atoms at time t,
3. the periodicity of respiration is described assuming a variation in lung unit volume with time,

4. gas flow is assumed to result from pressure gradients which produce a flow of gas $\emptyset_i(t)$ into the lung unit during inspiration and a flow of gas $\emptyset_e(t)$ out of the lung unit during expiration,
5. the exhaled gas is discharged into the atmosphere where it is infinitely diluted,
6. mixing in the lung unit is assumed to be complete, and
7. the radioactive decay of the tracer gas in the lung unit is taken into account.

The equations of the model were derived by considering the increase and the decrease in the number of radioactive atoms present in the lung unit during a breathing cycle. The lung unit is represented by the physical model shown in figure (3.1).

Figure 3.1. A Lung Unit and its behaviour during a breathing cycle.

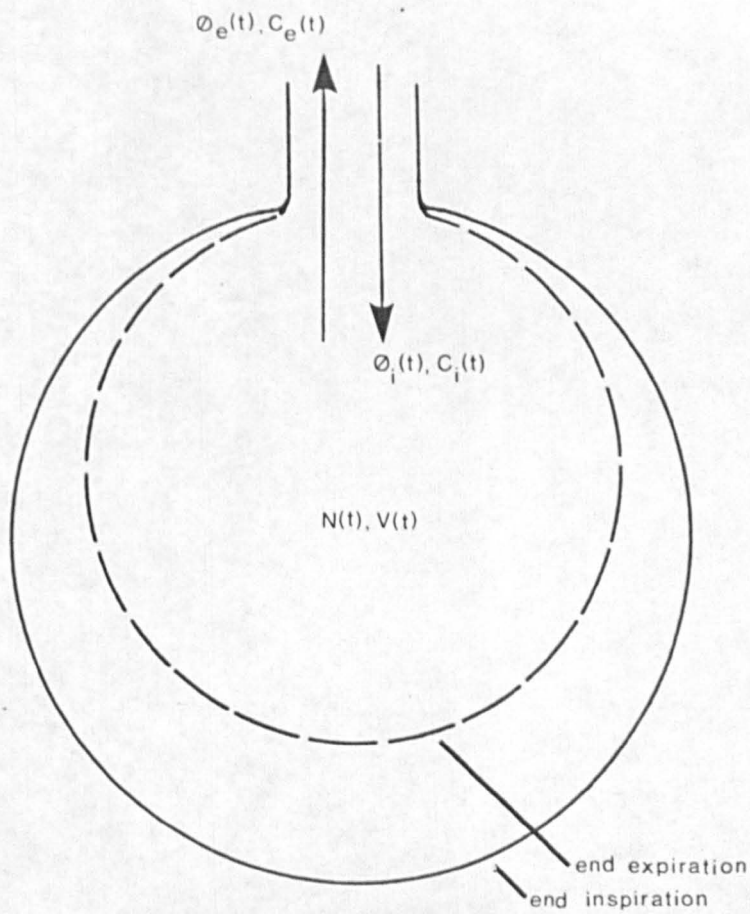

The increase in the number of radioactive atoms in the lung unit, in a small time Δt, caused by inspiration,

$$\Delta N_i = \emptyset_i(t) C_i(t) \Delta t \tag{3.1}$$

and the decrease in the number of radioactive atoms in the lung unit, in a small time Δt, caused by expiration,

$$\Delta N_e = \emptyset_e(t) C_e(t) \Delta t$$

$$= \emptyset_e(t) \frac{N(t)}{V(t)} \Delta t \tag{3.2}$$

Further, the decrease in the number of radioactive atoms in the lung unit, in a small time Δt, caused by radioactive decay,

$$\Delta N_d = \lambda N(t) \Delta t \tag{3.3}$$

where

$C_i(t)$ is the concentration of radioactive gas inspired, [atoms per litre].

$C_e(t)$ is the concentration of radioactive gas expired, [atoms per litre].

$N(t)$ is the number of radioactive atoms present in the lung unit.

$V(t)$ is the volume of the lung unit, [litre]

$\emptyset_i(t)$ is the flow rate of radioactive gas during inspiration, [litre per second].

$\emptyset_e(t)$ is the flow rate of radioactive gas during expiration, [litre per second].

λ is the decay constant of the radioactive gas, [per second].

These equations were combined to describe the behaviour of the radioactive gas during the inspiratory and the expiratory phases. The change in the number of radioactive atoms in the lung unit in a small time Δt, during inspiration,

$$\Delta N(t)=\Delta N_i-\Delta N_d \tag{3.4}$$

$$=\phi_i(t)C_i(t)\Delta t-\lambda N(t)\Delta t \tag{3.5}$$

Differentiating,

$$\frac{dN(t)}{dt}=\phi_i(t)C_i(t)-\lambda N(t) \tag{3.6}$$

Since,

$$\phi_i(t)=\frac{dV(t)}{dt}$$

$$=\dot{V}(t) \tag{3.7}$$

where

$\dot{V}(t)$ is the rate of change of lung unit volume [litre per second].

Then, equation (3.6) becomes,

$$\frac{dN(t)}{dt}=\dot{V}(t)C_i(t)-\lambda N(t) \tag{3.8}$$

The change in the number of radioactive atoms in the lung unit in a small time Δt, during expiration,

$$\Delta N(t)=-\Delta N_e-\Delta N_d \tag{3.9}$$

$$\Delta N(t)=-\phi_e(t)\frac{N(t)}{V(t)}\Delta t-\lambda N(t)\Delta t \tag{3.10}$$

Since,

$$\phi_e(t) = -\frac{dV(t)}{dt}$$

$$= -\dot{V}(t) \qquad (3.11)$$

Equation (3.10) becomes,

$$dN(t) = \dot{V}(t)\frac{N(t)}{V(t)}dt - \lambda N(t)dt \qquad (3.12)$$

Rearranging,

$$\frac{dN(t)}{N(t)} = \frac{dV(t)}{V(t)} - \lambda dt \qquad (3.13)$$

Integrating,

$$\log_e N(t) = \log_e V(t) - \lambda t + k \qquad (3.14)$$

Initial conditions at t=0 give,

$$k = \log_e\left[\frac{N(0)}{V(0)}\right] \qquad (3.15)$$

so that,

$$N(t) = \frac{N(0)}{V(0)}V(t)e^{-\lambda t} \qquad (3.16)$$

where

N(0) is the number of radioactive atoms present in the lung unit at the start of expiration.

V(0) is the volume of the lung unit at the start of expiration, [litre].

Unlike the equation for expiration, equation (3.12), the equivalent equation for inspiration equation (3.8), may not be solved without making further assumptions. During expiration the concentration of radioactive gas leaving the lung unit was taken to be constant, since a lung unit small enough to ensure complete mixing of the tracer gas in the lung unit was assumed. N(t) could, therefore, be related to lung unit volume. During inspiration, however, the concentration of radioactive gas entering the lung unit varied. This variation occurred because of the dead space and because the usual method of administration of $^{81}Kr^{m}$ gas, and the one used during this work, involved a face mask with a small volume which did not provide a reservoir of radioactive gas sufficiently large enough to ensure a constant concentration during an inspiration. N(t) could not therefore, be related to lung unit volume.

Integration of equations (3.8) and (3.16), necessary in order to calculate the number of radioactive atoms present in the lung unit, had to be performed over each phase (inspiration and then expiration) of each breathing cycle and the time variable had to be redefined for each phase. This was because the model considered that gas flow occurred in opposite directions during the inspiratory and the expiratory phases of the

breathing cycle. The history of the lung unit was conveyed to each phase of the analysis by passing the number of radioactive atoms present in the lung unit at end inspiration and end expiration to the subsequent phase of the calculation. A general solution was produced by introducing into the equations n (where n=0,1,2,3,.....), the number of the breathing phase under consideration, as shown in figure (3.2).

The pattern of variation in lung volume substituted into equations (3.8) and (3.16) was determined from spirometry traces obtained at tidal volumes published by Grenvik A., et. al., 1966. These indicated that the breathing pattern of normal subjects could be approximated by single exponential inspiratory and expiratory curves. Although it was probable that this pattern would change in disease, it was not possible to account for every pattern since each required a separate mathematical description to be substituted into the model. An estimate of the effect of changing this pattern, however, was provided by comparing the results obtained by substituting a sinusoidal variation in lung volume with those obtained by substituting the exponential variation in simulation studies.

Figure 3.2. The variation in activity in a Lung Unit as radioactive tracer gas is introduced.

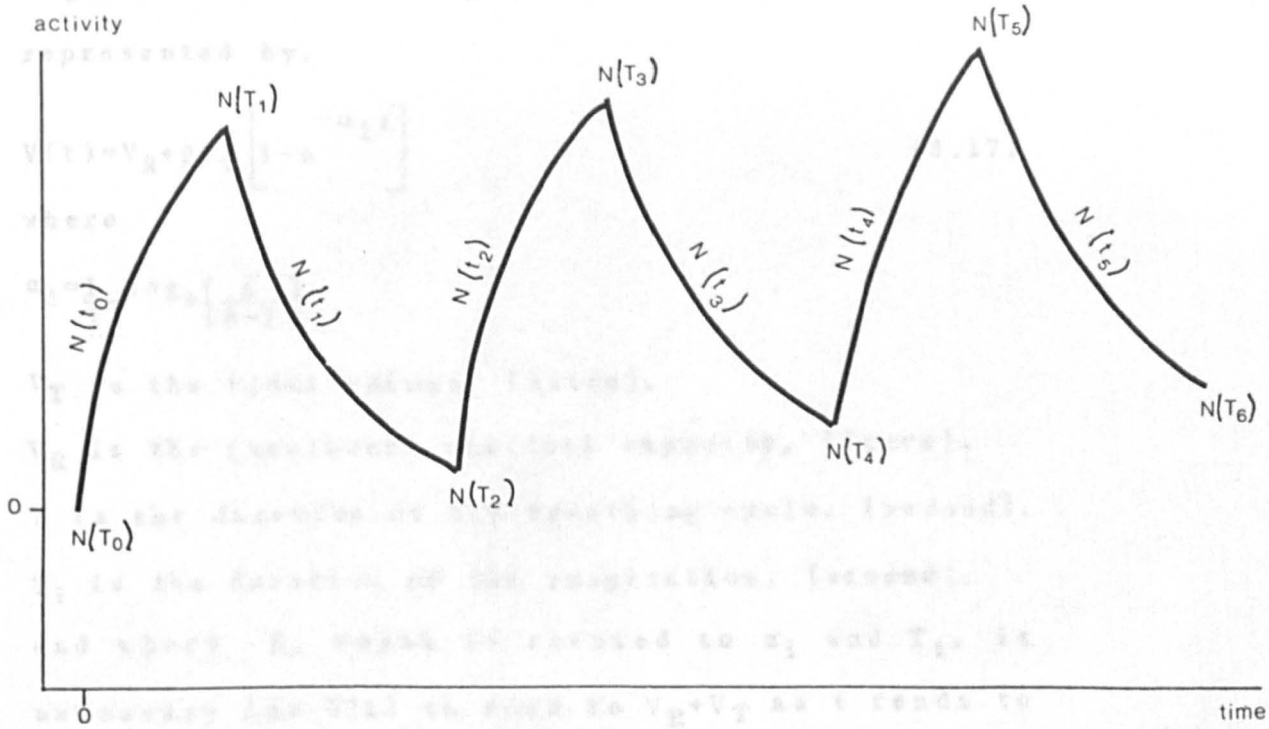

3.1.1 Exponential Variation in Lung Volume.

The exponential variation in lung volume assumed in the following equations is shown in figure (3.3). During inspiration it may be represented by,

$$V(t)=V_R+\beta V_T\left[1-e^{-\alpha_i t}\right] \qquad (3.17)$$

where

$$\alpha_i=\frac{1}{T_i}\log_e\left[\frac{\beta}{\beta-1}\right]$$

V_T is the tidal volume, [litre].

V_R is the functional residual capacity, [litre].

T is the duration of the breathing cycle, [second].

T_i is the duration of the inspiration, [second].

and where β, which is related to α_i and T_i, is necessary for V(t) to tend to V_R+V_T as t tends to T_i.

The value of β affected only the shape of the inspiratory volume curve and not the beginning or the end volume. This is demonstrated in figure (3.4). It did not affect the numerical results obtained from the model analysis and was used only in simulation studies to produce activity-time curves similar to those obtained during clinical studies.

Figure 3.3. The volume-time curve described by a Lung Unit when an exponential variation in lung volume is assumed.

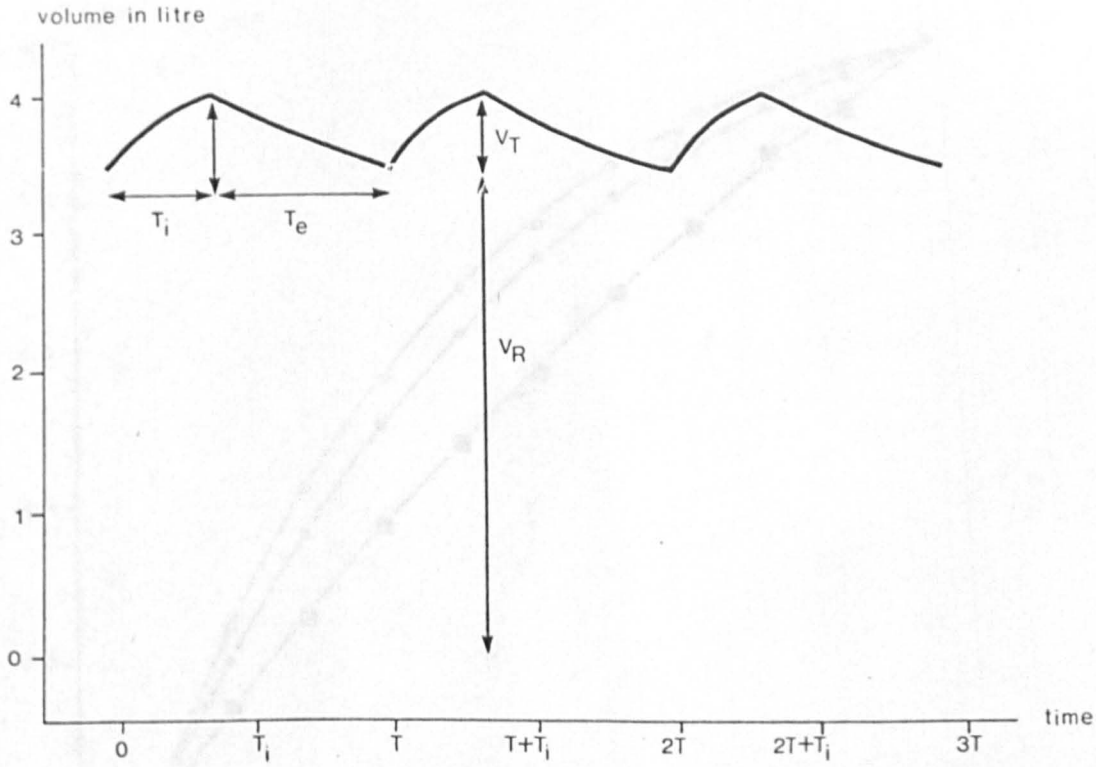

Figure 3.4. Inspiratory lung volume curves calculated from equation (3.17) for values of β of 1.1 (○), 1.2 (●) and 2.0 (■).

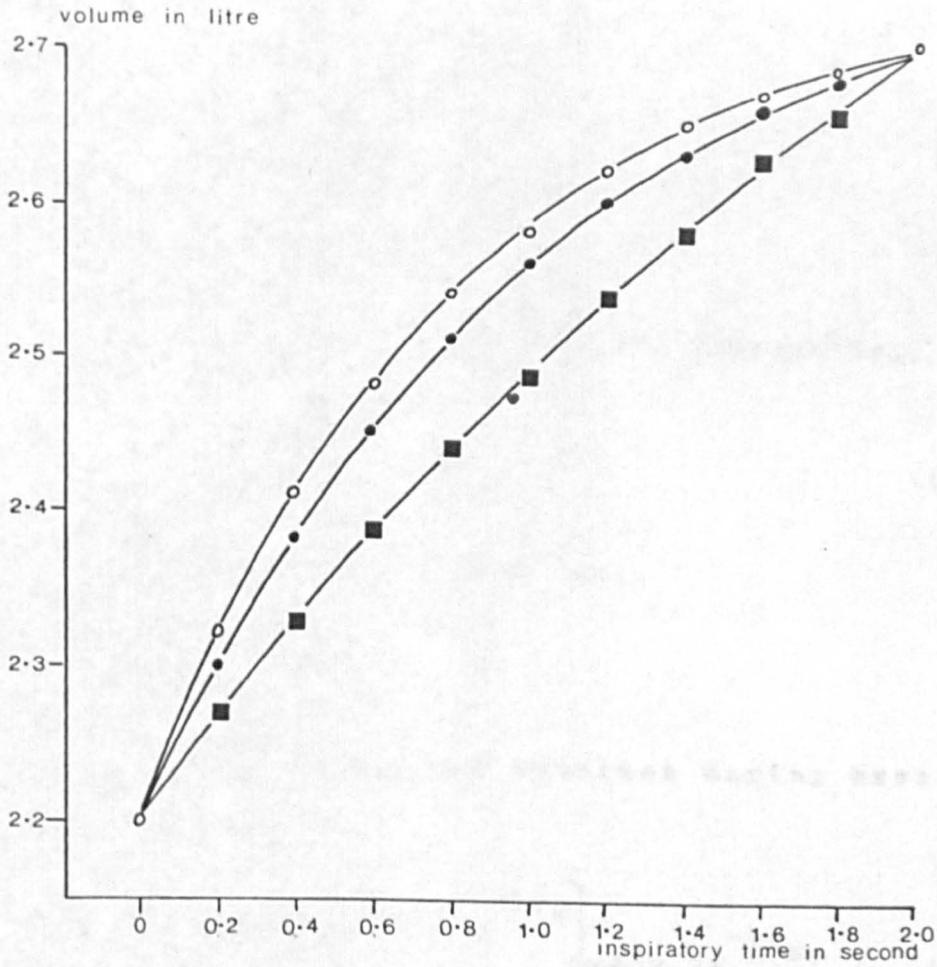

Substituting equation (3.17) into the equation of inspiration (3.8) with the assumption, for the moment, that the concentration of inspired radioactive gas, $C_i(t)$, is a constant, C_i, during the inspiratory period, the number of radioactive atoms present in the lung at time t is obtained,

From equation (3.8),

$$\frac{dN(t)}{dt}=C_i(t)\dot{V}(t)-\lambda N(t) \qquad (3.18)$$

$$N(t)e^{\lambda t}=C_i\int\frac{dV(t)}{dt}e^{\lambda t}dt \qquad (3.19)$$

Substituting equation (3.17) and integrating,

$$N(t)e^{\lambda t}=\frac{C_i\alpha_i\beta V_T e^{-\alpha_i t}}{\lambda-\alpha_i}+k \qquad (3.20)$$

Initial conditions at t=0 give,

$$k=N(T)-\frac{C_i\alpha_i\beta V_T}{\lambda-\alpha_i} \qquad (3.21)$$

Thus, the generalised equation during breathing phase number n,

$$N(t_n)=\frac{C_i\alpha_i\beta V_T}{\lambda-\alpha_i}\left[e^{-\alpha_i t_n}-e^{-\lambda t_n}\right]+N(T_n)e^{-\lambda t_n} \qquad (3.22)$$

n=0,2,4,6,.....

T_n is the time of the previous end expiration, T_{n+1} is the time of the next end inspiration, and $T_n < t_n \leqslant T_{n+1}$.

During expiration the exponential variation in lung volume was represented by,

$$V(t)=(V_R+V_T)e^{-\alpha_e t} \tag{3.23}$$

where

$$\alpha_e=\frac{1}{T_e}\log_e\left[\frac{V_R+V_T}{V_R}\right]$$

and T_e is the duration of the expiration, [second].

Substituting equation (3.23) into the equation of expiration (3.16), the number of radioactive atoms present in the lung at time t during breathing phase number n+1,

$$N(t_{n+1})=N(T_{n+1})e^{-(\alpha_e+\lambda)t_{n+1}} \tag{3.24}$$

$n=0,2,4,6,\ldots\ldots$

T_{n+1} is the time of the previous end inspiration, T_{n+2} is the time of the next end expiration, and $T_{n+1} < t_{n+1} < T_{n+2}$.

3.1.2 Sinusoidal Variation in Lung Volume.

The sinusoidal variation in lung volume assumed in the following equations is shown in figure (3.5). It may be represented by,

$$V(t)=V_R+\frac{V_T}{2}(1-\cos\omega t) \tag{3.25}$$

where,

$$\omega=\frac{2\pi}{T}$$

Substituting equation (3.25) into the equation of inspiration (3.8) again with the assumption, for the moment, that the concentration of inspired radioactive gas, $C_i(t)$, is a constant, C_i, during the inspiratory period, the number of radioactive atoms present in the lung at time t is obtained, From equation (3.8),

$$\frac{dN(t)}{dt}=C_i(t)\dot{V}(t)-\lambda N(t) \tag{3.26}$$

$$\frac{d}{dt}\left[N(t)e^{\lambda t}\right]=C_i\dot{V}(t)e^{\lambda t} \tag{3.27}$$

Substituting the first derivative of equation (3.25),

$$\dot{V}(t)=\frac{V_T}{2}\omega\sin\omega t \tag{3.28}$$

Integrating,

$$N(t)e^{\lambda t}=\frac{C_iV_T\omega}{2}\int\sin\omega t\ e^{\lambda t}dt+k \tag{3.29}$$

Integrating,

$$N(t)e^{\lambda t}=\frac{C_i V_T \omega e^{\lambda t}}{2(\lambda^2+\omega^2)}(\lambda \sin\omega t-\omega\cos\omega t)+k \qquad (3.30)$$

Initial conditions at t=0 give,

$$k=N(T)+\frac{C_i V_T \omega^2}{2(\lambda^2+\omega^2)} \qquad (3.31)$$

Thus, the generalised equation during breathing phase number n,

$$N(t_n)=\frac{C_i V_T \omega}{2(\lambda^2+\omega^2)}(\lambda \sin\omega t_n-\omega\cos\omega t_n)$$

$$+\ N(T_n)+\frac{C_i V_T \omega^2}{2(\lambda^2+\omega^2)}\ e^{-\lambda t_n} \qquad (3.32)$$

where, n=0,2,4,6,.....

T_n is the time of the previous end expiration, T_{n+1} is the time of the next end inspiration, and $T_n < t_n \leqslant T_{n+1}$.

Substituting equation (3.25) into the equation of expiration (3.16), the number of radioactive atoms present in the lung at time t during breathing phase number n+1,

$N(t_{n+1})=$

$$\frac{N(T_{n+1})}{V_R+V_T}\left[V_R+\frac{V_T}{2}(1-\cos\omega t_{n+1})\right]e^{-(\lambda t_{n+1}+\lambda T/2)} \qquad (3.33)$$

where, n=0,2,4,6,.....

T_{n+1} is the time of the previous end inspiration, T_{n+2} is the time of the next end expiration, and $T_{n+1} < t_{n+1} \leqslant T_{n+2}$.

Figure 3.5. The volume-time curve described by a Lung Unit when a sinusoidal variation in lung volume is assumed.

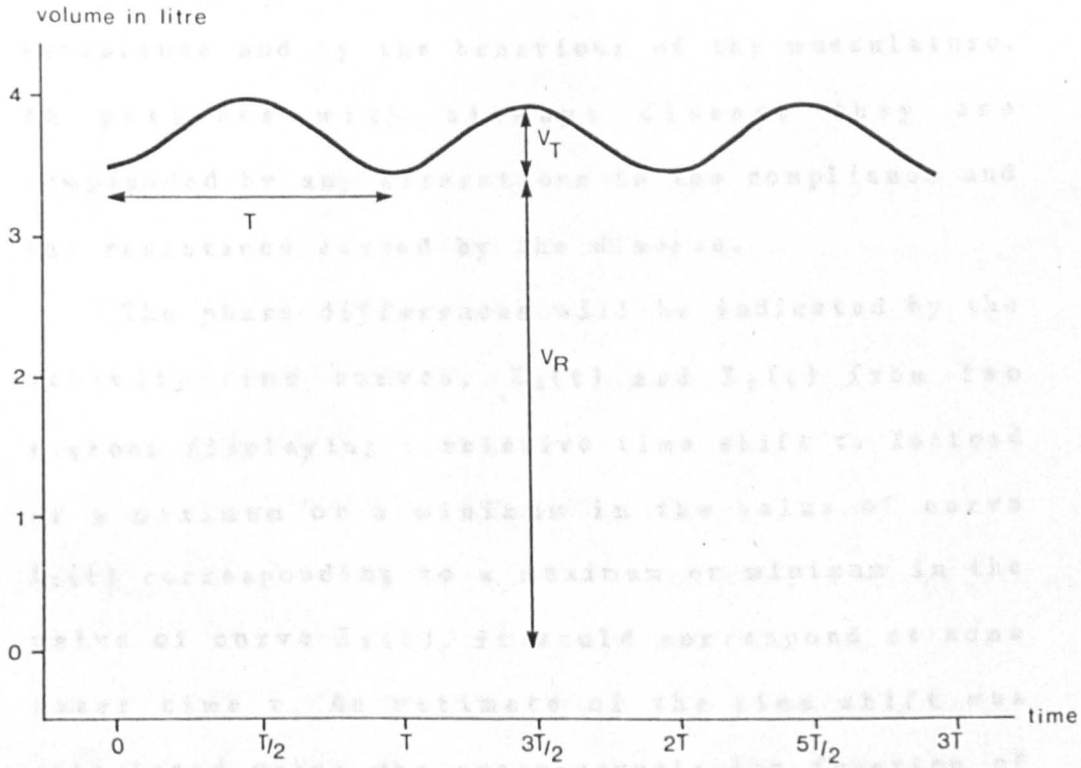

3.2 Cross-Correlation.

As well as exhibiting amplitude variations, different regions of the lung also exhibit phase variations. In normal subjects these are caused by the normal regional variations in compliance and resistance and by the behaviour of the musculature. In patients with airways disease they are compounded by any alterations to the compliance and the resistance caused by the disease.

The phase differences will be indicated by the activity-time curves, $X_1(t)$ and $X_2(t)$ from two regions displaying a relative time shift τ. Instead of a maximum or a minimum in the value of curve $X_1(t)$ corresponding to a maximum or minimum in the value of curve $X_2(t)$, it would correspond at some later time τ. An estimate of the time shift was calculated using the cross-correlation function of the signals $X_1(t)$ and $X_2(t+\tau)$. (Brigham E.O., 1974, Cooper G.R., and McGillem C.D., 1967 and Douce J.L., 1963).

Data were acquired at equilibrium, and therefore, the mean values of the activity signals $X_1(t)$ and $X_2(t+\tau)$ did not vary. The cross-correlation function, assuming an infinite amount of data, could be defined as,

$$\phi_{X_1X_2}(\tau)=\lim_{t\to\infty}\frac{1}{2T}\int_{-T}^{T}X_1(t)X_2(t+\tau)dt \qquad (3.34)$$

The time displacement when the two signals

achieve their maximum correlation was found by moving one curve with respect to the other curve used as a reference.

The continuous equation of the cross-correlation function was altered to describe the discrete process of the activity-time curves,

$$\phi_{X_1X_2}(kT) = \frac{1}{n}\sum_{i=1}^{n} X_1(iT)X_2[(i+k)T] \qquad (3.35)$$

where k is the number of points of the test curve shifted with respect to the reference curve, T is the time interval between points, n is the total number of points in each curve and $n \gg k$.

The following equations were used to determine the position of maximum cross-correlation.

The equation used when the test activity-time curve was advanced in time against the reference activity-time curve, when k was greater than or equal to zero,

$$\phi_{X_1X_2}(kT) = \frac{1}{n-k}\sum_{i=1}^{n-k} X_1(iT)X_2[(i+k)T] \qquad (3.36)$$

where n-k is the number of overlapping points in the curves.

The equation used when the test activity-time curve was delayed in time against the reference activity-time curve, when k was less than or equal to zero,

$$\phi_{X_1X_2}(kT) = \frac{1}{n+k}\sum_{i=k+1}^{n} X_1(iT)X_2[(i-k)T] \qquad (3.37)$$

where n+k is the number of overlapping points in

the curve.

In order to compare the cross-correlation values and find the time of the maximum cross-correlation, the equations were normalised. Since as k, the number of points moved, increased $\emptyset_{X_1X_2}(kt)$ became smaller because of the fewer overlapping points.

3.3 Data.

The model analysis concerned only the activity variation over a single breath but the statistics of the single breath data were so poor that a series of sequential breaths had to be acquired in the form of activity-time curves obtained at equilibrium during tidal breathing.

Superimposed onto these traces was Poisson noise of radioactive decay. Since the standard deviation of this is equal to the square root of the activity, the higher the activity the better the signal to noise ratio. The activity was limited by the amount of gas which could be eluted from the generator. This problem was exaggerated when the lung was divided into regions and the data acquisition frequency was increased.

3.3.1 Model Application.

The expiratory equation only of the mathematical model was used in the analysis. To use the inspiratory equation a description of the variation in the radioactive gas concentration

during an inspiration would be required. This was not possible because of the re-inspiration previously exhaled radioactive gas in the dead space. Expiration was also chosen because it is the passive part of the breathing cycle and is influenced by the elastic recoil of the lung parenchyma.

Initially, the model was applied to the expiratory phase of each breath in the activity-time curve. This produced too many values for practical interpretation, approximately 30 per patient per study, and the values varied considerably because of poor counting statistics. Therefore, before application of the mathematical model, a series of similar cycles were averaged. The averaging procedure consisted of identifying the individual breaths in the activity-time curve and averaging those which were similar. Atypical breathing cycles, corresponding to irregular breathing volumes, either too short or too long, were omitted.

The statistical fluctuations of the activity-time curve were reduced by smoothing using a three-point linear average. This replaced the mid-point of three with their arithmetic mean. A smoothed curve was obtained by moving this low pass filter from the beginning to the end of the original

curve. The smoothed curve was then smoothed a second time.

The positions of activity maxima and minima in the smoothed curve were identified by searching from beginning to end for reversals in the gradient of the activity variation. The average durations of both the inspiratory and the expiratory phases were then calculated. The curve was searched a second time to exclude atypical breathing cycles. Only those breaths whose inspiratory and expiratory phases had durations within ± 0.50 of their means were retained.

Having identified the positions of those breathing cycles which satisfied the acceptance criteria, the remainder of the analysis was conducted on the original unsmoothed activity-time curve.

Because the duration of the single breaths varied slightly, the data had to be centred before an average breath could be constructed. Two series of single breaths were therefore produced from the original activity-time curve, one series were centred on activity maxima and the other series were centred on activity minima. Two series were produced because there was a possibility that the shape of the breathing cycle would influence the repeatability with which the position of an activity maximum or an activity minimum could be

identified.

The limit of each breath was extended to include some of the data points from adjacent breaths, as shown in figures (3.6) and (3.7), in order to reduce noise in the following mathematical manipulations. Each series of single breaths was then summed to form an average breath.

An extension to this averaging procedure was attempted in order to reduce the effect Poisson noise had on the identification of activity maxima and minima. The single breaths were cross-correlated with their average to obtain the time shift at which a maximum in the cross-correlogram occurred. A correlated average was then constructed for the time displaced single breaths.

Both curves were first processed by subtracting a value from each data point so that the activity at the end points approximated to zero, as shown in figure (3.8). This was to reduce the effect on the cross-correlogram of any error in the identifiction of the end points.

Figure 3.6. A single breath activity-time curve centred on an activity maximum, showing extra data points included at each side to improve the accuracy of the mathematical analysis.

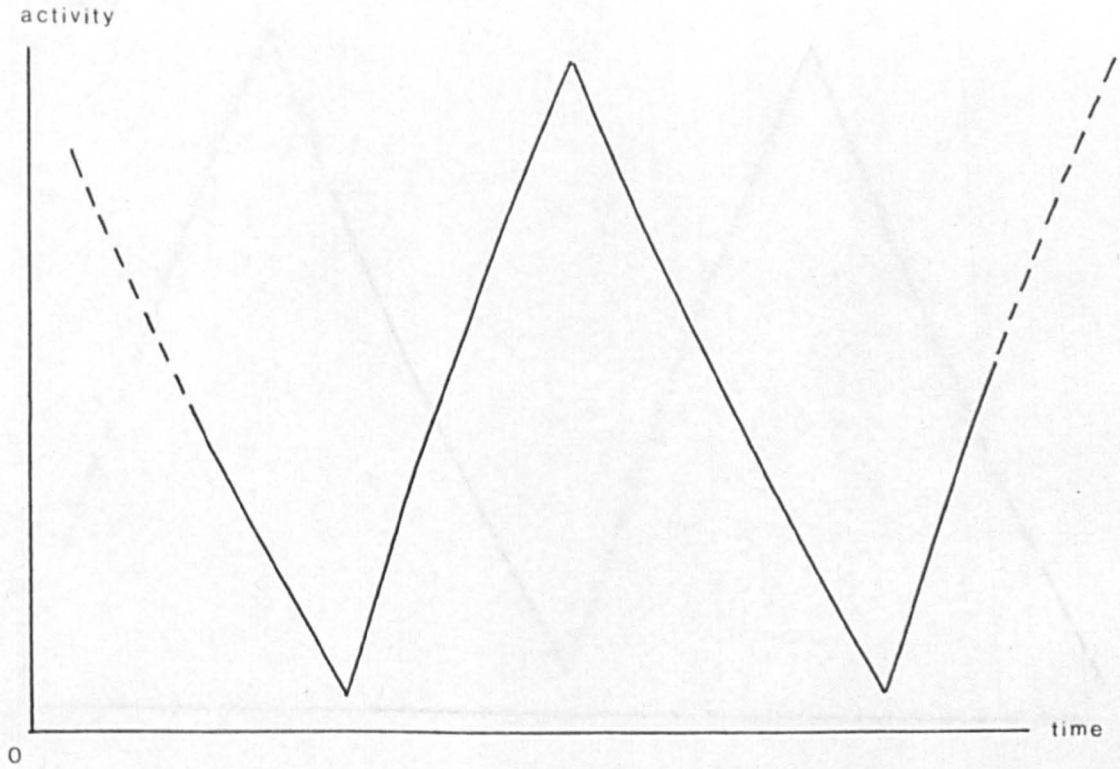

Figure 3.7. A single breath activity-time curve centred on an activity minimum, showing extra data points included at each side to improve the accuracy of the mathematical analysis.

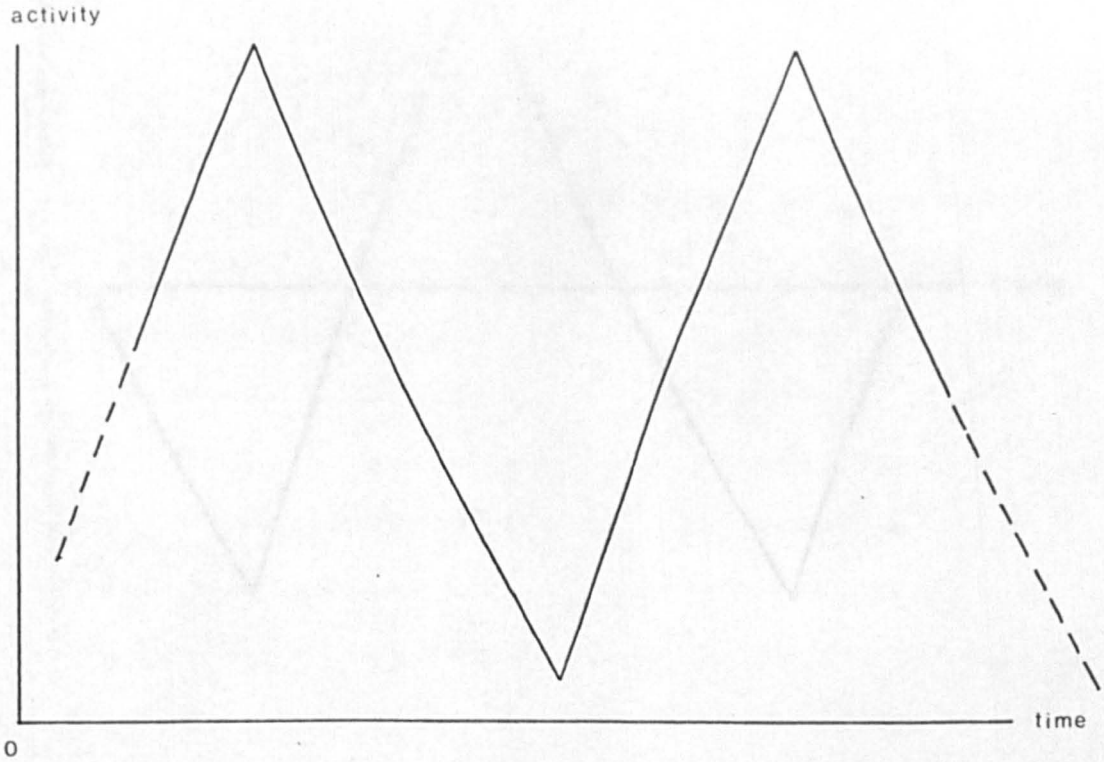

Figure 3.8. A single breath activity-time curve processed so that the activity varies about zero.

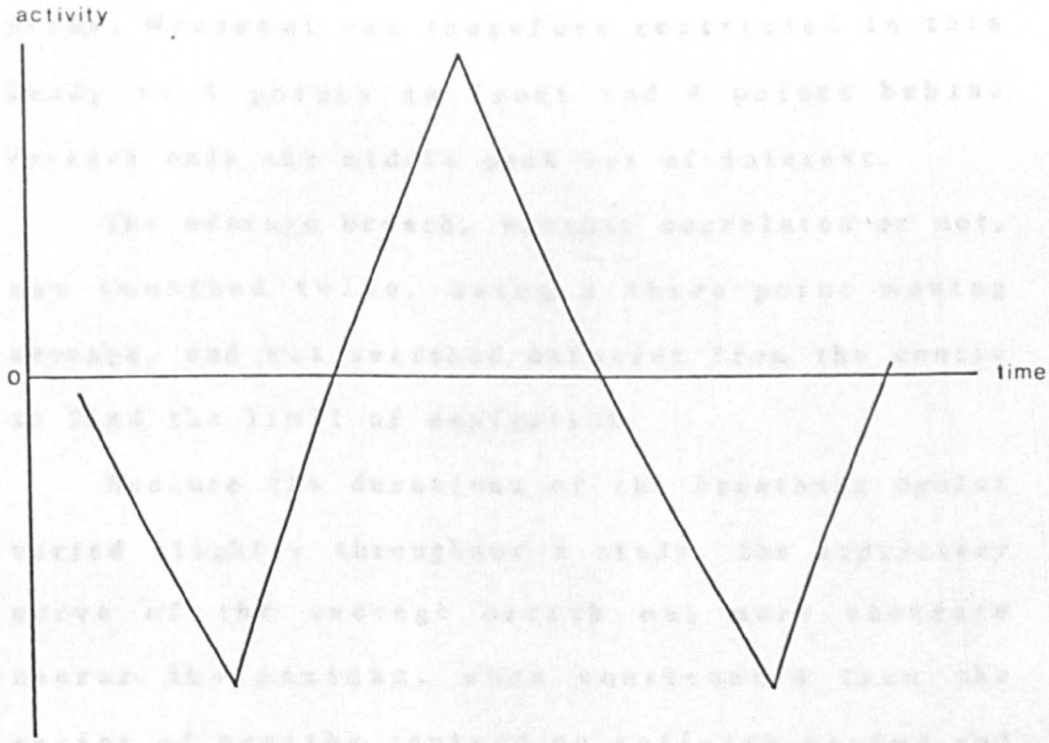

Figure (3.9) shows the cross-correlogram of a simulated noiseless single breath moved across a simulated noiseless average. It can be seen from this graph that there is a middle peak and two side peaks. Movement was therefore restricted in this study to 4 points in front and 4 points behind because only the middle peak was of interest.

The average breath, whether correlated or not, was smoothed twice, using a three-point moving average, and was searched outwards from the centre to find the limit of expiration.

Because the durations of the breathing cycles varied slightly throughout a study, the expiratory curve of the average breath was more accurate nearer the maximum, when constructed from the series of breaths centred on activity maxima and was more accurate nearer the minimum when constructed from the series of breaths centred on activity minima. Composite expiration curves were therefore constructed, as shown in figure (3.10), by combining the points nearest the maximum from the average breath constructed from the series of breaths centred on activity maxima with the points nearest the minima from the average breath constructed from the series of breaths centred on activity minima.

Figure 3.9. A cross-correlogram constructed for a noiseless single breath activity-time curve moved across a noiseless average single breath.

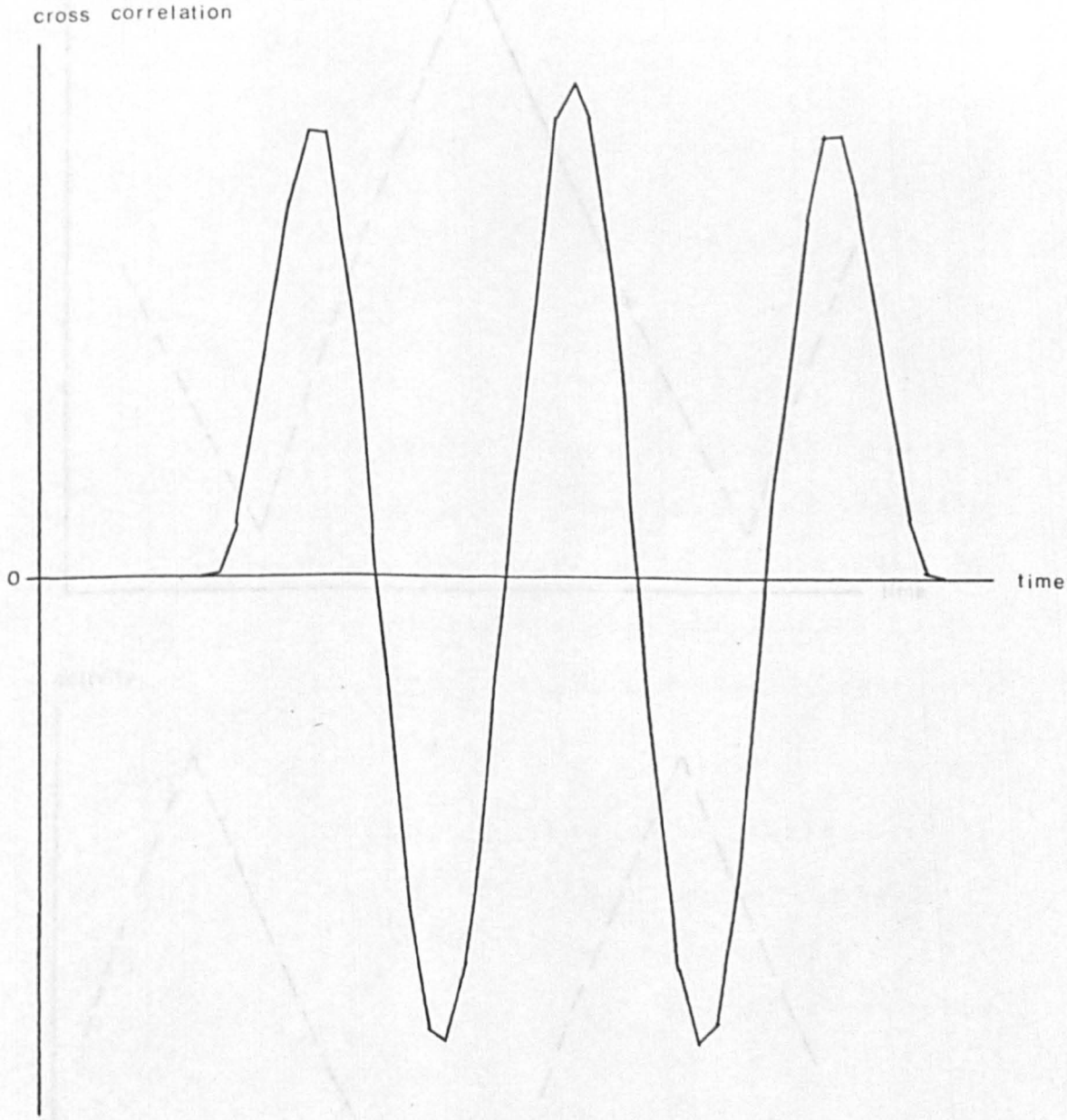

Figure 3.10. The parts of the expiratory phases, shown as continuous lines, which were used to construct composite expiration curves.

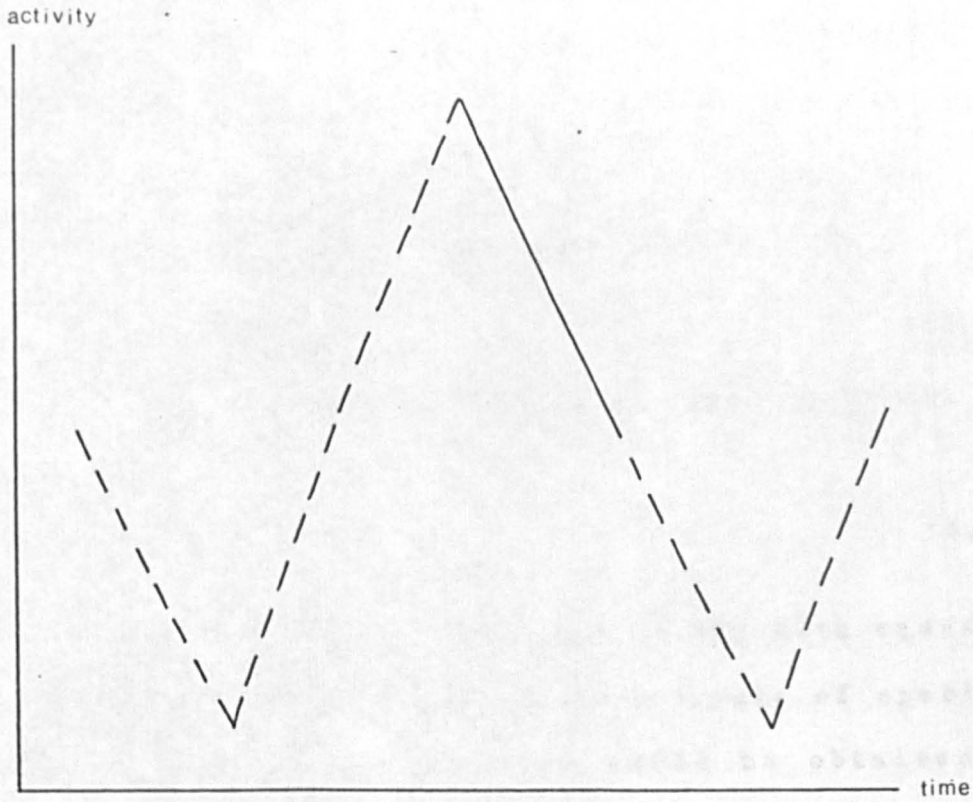

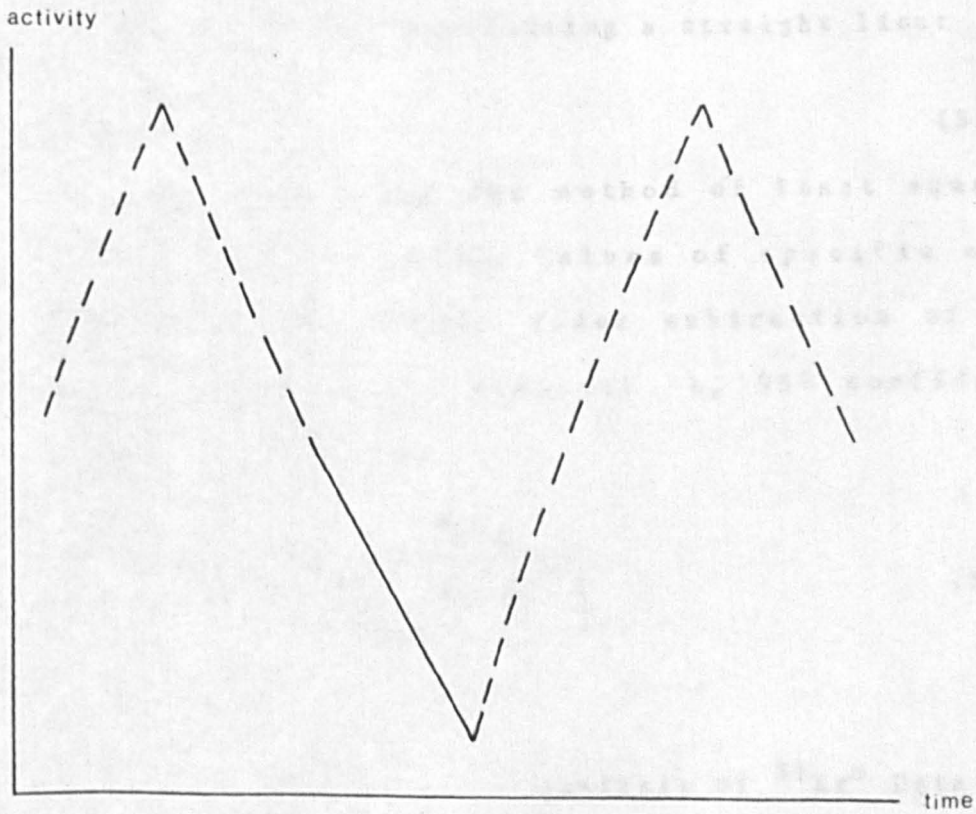

Equation (3.12) was rearranged to make it suitable for application to the six expiratory curves and the exponential variation in lung volume, described by equation (3.23), was assumed for the reasons described in the last paragraph of section (3.1). An expression in specific mean expiratory gas flow during an expiration, was obtained by differentiating equation (3.23):

$$\dot{V}(t)=-\alpha_e(V_R+V_T)e^{-\alpha_e t} \tag{3.38}$$

and dividing equation (3.38) by equation (3.23),

$$\frac{\dot{V}(t)}{V(t)}=-\alpha_e \tag{3.39}$$

Comparison of this equation (3.39) with equation (3.24) demonstrated that an estimate of specific mean expiratory gas flow could be obtained by taking natural logarithms of the data points on the expiratory curve, and fitting a straight line:

$$\bar{y}=\hat{a}_0+\hat{a}_1 x \tag{3.40}$$

to this data using the method of least squares (Chatfield C., 1975). Values of specific mean expiratory gas flow, after subtraction of the radioisotope decay constant λ, 95% confidence limits cl, given by,

$$cl=t_{0.025,n-2}\frac{s_{y/x}}{\sqrt{\left[\sum_{i=1}^{n}(x_i-\bar{x})^2\right]}} \tag{3.41}$$

where

$$s^2_{y/x}=\frac{\sum_{i=1}^{n} y^2_i-\hat{a}_0\sum_{i=1}^{n} y_i-\hat{a}_1\sum_{i=1}^{n} x_i y_i}{n-2}$$

and coefficient of determination r, given by,

$$r=\frac{\sum_{i=1}^{n} (\hat{y}_i-\bar{y})^2}{\sum_{i=1}^{n} (y_i-\bar{y})^2} \qquad (3.42)$$

were obtained. The coefficient of determination estimated how well the straight line fitted the logarithmic data, its maximum value was 1.00, which indicated that all the data points lay on the straight line. For the number of points on the curves, approximately 10, a value of 0.66 indicated that most of the data points lay reasonably near the straight line and a value of 0.80 indicated that most of the data points lay very near to the straight line.

3.3.2 Cross-Correlation Application.

The cross-correlation techniques used for the phase analysis were applied to the unsmoothed multiple breath activity-time curves. The only pre-processing undertaken was the subtraction of a value from each data point such that the average value of each curve approximated zero. The curve from one region was used as reference and the curve from another region was moved across it to construct the cross-correlogram.

CHAPTER 4 Simulation Studies.

Simulation studies were undertaken to assess the adequacy of the mathematical model and the susceptibility of both the model and the cross-correlation analyses to the effects of Poisson noise.

The adequacy of the mathematical model was assessed by simulating washin, equilibrium and washout activity-time curves, using the model, for different values of a number of physiological parameters. The equilibrium activity levels obtained were compared to those calculated, for the same values of the physiological parameters, using equation (2.1) published by Fazio F., and Jones T., 1975. The washout curves were analysed, using techniques published by Ciofetta G., et. al., 1980, Spaventi S., et. al., 1978 and Bajzer Z., and Nosil J., 1980 reviewed in section (2.4), to obtain values of specific ventilation which were compared to values predicted by two mathematical descriptions of specific ventilation.

The susceptibility of the analyses to the effects of Poisson noise was assessed by simulating equilibrium activity-time curves, using the model, for a number of activity levels. Poisson noise was superimposed on these curves and the analysis techniques were applied to retrieve the simulation variables. The results were used to indicate the

lowest activity levels for which the techniques could provide reliable information.

4.1 Simulation.

The activity-time curves used in the simulation studies were generated for both an exponential and a sinusoidal variation in lung volume. Data points were calculated every 0.2 second, consistent with data acquisition during clinical studies, using equations (3.22), (3.24), (3.32) and (3.33), as described in Appendix I Simulation Programming.

A number of curves were generated for different values of the following variables, which were assumed to be constant during each curve:

C_i: The concentration of the radioactive tracer gas breathed into the lungs. The value of this variable was adjusted to alter the activity level of the simulated curve, as explained later in the text.

T: The duration of the breathing cycle. It was usually specified to be 4 or 5 seconds which gave a respiratory rate of 15 and 12 breaths per minute.

V_T: Tidal volume. The lung volume change during a single respiratory manouevre in quiet breathing. It was usually specified to be one of: 0.3, 0.4, 0.5 or 0.6 litre which provided

a variation around the normal value of 0.5 litre (Cotes J.E., 1975).

V_R: Functional residual capacity. The lung volume remaining at end expiration in quiet breathing. This was usually specified to be one of: 1.8, 2.0, 2.2, 2.8, 3.5, 4.2 litre which provided a variation around the normal value of 3.5 litre for a healthy man of height 1.72 metre, age 30 years and weight 70 kilogramme (Cotes J.E., 1975).

The values of V_T and V_R were chosen as representative of the volumes of both lungs taken together. For regional volumes, comparably smaller values could be specified. If, however, the values were in the same proportion as those representing total lung volumes similar results would be produced by the simulation.

For a simulation assuming an exponential variation in lung volume, two additional variables were specified.

R: The ratio of the durations of expiration and inspiration. In quiet breathing, inspiratory time is shorter than expiratory time. The ratio was usually specified to be 2.0 which, for a 4 second duration, would give an inspiratory duration of 1.4 seconds and an expiratory duration of 1.6 second, when rounded to the nearest 0.2 second data

interval.

β: The factor which determines the shape of the inspiratory volume-time curve. It was usually specified to be 1.1 for the reasons described in section (3.1.1) and in order to produce simulated activity-time curves which resembled those obtained during clinical studies.

4.2 Adequacy of the Model.

The behaviour of the mathematical model was investigated under ideal conditions using equilibrium activity-time curves simulated assuming a high inspiratory concentration of radioactive tracer gas and without superimposed Poisson noise. C_i was set at 3000 counts per 0.2 seconds per litre of air inspired. This produced equilibrium activity levels which approximated to the highest observed during clinical studies.

The effect of the breathing pattern on the results obtained from the analysis was assessed by assuming both an exponential and a sinusoidal variation in lung volume.

4.2.1 Washin.

Washin activity-time curves were simulated over a number of breathing cycles, from an initial condition of zero radioactive gas in the lungs until the equilibrium activity level was attained. Typical curves are shown in figure (4.1) for an exponential variation in lung volume and in figure (4.2) for a sinusoidal variation in lung volume. The equilibrium activity levels are indicated in these figures by the horizontal lines.

A number of equilibrium activity levels were calculated for the model and for the equilibrium equation of Fazio F., and Jones T., 1975,

$$N(t) \propto \frac{\dot{V}}{\frac{\dot{V}}{V}+\lambda} = \frac{k\dot{V}}{\frac{\dot{V}}{V}+\lambda} \qquad (4.1)$$

k is the constant of proportionality and includes the efficiency of detection of the radioactivity in the lung. A value of k was chosen which produced activity levels similar to those predicted by the model.

Assuming certain values for the constants of proportionality does not affect the assessment of the validity of the model because the important measurement is the variation in activity levels for different values of the physiological parameters.

Figure 4.1. A simulated washin to equilibrium activity-time curve for parameter values: C_i=3000, V_T=0.5, V_R=2.2, T=4, R=1:2 and β=1.1, assuming an exponential variation in lung volume. The mean equilibrium activity level is indicated by the horizontal line.

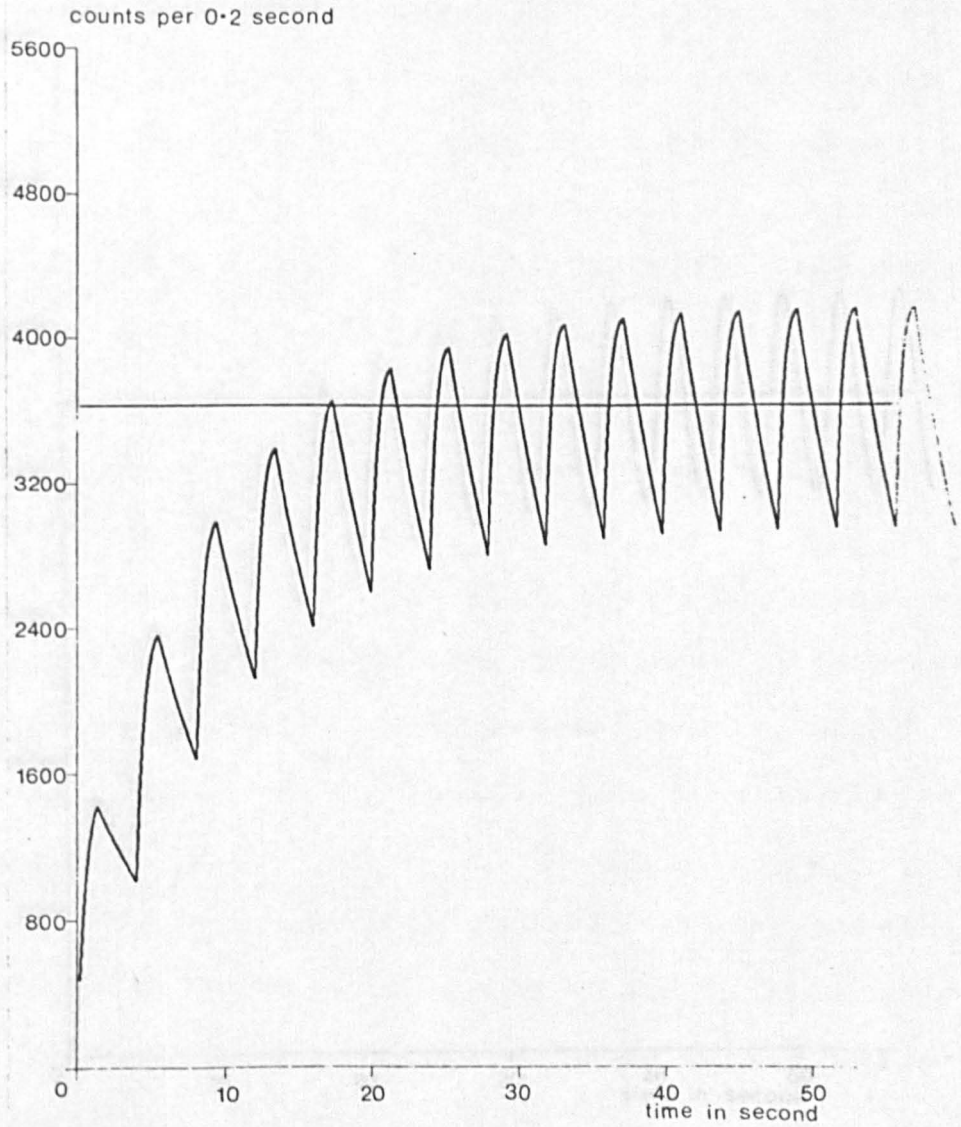

Figure 4.2. A simulated washin to equilibrium activity-time curve for parameter values: C_i=3000, V_T=0.5, V_R=2.2, T=4, assuming a sinusoidal variation in lung volume. The mean equilibrium activity level is indicated by the horizontal line.

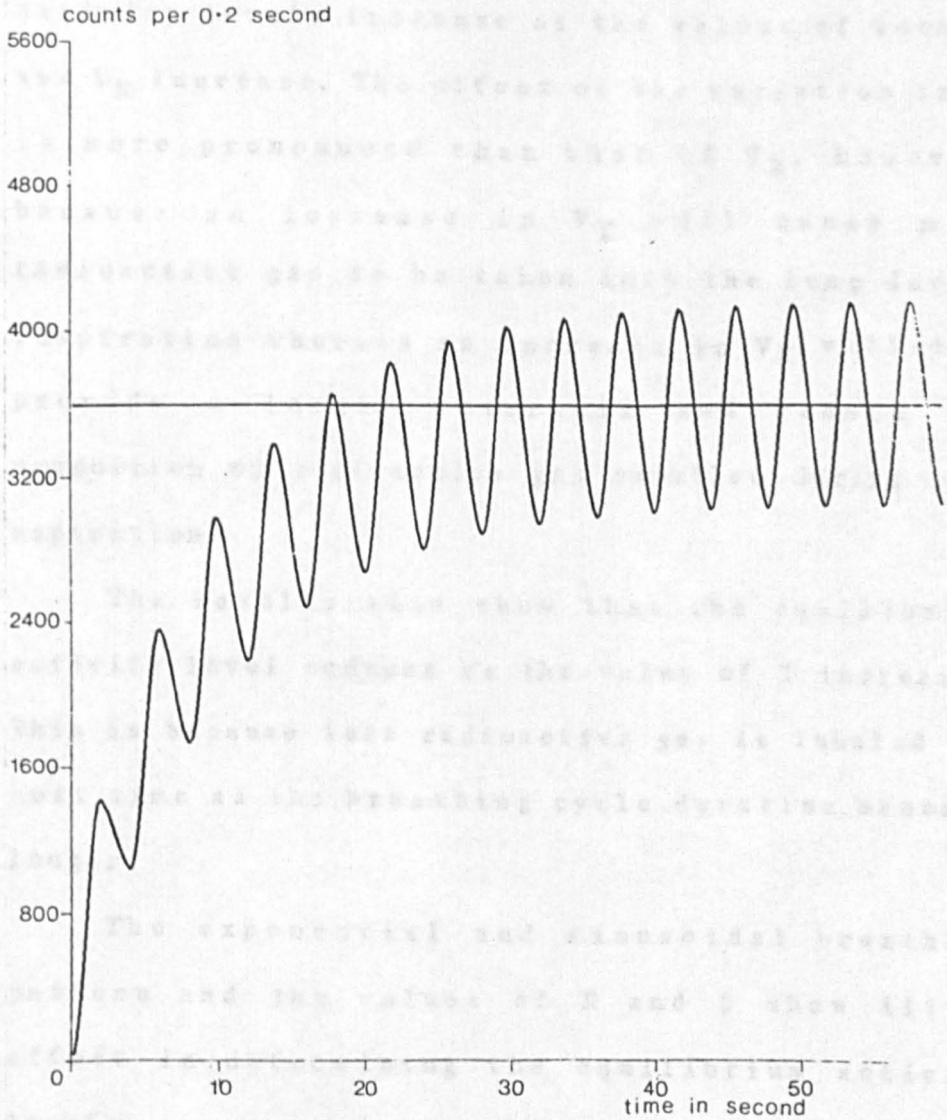

Equilibrium activity levels [in counts per 0.2 second] are shown in table (4.1) for a breathing cycle duration of 4 seconds and in table (4.2) for a breathing cycle duration of 5 seconds. Values obtained from equation (4.1) and from the model assuming both an exponential and a sinusoidal variation in lung volume are listed against the values of the physiological parameters, V_T and V_R.

These results demonstrate that the equilibrium activity levels increase as the values of both V_T and V_R increase. The effect of the variation in V_T is more pronounced than that of V_R, however, because an increase in V_T will cause more radioactive gas to be taken into the lung during inspiration whereas an increase in V_R will only provide a larger reservoir and reduce the proportion of radioactive gas expelled during each expiration.

The results also show that the equilibrium activity level reduces as the value of T increases. This is because less radioactive gas is inhaled per unit time as the breathing cycle duration becomes longer.

The exponential and sinusoidal breathing pattern and the values of R and β show little effect in determining the equilibrium activity levels.

Table 4.1. Equilibrium activity levels [counts per 0.2 second] obtained from equation (4.1) and from the mathematical model for T=4 seconds. Results are listed against values of V_R and V_T [litre], and for both a sinusoidal (S) and an exponential (E) variation in lung volume.

				R= 1	1	2
				β= 1.1	1.2	1.1
V_R	V_T	(4.1)	(S)	(E)	(E)	(E)
1.8	0.3	2452	2457	2487	2479	2475
	0.4	2936	2912	2958	2947	2940
	0.5	3357	3294	3356	3340	3331
	0.6	3736	3625	3703	3682	3670
2.0	0.3	2544	2555	2584	2577	2573
	0.4	3057	3045	3089	3078	3072
	0.5	3503	3456	3516	3501	3492
	0.6	3903	3813	3889	3869	3857
2.2	0.3	2627	2643	2671	2664	2661
	0.4	3168	3166	3208	3197	3192
	0.5	3638	3605	3663	3649	3640
	0.6	4058	3987	4060	4041	4030
2.8	0.3	2833	2859	2883	2877	2874
	0.4	3449	3467	3505	3496	3491
	0.5	3986	3986	4038	4025	4018
	0.6	4466	4437	4505	4488	4479
3.5	0.3	3014	3046	3066	3061	3059
	0.4	3705	3737	3770	3762	3758
	0.5	4311	4334	4381	4370	4364
	0.6	4855	4860	4921	4906	4898
4.2	0.3	3153	3186	3204	3200	3198
	0.4	3906	3946	3975	3968	3965
	0.5	4573	4611	4653	4643	4637
	0.6	5173	5201	5257	5244	5236

Table 4.2. Equilibrium activity levels [counts per 0.2 second] obtained from equation (4.1) and from the mathematical model for T=5 seconds. Results are listed against values of V_R and V_T [litre], and for both a sinusoidal (S) and an exponential (E) variation in lung volume.

				R= 1	1	2
				β= 1.1	1.2	1.1
V_R	V_T	(4.1)	(S)	(E)	(E)	(E)
1.8	0.3	2140	2077	2103	2098	2160
	0.4	2596	2504	2543	2534	2602
	0.5	2998	2868	2920	2908	2980
	0.6	3363	3187	3254	3238	3312
2.0	0.3	2210	2148	2173	2168	2234
	0.4	2690	2602	2640	2632	2705
	0.5	3114	2991	3042	3031	3109
	0.6	3497	3333	3398	3383	3464
2.2	0.3	2272	2210	2234	2230	2299
	0.4	2776	2690	2726	2719	2797
	0.5	3220	3103	3152	3142	3225
	0.6	3621	3467	3530	3516	3603
2.8	0.3	2424	2360	2381	2378	2456
	0.4	2989	2907	2939	2933	3023
	0.5	3490	3384	3428	3419	3518
	0.6	3943	3807	3864	3852	3956
3.5	0.3	2556	2486	2505	2502	2589
	0.4	3179	3095	3124	3119	3221
	0.5	3736	3633	3674	3666	3779
	0.6	4242	4116	4169	4158	4279
4.2	0.3	2655	2579	2597	2594	2688
	0.4	3327	3237	3264	3260	3371
	0.5	3932	3827	3864	3857	3982
	0.6	4484	4360	4409	4399	4535

To facilitate simple comparison, the results are shown in figure (4.3) plotted against specific ventilation. Specific ventilation was calculated from the values of the physiological variables used in the simulation of the activity-time curves according to the definition,

$$SV=\frac{V_T}{T(V_T+V_R)} \qquad (4.2)$$

Figure (4.3) indicates that the model predicts a similar variation in the equilibrium activity levels in the lung, for both the exponential and the sinusoidal variation in lung volume, as equation (4.1). This demonstrates both the adequacy of the model and the dependence of the equilibrium activity levels on functional residual capacity as well as on tidal volume. Both these parameters are involved in the description of specific ventilation in equation (4.2) and it is apparent from the figure that multiple equilibrium activity levels are possible for the same value of specific ventilation.

Figure 4.3. Equilibrium activity levels plotted against values of specific ventilation calculated from equation (4.2), determined from equation (4.1)(■) and from the mathematical model assuming both an exponential (○) and a sinusoidal (●) variation in lung volume. Parameter values: C_i=3000, T=4, R=1:2 and β=1.1.

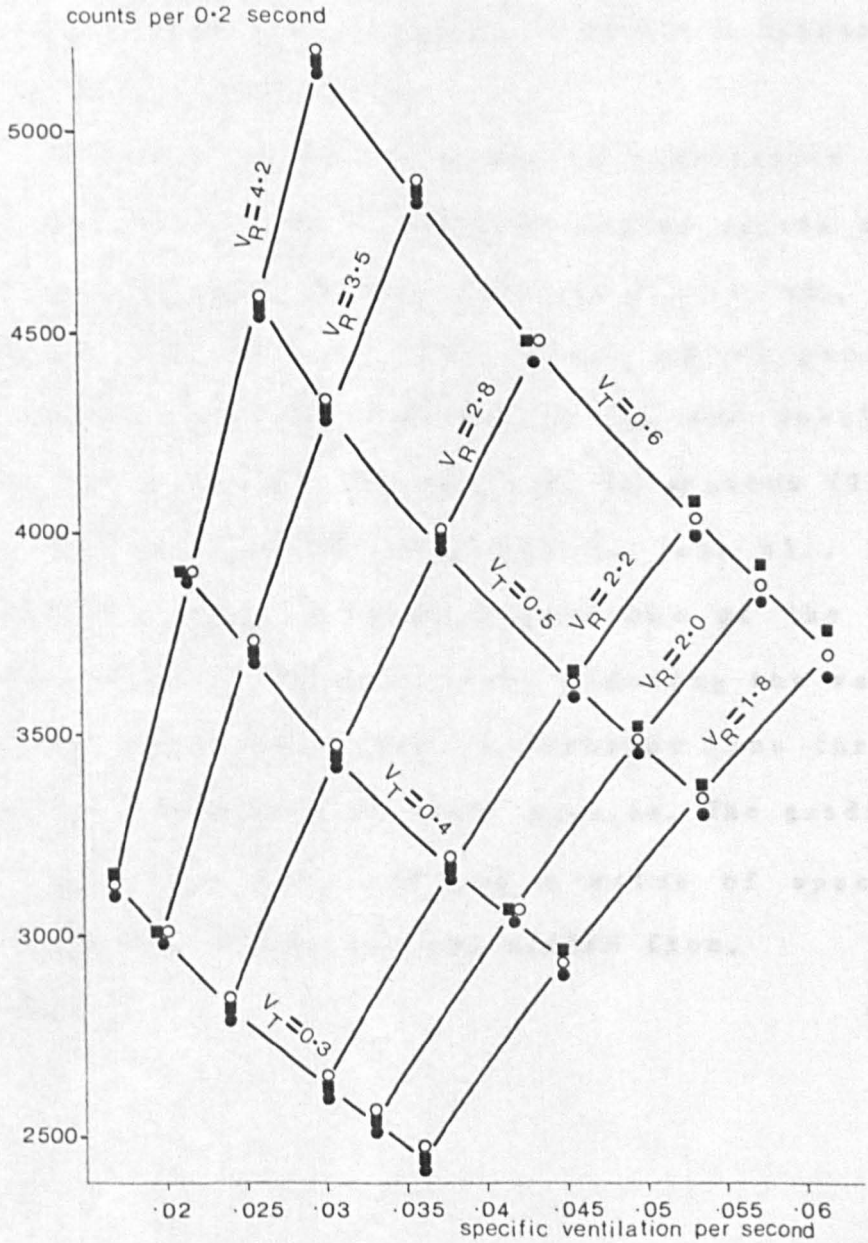

4.2.2 Washout.

Washout activity-time curves were simulated by setting C_i to zero once the equilibrium activity level had been attained and continuing the simulation over a number of breathing cycles until the initial condition of zero radioactive gas in the lungs was re-established. Typical traces are shown in figure (4.4) for an exponential variation in lung volume and in figure (4.5) for a sinusoidal variation in lung volume.

Absolute values of specific ventilation were calculated from the simulated washout curves using the methods described by Ciofetta G., et. al., 1980 and Spaventi S., et. al., 1978, which produce identical results, and Bajzer Z., and Nosil J., 1980. These methods are reviewed in section (2.4).

The method of Ciofetta G., et. al., 1980 involved taking natural logarithms of the data points on the washout curve, plotting the values against time and fitting a straight line through them by the method of least squares. The gradient, g_1, was then obtained and a value of specific ventilation, SV(C), was calculated from,

$$SV(C)=g_1+\lambda \qquad (4.3)$$

Figure 4.4. A simulated washout activity-time curve for parameter values: C_i=3000, V_T=0.5, V_R=2.2, T=4, R=1:2 and β=1.1 assuming an exponential variation in lung volume.

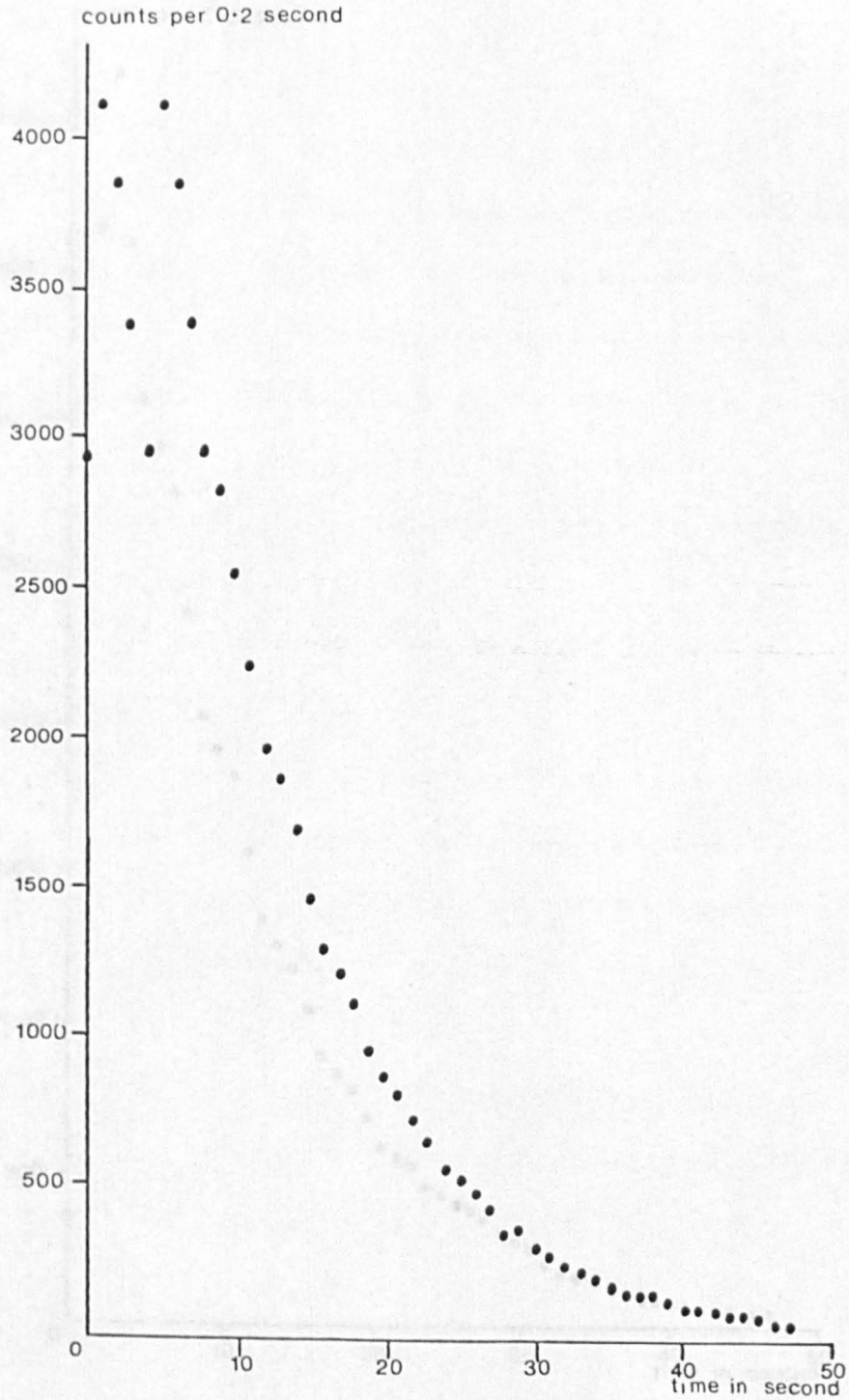

Figure 4.5. A simulated washout activity-time curve for parameter values: C_i=3000, V_T=0.5, V_R=2.2 and T=4 assuming a sinusoidal variation in lung volume.

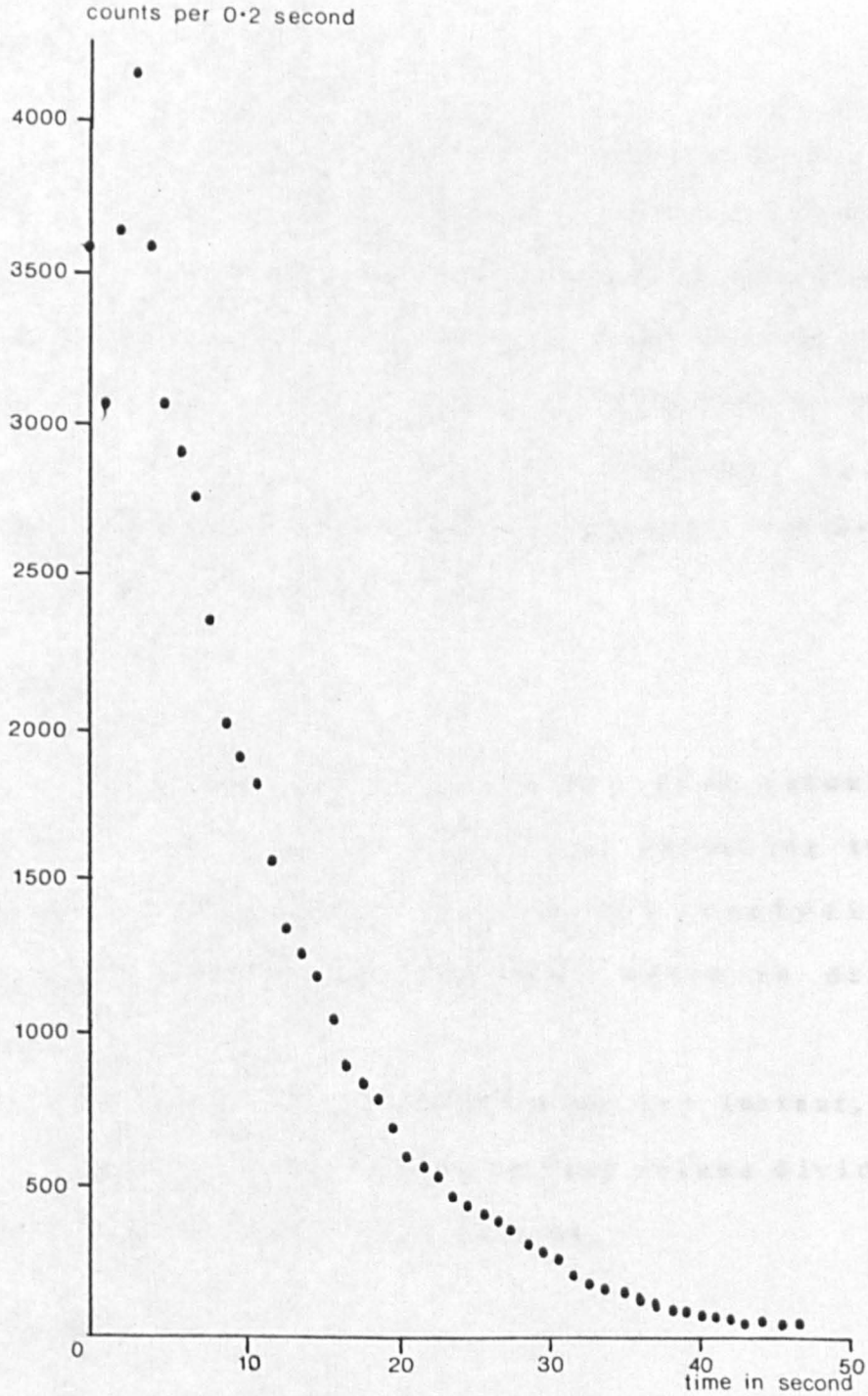

The method of Spaventi S., et. al., 1978 involved measuring the number of counts obtained in the first breath of the washout, A_b, and during the complete washout, A_w. A value of specific ventilation, SV(S), was then calculated from,

$$SV(S) = \frac{1}{T} \log_e \left[\frac{1-A_b}{A_w} \right] + \lambda \qquad (4.4)$$

The method of Bajzer Z., and Nosil J., 1980 involved summing the counts in each breath during the washout, taking the natural logarithms of these, plotting the values against breath number and fitting a straight line through them using the method of least squares. The gradient, g_2, was then obtained and a value of specific ventilation, SV(B), was calculated from,

$$SV(B) = \frac{g_2}{T} + \lambda \qquad (4.5)$$

Specific ventilation was also calculated according to equation (4.2) and according to the equation appropriate to the analysis of radioisotope washout curves, which is derived below.

The specific ventilation at any instant, SV_i, is given by the variation in lung volume divided by the lung volume at that instant,

$$SV_i = \frac{\dot{V}}{V} \qquad (4.6)$$

The value calculated by the radioisotope washout technique, SV_w, is this value averaged over a complete breath,

$$SV_w = \overline{SV}_i = \frac{1}{T}\int_0^{T_i} \frac{\dot{V}}{V} dt \tag{4.7}$$

$$SV_w = \frac{1}{T}\Big[\log_e V\Big]_0^{T_i} \tag{4.8}$$

$$= \frac{1}{T}\Big[\log_e(V_T+V_R) - \log_e(V_R)\Big] \tag{4.9}$$

$$= \frac{1}{T}\log_e\left[\frac{V_T+V_R}{V_R}\right] \tag{4.10}$$

The values of specific ventilation calculated from simulated washout curves and from equations (4.2) and (4.10) are shown in table (4.3) for T equal to 4 seconds and in table (4.4) for T equal to 5 seconds listed against the values of the physiological parameters V_T and V_R.

Table 4.3. Specific ventilation [per second] obtained from equations (4.2) and (4.10) and from washout curves, simulated by the mathematical model, for T=4 seconds. Results are listed against values of V_R and V_T [litre] and for the analysis techniques of Ciofetta G., et. al., 1980 (C), Spaventi S., et. al., 1978 (S) and Bajzer Z., and Nosil J., 1980 (B).

V_R	V_T	(4.2)	(4.10)	C + S	B
1.8	0.3	0.036	0.039	0.042	0.044
	0.4	0.045	0.050	0.053	0.041
	0.5	0.054	0.061	0.064	0.041
	0.6	0.063	0.072	0.075	0.042
2.0	0.3	0.033	0.035	0.038	0.045
	0.4	0.042	0.046	0.049	0.043
	0.5	0.050	0.056	0.059	0.042
	0.6	0.058	0.066	0.069	0.042
2.2	0.3	0.030	0.032	0.035	0.050
	0.4	0.038	0.042	0.045	0.044
	0.5	0.046	0.051	0.054	0.043
	0.6	0.054	0.060	0.064	0.043
2.8	0.3	0.024	0.025	0.029	0.055
	0.4	0.031	0.033	0.037	0.046
	0.5	0.038	0.041	0.044	0.044
	0.6	0.044	0.049	0.052	0.043
3.5	0.3	0.020	0.021	0.024	0.061
	0.4	0.026	0.027	0.030	0.049
	0.5	0.031	0.033	0.037	0.045
	0.6	0.037	0.040	0.043	0.044
4.2	0.3	0.017	0.017	0.021	0.059
	0.4	0.022	0.023	0.026	0.053
	0.5	0.027	0.028	0.031	0.048
	0.6	0.031	0.033	0.037	0.044

Table 4.4. Specific ventilation [per second] obtained from equations (4.2) and (4.10) and from washout curves, simulated by the mathematical model, for T=5 seconds. Results are listed against values of V_R and V_T [litre] and for the analysis techniques of Ciofetta G., et. al., 1980 (C), Spaventi S., et. al., 1978 (S) and Bajzer Z., and Nosil J., 1980 (B).

V_R	V_T	(4.2)	(4.10)	C + S	B
1.8	0.3	0.029	0.031	0.033	0.034
	0.4	0.036	0.040	0.042	0.039
	0.5	0.043	0.049	0.050	0.043
	0.6	0.050	0.058	0.059	0.047
2.0	0.3	0.026	0.028	0.030	0.053
	0.4	0.033	0.036	0.038	0.047
	0.5	0.040	0.045	0.046	0.045
	0.6	0.046	0.052	0.054	0.046
2.2	0.3	0.024	0.026	0.028	0.065
	0.4	0.031	0.033	0.035	0.052
	0.5	0.037	0.041	0.043	0.047
	0.6	0.043	0.048	0.050	0.044
2.8	0.3	0.019	0.020	0.023	0.065
	0.4	0.025	0.027	0.029	0.053
	0.5	0.030	0.033	0.035	0.046
	0.6	0.035	0.039	0.041	0.043
3.5	0.3	0.016	0.016	0.019	0.056
	0.4	0.021	0.022	0.024	0.047
	0.5	0.025	0.027	0.029	0.045
	0.6	0.029	0.032	0.034	0.041
4.2	0.3	0.013	0.014	0.017	0.058
	0.4	0.017	0.018	0.021	0.046
	0.5	0.021	0.022	0.025	0.039
	0.6	0.025	0.027	0.029	0.039

The results indicate that the values obtained from equation (4.10) are similar to those obtained from equation (4.2). The similarity of the results increases as both V_R and T increase but diminishes as V_T increases.

The results also indicate that the values obtained using the analyses reported by Ciofetta G., et. al., 1980 and Spaventi S., et al., 1978 are similar to those obtained from equation (4.2) but are more similar to those obtained from equation (4.10). The similarity to the results obtained from equation (4.10) is not affected by variations in the values of V_T, V_R or T. This suggests that the model predicts realistic washout curves when supplied with reasonable values of the physiological parameters and that equation (4.10) is a better description of the values obtained using a washout analysis than is equation (4.2).

The results obtained from the simulated washout curves are similar to previously published values of specific ventilation (0.031±0.006 by Rosenzweig D.Y., et. al., 1969, 0.015 by Ciofetta G., et. al., 1980, 0.022±0.002 by Spaventi S., et. al., 1978 and 0.033± 0.003 by Bajzer Z., and Nosil J., 1980)[per second].

The adequacy of the model is demonstrated by the similarity of the values of specific ventilation calculated from the simulated washout

curves to the values obtained from equations (4.2) and (4.10) and to previously published values.

The values obtained using the analysis reported by Bajzer Z., and Nosil J., 1980 are not similar to the values obtained using any of the other analyses. The most striking feature of these results is that they diminish as V_T increases. This is not expected according to the classical definition of specific ventilation by equation (4.2). It is probably caused by the count reducing very quickly as V_T increases, causing relatively little variation near the end of washout and resulting in a poor line fit. This is confirmed by an increase in the size of the 95% confidence limits as V_T increases.

The specific ventilation obtained from the analysis of the simulated washout curves was not affected by the value of the parameter β, the ratio $T_i:T_e$ or the pattern of variation in lung volume.

4.3 Susceptibility to Poisson Noise.

The susceptibility of the model and the cross-correlation analysis techniques to the effects of Poisson noise only, ignoring for the moment noise from all other sources, was assessed using activity-time curves simulated assuming low inspiratory concentrations of radioactive tracer gas. This resulted in activities similar to those

encountered in small or poorly ventilated lung regions in clinical studies.

Equilibrium activity-time curves for a number of activity levels were generated assuming an exponential variation in lung volume. Only the exponential pattern was considered in this simulation since this was the only pattern assumed in clinical studies. Values of specific mean expiratory gas flow of 0.15 per second, breathing cycle duration of 2.8 second and ratio $T_i:T_e$ of 1.2:1.6 were assumed.

The curves were simulated in a different manner to the washin and washout curves. In order that the model analysis operate under ideal conditions it was important to ensure that the mean activity level did not vary during a simulation. The simulated activity was therefore varied between a defined peak activity and a trough activity which was calculated from the peak activity such that exactly the same activity was achieved at the end of the next inspiration.

Poisson noise was superimposed on the equilibrium activity-time curves using a random number generator.

4.3.1 **Data Reduction.**

The reliability of the cross-correlation of single breath activity-time curves against the average curve during data reduction in the model

analysis was assessed using equilibrium activity-time curves simulated for a number of peak activities.

The results, expressed as the time of maximum cross-correlation, are shown in table (4.5) for single breath activity-time curves centred on activity maxima and in table (4.6) for single breath activity-time curves centred on activity minima.

Table 4.5. Time displacements [in multiples of 0.2 second] at which maximum cross-correlation occurs when one breathing cycle from a multiple breath activity-time curve was moved against the average single breath curve constructed from the multiple breath curve, both centred on activity maxima. Results are listed against peak activity and breath number (#) in the multiple breath curve.

Peak activity [counts per 0.2 second]

#	20	25	30	40	50	60	80	100	120	150	160	170	200
1			-1	-1	-1	-1	-1	-1	-1	-1	-1	-1	-1
2	-3	-2	-2	-2	-2	-2	-2	-1	-1	-1	-1	-1	-1
3	-3	-3	0	1	1	0	0	1	0	0	0	0	0
4		0	2	2	2	0	0	0	0	1	0	1	0
5		1	0	0	0	0	1	1	1	1	1	1	1
6	0			1	1	1	0	0	0	0	0	0	0
7	-4			0	3	0	0	0	0	0	0	0	0
8	0	1	0	-1	0	0	0	0	0	0	0	0	0
9	0	0	0	0	0	0	0	0	0	0	0	0	0
10	0	0	-2	-2	-1	0	-1	-1	-1	-1	-1	-1	-1
11	0	0	-1	-1	-1	-1	-2	-2	-1	0	0	-1	-1
12	0	0		0	0	0	0	0	0	0	0	0	0
13				0	1	1	0	0	0	0	0	0	0
14			-4	-3	-2	-2	-2	-2	-1	0	0	0	0
15		-2	0	0	0	0	0	0	0	0	0	0	0
16		1	0	0	0	0	0	0	0	0	0	0	0
17		0	0	0	0	0	0	0	0	0	0	0	0
18	0	0	0	0	0	0	0	0	0	0	0	0	0
19	-3	0	0	1	0	-1	0	0	0	0	0	0	0
20	0	0	4	0	0	0	0	0	0	0	0	0	0
21	0	0	3	2	2	2	1	1	1	1	1	1	1
22	0	2	0	0	0	0	0	0	0	0	0	0	0
23	3	0	0	0	0	0	0	0	0	0	0	0	0
24	0	0	0	0	0	0	0	0	0	0	0	0	0
25	1	-1	-1	-2	-1	-1	-1	-1	0	-1	0	-1	-1
26		-3		-1	-1	-1	-1	0	0	0	0	0	0
27				2	1	1	0	0	0	0	0	0	0
28			0	0	0	0	0	0	1	0	0	0	0
29		0	1	1	1	1	1	0	0	0	0	0	0
30	2	1	0	0	1	1	0	0	1	0	0	0	0
31	-2	0	3	3	3	2	1	1	1	1	1	1	0
32	0	3	2	1	2	2	1	1	1	1	1	1	1
33	3	2	-1	0	0	0	0	0	0	0	0	0	0
34	3	-1	0	0	0	0	0	0	-1	-1	-1	-1	0
35	-1	0		0	0	0	1	1	0	0	0	0	0
36	0				-2	-2	-2	-2	-1	-1	-1	-1	-1
37			0		0	0	0	0	0	0	0	0	0
38		0		0	1	1	0	0	1	0	0	0	0
39				0	0	0	1	0	0	0	0	0	0
40			-2	-1	-1	-1	-1	0	0	0	0	0	0
41													
42	-2	-1											

Table 4.6. Time displacements [in multiples of 0.2 second] at which maximum cross-correlation occurs when one breathing cycle from a multiple breath activity-time curve was moved against the average single breath curve constructed from the multiple breath curve, both centred on activity minima. Results are listed against peak activity and breath number (#) in the multiple breath curve.

	Peak activity [counts per 0.2 second]												
#	20	25	30	40	50	60	80	100	120	150	160	170	200
1			-2	-1	-1	-1	-1	-1	-1	-1	-1	-1	-1
2	-2	-3	-3	-2	-3	-3	-2	-2	-2	-2	-2	-2	-1
3	-4	0	-4	-4	0	0	0	0	0	0	1	1	1
4	0	4	4	4	0	0	0	0	1	1	1	1	1
5			2	2	2	2	2	1	1	1	1	1	1
6				1	1	1	0	1	1	1	1	1	1
7		-1		-3	0	0	0	0	0	0	0	0	0
8	0	0	0	-1	-1	-1	-1	0	0	0	0	0	0
9	0	0	0	0	0	0	0	0	0	0	0	0	0
10	1	-1	-1	0	0	0	0	0	0	0	0	0	0
11	-1			-1	-1	-1	-1	-1	-1	-1	-1	-1	-1
12				-1	-1	-1	-1	-1	-1	-1	-1	-1	-1
13		0	0	0	1	1	1	0	0	0	0	0	0
14		0	0	0	0	0	0	0	0	0	0	0	0
15		-1	0	-1	-1	-1	-1	0	-1	0	0	0	0
16	0	0	3	0	0	0	0	0	0	0	0	0	0
17	0	0	-2	0	0	0	0	0	0	0	0	0	0
18	0	0	0	-2	0	0	0	0	0	0	0	0	0
19	1	0	0	0	0	0	0	0	0	0	0	0	0
20	0	0	1	0	0	0	0	0	0	0	0	0	0
21	1	0	2	1	1	1	1	1	1	1	1	1	1
22	1	0	0	1	1	1	1	1	1	1	1	1	1
23	0	0	0	0	0	0	0	0	0	0	0	0	0
24	0	0	-1	0	0	0	0	0	0	0	0	0	0
25				0	0	0	0	-1	-1	0	-1	0	-1
26				-1	0	0	0	0	0	0	0	0	0
27		3	3	3	0	0	0	0	0	0	0	0	0
28	3	4	4	3	3	3	3	1	1	1	1	1	1
29	0	-2	-2	4	0	0	0	0	0	1	1	1	1
30	2	1	0	-2	-2	1	0	0	0	0	0	0	0
31	0	2	2	0	0	0	0	0	0	0	0	0	0
32	0	0	0	2	0	1	1	1	1	1	1	1	1
33	1	-2	-2	0	0	0	0	0	0	0	0	0	0
34	0	0	0	-1	0	0	0	0	0	0	0	0	0
35				0	-1	0	-1	0	-1	-1	0	-1	0
36					0	0	0	-1	-2	-1	-1	0	-1
37			0		0	0	-2	-1	-1	-1	-1	-1	-1
38				0	0	0	0	0	0	0	0	0	0
39		0		2	1	1	1	1	1	1	1	1	1
40	0	0	0	0	-1	0	0	0	0	0	0	0	0
41	0			0	0	0	0	0	0	0	0	0	0

The results indicated that at peak activity levels higher than 40 counts per 0.2 second all breaths in the activity-time curve fulfilled the acceptance criteria. This is indicated in the tables by a time displacement being listed for all breath numbers. At all activity levels, non-zero time displacements were measured, however. They varied between ± 4, the maximum displacement undertaken during this procedure. When the same procedure was conducted with noise free data all breaths at all peak activity levels were detected with time displacements of zero.

From these results it was concluded that, at the activities available for clinical studies, cross-correlation of single breath activity-time curves against average single breath activity-time curves during data reduction was unreliable. This practice was therefore abandoned and the average single breath activity-time curve was used in the application of the model analysis to the data.

4.3.2 Model Application.

The reliability of the model analysis for determining values of specific mean expiratory gas flow was assessed using activity-time curves simulated for three activity levels. Values of specific mean expiratory gas flow (f), 95% confidence limits (cl) and coefficient of determination (cd) were calculated from the expiratory phase of the average single breath activity-time curve using equations (3.39), (3.41) and (3.42). The results are listed against peak activity in table (4.7) for both noise free data and for data on which Poisson noise had been superimposed.

The three activity levels used were chosen to represent the activity measured in each of eight lung regions, of equal volume. The levels were equivalent to mean activity levels of 168, 552 and 1376 counts per 0.2 second summed over the eight regions and 1.4, 4.6 and 11.5 kcounts per second over the whole lung field, assuming only 60% of the complete field was used in the definition of the lung regions.

Table 4.7. Specific mean expiratory gas flow (f) [per second], 95% confidence limits (cl) and coefficient of determination (cd) obtained using the mathematical model analysis applied to simulated activity-time curves. Results are listed against peak activity (pa) [counts per 0.2 second] and for the three types of model application: Max: the series of single breath curves centred on activity maxima, Min: the series of single breath curves centred on activity minima and Com: the combination of the peak and trough expiratory phase data.

	Max			Min			Com		
pa	f	cl	cd	f	cl	cd	f	cl	cd
noise free data.									
25	.149	.019	.989	.149	.019	.989	.149	.019	.989
80	.155	.006	.999	.154	.003	.999	.124	.017	.986
200	.151	.006	1.00	.151	.006	1.00	.151	.006	1.00
data with superimposed Poisson noise.									
25	.156	.069	.855	.180	.067	.902	.146	.055	.895
80	.169	.040	.960	.158	.025	.983	.151	.027	.978
200	.164	.021	.988	.151	.020	.987	.149	.013	.992

The results indicated that even at the lowest activity level the estimated values of specific mean expiratory gas flow were similar to the simulated value of 0.15 per second. Also the 95% confidence limits were narrow and the coefficient of determination was high. This demonstrated that, with generator activities and detection system sensitivities presently available, resulting in approximately 3 kcounts per second over a complete lung field, it was theoretically possible to obtain accurate values of specific mean expiratory gas flow in eight regions of the lung from a two minute data acquisistion.

Greater accuracy, by for example incorporating cross-correlation techniques into the multiple breath to single breath data reduction or an analysis of smaller lung regions, would be possible with higher activity generators which should be available in the future.

4.3.3 Cross-Correlation Application.

The reliability of the cross-correlation of activity-time curves from two different lung regions as an estimate of phase differences was assessed using activity-time curves simulated for a number of activity levels. Curves were generated for eight lung regions, assumed to divide each lung field vertically into four regions with equal volumes. The curves generated for regions in the right lung (numbers 2,4,6,8) were time advanced by one data interval compared with those generated for regions in the left lung (numbers 1,3,5,7).

The results of the cross-correlation are listed against peak activity in tables (4.8), (4.9) and (4.10).

The results indicate that above a peak activity of 200 counts per 0.2 second or 11.5 kcounts per second over the whole lung field, again assuming only 60% of the field was used in the definition of the lung regions, the cross-correlation technique is reliable. At activity levels presently seen (3 kcounts per second over the whole lung field) however, the values simulated were not extracted.

When this procedure was undertaken with noise free data correct time displacements were detected at all activity levels.

Table 4.8. Time displacements [in multiples of 0.2 second] at which maximum cross-correlation occurs when a simulated activity-time curve from one lung region is moved against a simulated activity-time curve from another lung region. Results are listed against peak activity (pa) [counts per 0.2 second] and for curves of regions in the right lung (2,4,6,8) moved against curves of regions in the left lung (1,3,5,7) used as reference.

	Lung Regions															
	1				3				5				7			
pa	2	4	6	8	2	4	6	8	2	4	6	8	2	4	6	8
20	1	0	-1	0	0	1	0	1	1	0	0	1	0	1	-1	1
25	1	0	0	0	0	1	0	1	1	0	0	1	2	1	1	1
30	1	0	0	1	0	1	0	1	1	0	0	1	0	1	1	1
40	1	0	0	1	0	1	0	1	1	0	0	1	1	1	1	1
50	1	0	0	1	0	1	0	1	1	0	0	1	1	1	1	1
60	1	0	0	1	0	1	0	1	1	0	0	1	1	1	1	1
80	1	0	0	1	0	1	0	1	1	1	0	1	1	1	1	1
100	1	0	1	1	1	1	1	1	1	1	1	1	1	1	1	1
120	1	0	1	1	1	1	1	1	1	1	1	1	1	1	1	1
150	1	1	1	1	1	1	1	1	1	1	1	1	1	1	1	1
160	1	1	1	1	1	1	1	1	1	1	1	1	1	1	1	1
170	1	1	1	1	1	1	1	1	1	1	1	1	1	1	1	1
200	1	1	1	1	1	1	1	1	1	1	1	1	1	1	1	1

Table 4.9. Time displacements [in multiples of 0.2 second] at which maximum cross-correlation occurs when a simulated activity-time curve from one lung region is moved against a simulated activity-time curve from another lung region. Results are listed against peak activity (pa) [counts per 0.2 second] and for curves of regions in the left lung (1,3,5,7) moved against curves of regions in the left lung (1,3,5,7) used as reference.

	Lung Regions			
	1	3	5	7
pa	1 3 5 7	1 3 5 7	1 3 5 7	1 3 5 7
20	1 1-1	-1 -1 1	-1 1 0	1-1 0
25	-1 1-1	1 1 1	-1-1 0	1-1 0
30	1 1-1	-1 -1 0	-1 1 0	1 0 0
40	1 0-1	-1 -1 0	0 1 0	1 0 0
50	-1 0 0	1 -1 0	0-1 0	0 0 0
60	-1 0 0	1 -1 0	0 1 0	0 0 0
80	-1 0 0	1 0 0	0 0 0	0 0 0
100	-1 0 0	1 0 0	0 0 0	0 0 0
120	-1 0 0	1 0 0	0 0 0	0 0 0
150	-1 0 0	1 0 0	0 0 0	0 0 0
160	-1 0 0	1 0 0	0 0 0	0 0 0
170	-1 0 0	1 0 0	0 0 0	0 0 0
200	0 0 0	0 0 0	0 0 0	0 0 0

Table 4.10. Time displacements [in multiples of 0.2 second] at which maximum cross-correlation occurs when a simulated activity-time curve from one lung region is moved against a simulated activity-time curve from another lung region. Results are listed against peak activity (pa) [counts per 0.2 second] and for curves of regions in the right lung (2,4,6,8) moved against curves of regions in the right lung (2,4,6,8) used as reference.

	Lung Regions			
	2	4	6	8
pa	2 4 6 8	2 4 6 8	2 4 6 8	2 4 6 8
20	0-1 1	0 0-1	1 0 1	-1 1-1
25	0-1 0	0 0-1	1 0 0	0 1 0
30	0-1 0	0 0-1	1 0 1	0 1-1
40	0-1 0	0 0-1	1 0 0	0 1 0
50	0-1 0	0 0-1	1 0 0	0 1 0
60	0-1 0	0 0-1	1 0 0	0 1 0
80	0 0 0	0 0-1	0 0 0	0 1 0
100	0 0 0	0 0 0	0 0 0	0 0 0
120	0 0 0	0 0 0	0 0 0	0 0 0
150	0 0 0	0 0 0	0 0 0	0 0 0
160	0 0 0	0 0 0	0 0 0	0 0 0
170	0 0 0	0 0 0	0 0 0	0 0 0
200	0 0 0	0 0 0	0 0 0	0 0 0

CHAPTER 5 **Clinical Studies.**

Clinical studies were undertaken to assess the reproducibility of both the model and the cross-correlation analyses and to assess the sensitivity of the model analysis.

The reproducibility of the analysis techniques was assessed by applying the model and the cross-correlation analyses to data acquired during two consecutive studies on 14 patients. An estimate of the reproducibility was obtained by observing the similarity of the results obtained from the consecutive studies in each patient.

The sensitivity of the model analysis was assessed by applying the analysis to data acquired during single studies on six normal subjects and 30 patients with a variety of respiratory disorders. An estimate of the sensitivity was obtained by comparing the results obtained from the normal subjects with those obtained from the patients.

5.1 $^{81}Kr^{m}$ Administration.

$^{81}Kr^{m}$ gas was administered via a 24% clear plastic disposable 'Ventimask' face mask placed over the mouth and nose and adjusted to be a good fit.

The gas was obtained from a $^{81}Rb/^{81}Kr^{m}$ generator, shown in photograph (5.1), which was supplied by the MRC Cyclotron Unit of the Hammersmith Hospital. $^{81}Kr^{m}$ was eluted by passing

moist air at approximately 1.0 bar pressure through an alumina column onto which ^{81}Rb had been adsorbed. The air was obtained from a compressed air cylinder and its pressure was regulated by a constant pressure nitrogen valve type 'BOC M.30-NG' to maintain a good yield of $^{81}Kr^{m}$ when the density of the alumina column varied.

Standard gauge oxygen tubing carried the compressed air, via a humidifier, to the radioactive column. Portex PP40 0.5mm small bore plastic tubing carried the air mixed with radioactive $^{81}Kr^{m}$ to the face mask. The cross-sectional area of the tubing from the radioactive column to the face mask was very small to avoid excessive decay of the radioisotope during transit.

5.2 Data Acquisition.

Inhalation data was acquired by the nuclear medicine acquisition and processing system Dycom-80 (Ram G., 1979) shown in photograph (5.2), from either a Searle large field of view, shown in photograph (5.3) or an Elscint gamma camera. A low energy, low resolution, high sensitivity collimator suitable for gamma energies upto approximately that of $^{81}Kr^{m}$ was used. Data was acquired using a mini-computer, shown in photograph (5.4), which divided the gamma camera image into a two dimensional matrix of 32 x32, 64 x 64 or 128 x 128 picture

elements or pixels.

The subject was seated with his back against the gamma camera in the postero-anterior orientation as close as possible to the camera face in order to reduce the loss of spatial resolution with increasing separation experienced using these instruments. The procedure was explained and the subject was asked to relax for five minutes.

Photograph 5.1. MRC Cyclotron Unit $^{81}Rb/^{81}Kr^{m}$ gas generator.

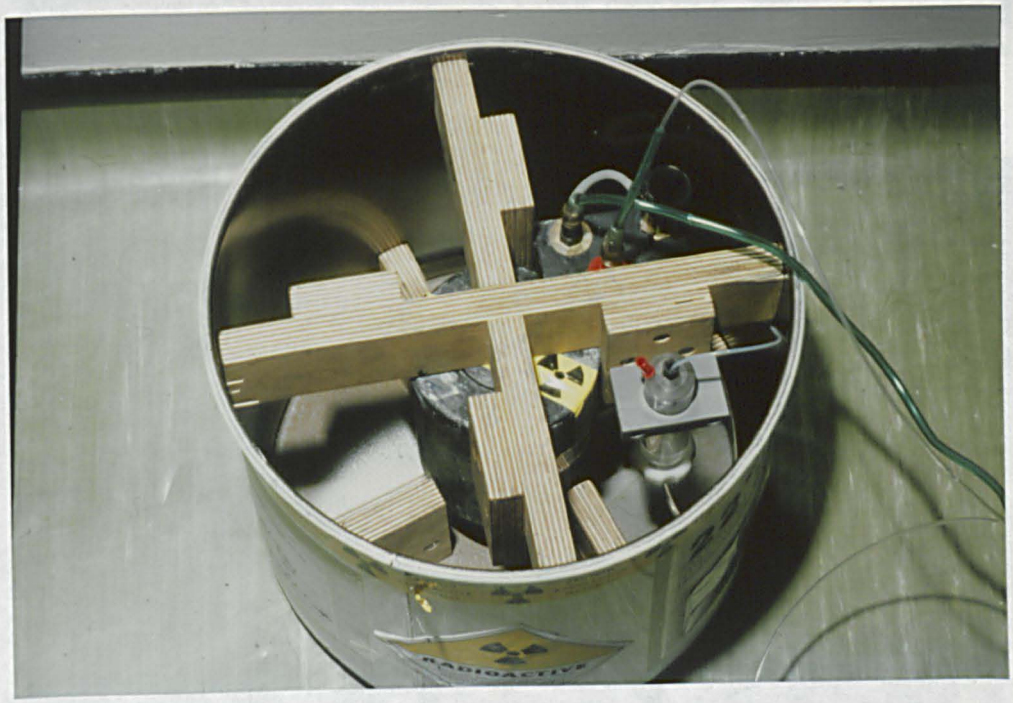

Photograph 5.2. Console of the Elscint Dycom-80, nuclear medicine data acquisition and processing system.

Photograph 5.3. Searle large field of view Gamma Camera.

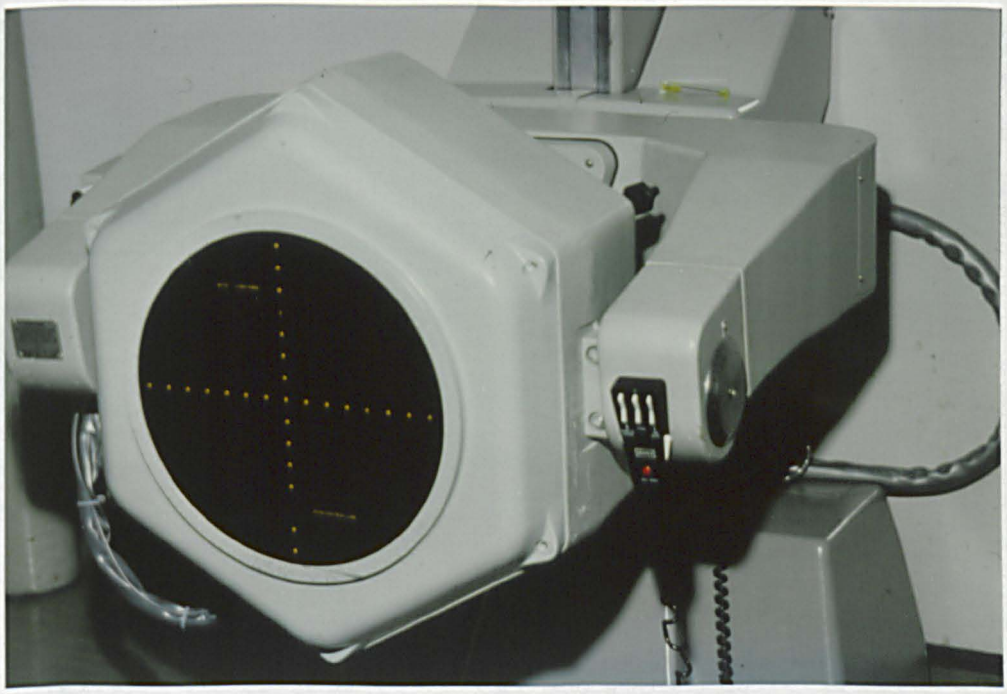

Photograph 5.4. Data General Nova 3/12 mini-computer.

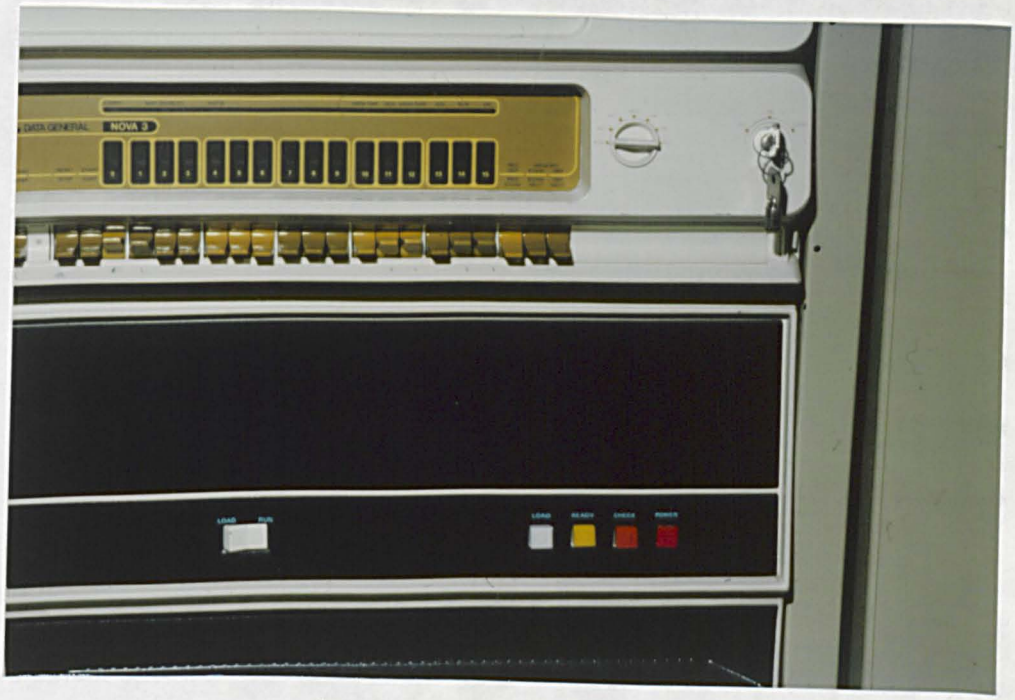

Photograph 5.5. Gamma Camera analogue electronics and console.

The mask was placed over the mouth and nose of the subject and the flow of $^{81}Kr^{m}$ was started. The patient breathed quietly at tidal volumes and was given one minute to equilibrate before data was acquired. During this time the position of the subject relative to the camera face was adjusted to ensure that the lung image was central in the field of view and that the face mask was excluded. The latter was important since the analysis program would have considered this as part of the lung field.

If the subject had recently received an injection of $^{99}Tc^{m}$ as part of a perfusion investigation, a 128 x 128 image of short duration was acquired to localise the lungs and position the patient.

To acquire this image the single channel analyser on the camera electronics, shown in photograph (5.5), was set to an energy of 140 kev with a window of 40 kev which was slightly wider than normal. It was the one used for the $^{81}Kr^{m}$ acquisition and was left at 40 kev because only an approximate guide was required from this acquisition.

If the subject had not recently received an injection of $^{99}Tc^{m}$ localisation of the lungs was accomplished by the acquisition of a 128 x 128 image of short duration during the equilibration

phase. Data was acquired during this period in order to keep the radiation dose as low as possible.

Even when $^{99}Tc^{m}$ was present, acquiring an image during the equilibration phase provided confirmation that the face mask did not appear in the field of view of the gamma camera.

The single channel analyser was set for an energy of 190 kev. There was a breakthrough of only 5% from the gamma emissions of any $^{99}Tc^{m}$ present in the lung field into the energy window used for the inhalation study.

A fan was used to provide a flow of air across the gamma camera face to ensure that build-up of $^{81}Kr^{m}$ gas near the face of the camera was avoided.

After equilibration, the subject was asked to ramain still and a two minute data acquisition was started.

There was no regulation in the depth of breathing other than requesting the patient to breath quietly at tidal volumes. Observation of the acquired data, however, indicated that this resulted in a regular activity-time curve for most patients.

Data was acquired in the form of a sequential series of images of short duration. Spatial resolution of the lung image was sacrificed in

favour of a fast frame rate in order to provide an accurate representation of the behaviour of radioactive gas in the lung. The frame rate was set at five per second and the image matrix at 32 x 32, each pixel thus representing either 1.0 or 1.5 cm^2 approximately of the lung field depending which camera was in use. The maximum study length available for the frame rate and matrix size chosen was used, which was 600 frames and which provided 120 seconds of imaging time.

The additional resolution afforded by the larger matrices available was not helpful and the rapid utilisation of available external computer storage space was a great disadvantage. Acquisition speeds of upto 25 frames per second were available but the counting statistics would have deteriorated from their already poor state at rates faster than 0.2 second.

On completion of an acquisition, the data was stored on hard disk for future analysis. 5 studies were stored on each disk which, when full, were dumped to 9 track magnetic tape. Two disks could be dumped to one tape. In this way patients and subjects for the clinical studies were acquired over two years and were available for off-line analysis at any time.

5.3 Data Processing.

The data acquired during a clinical study was processed into a form which could be analysed by the model and the cross-correlation techniques.

Using libraries and file structure supplied by Elscint (Europe) Ltd., a program was written which interfaced with the Dycom 80 system.

An outline of the lungs was defined and each lung divided vertically into four equal regions. Multiple breath activity-time curves were generated for each region and for seven larger regions obtained from combinations of the original eight. The analysis techniques were applied to this data.

To produce an outline of the lungs the 600 frames of the study were summed and, to reduce statistical fluctuation, the resulting matrix was spatially smoothed twice using a nine-point average. The highest pixel count in the smoothed image was obtained and an outline of the lungs defined by excluding all pixels with counts less than 40% of this maximum. This contour level was chosen, by reference to profile data published by Nosil J., et. al., 1977, Alpert N.M., 1975 and by experience, to produce consistent outlines of each lung without excluding data from diseased areas. Eight regions were defined within the 40% contour by dividing each lung into four equal vertical sections. The 40% contour and the regional

boundaries were printed out for each study, a typical example of which is shown in figure (5.1), to confirm that the face mask was not included and that areas of lung were not excluded from the analysis. Activity-time curves were constructed from the original 600 frames of unprocessed data by summing the counts obtained in each region in each frame. Curves were generated for each of 15 regions shown in figure (5.2), eight for region numbers 1 to 8 and seven more for combinations of these, region numbers 9 to 15. The seven regions obtained from combinations of the original eight were: the upper (12) and lower (14) halves of the left lung, the upper (13) and lower (15) halves of the right lung, the complete left lung (9), the complete right lung (10) and both lungs taken together (11).

By constructing data from lung regions of different sizes, the behaviour of the analysis techniques could be assessed for four levels of spatial resolution.

Figure 5.1. Lung regions defined by a 40% of maximum count contour and four vertical divisions, shown in the postero-anterior orientation.

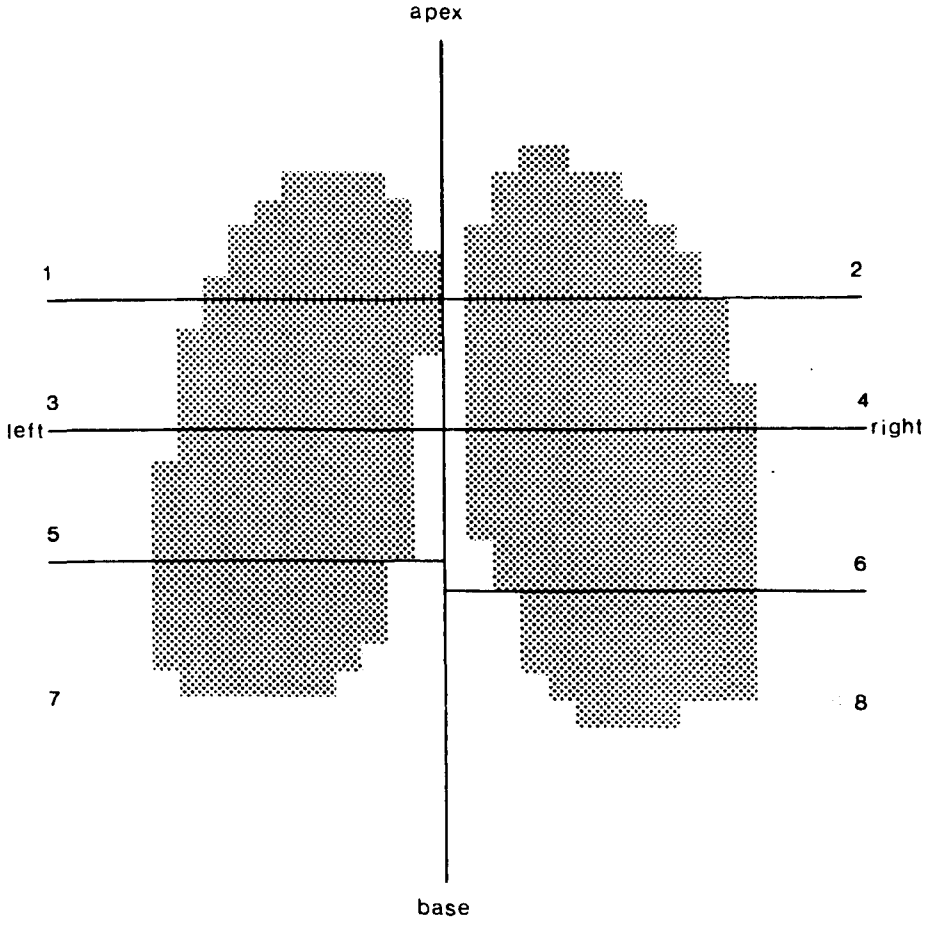

Figure 5.2. The numbering and position of the 8, 4 and 2 lung regions and both lungs taken together, shown in the postero-anterior orientation.

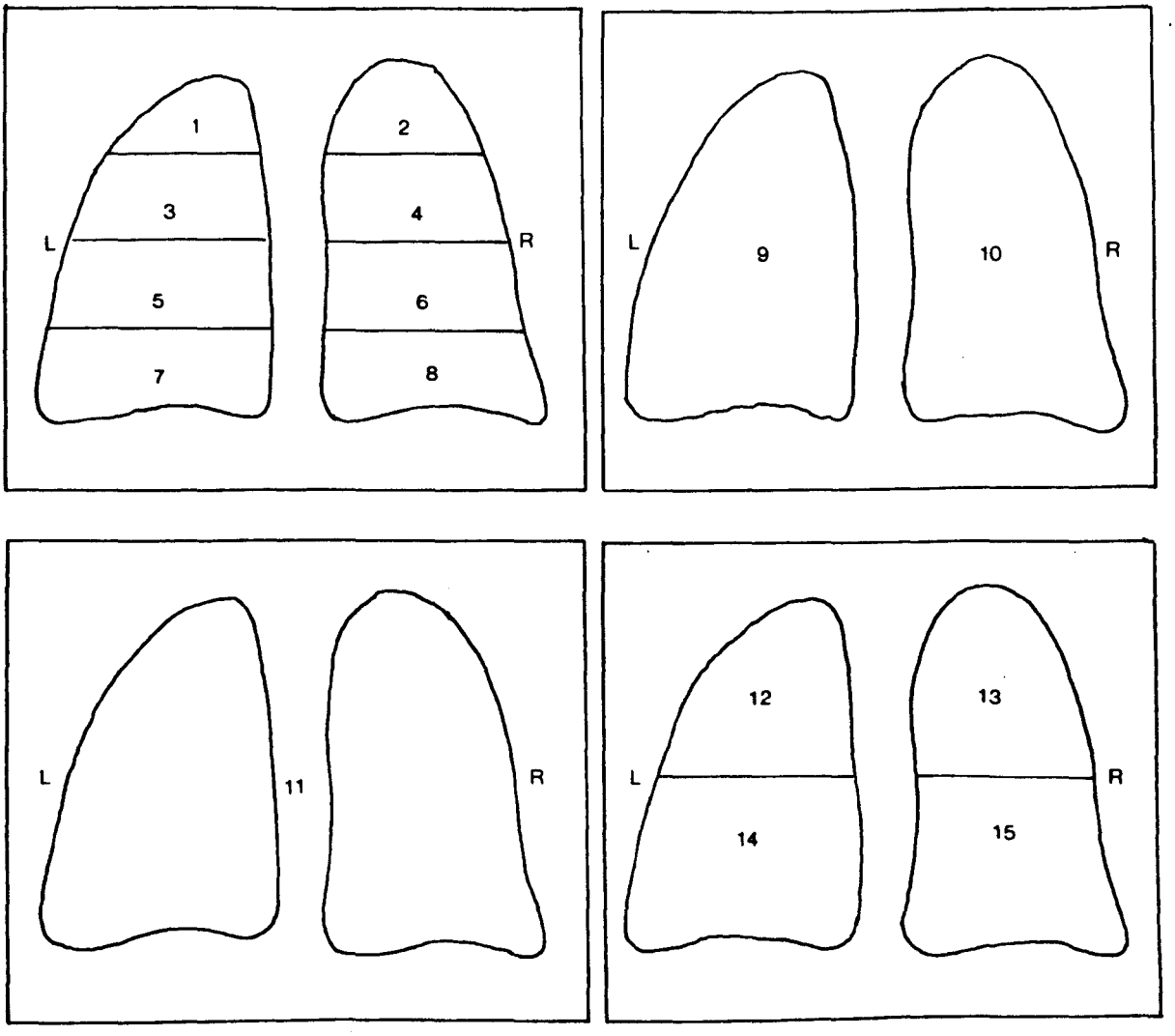

5.3.1 Model.

For each region an average single breath curve was constructed and a value of specific mean expiratory gas flow was calculated by applying the mathematical model to the expiratory phase of this curve.

To condense each multiple breath curve into a single breath curve, the series of individual breaths in the curve were centred first on activity maxima and summed to produce an average breath and then centred on activity minima and summed to produce an average breath. Single breath curves centred on activity minima observed in a typical patient are shown for regions 1 to 8 in figure (5.3) and for regions 9 to 15 in figure (5.4). They illustrate the increase in definition of the single breath activity-time curves with increasing region size as the counting statistics improve. For the larger regions of the lung where more pixels are included and more counts are obtained the standard deviation is relatively less and the curves are smoother.

Figure 5.3. Single breath activity-time curves centred on activity minima observed in a typical patient in lung regions one to eight.

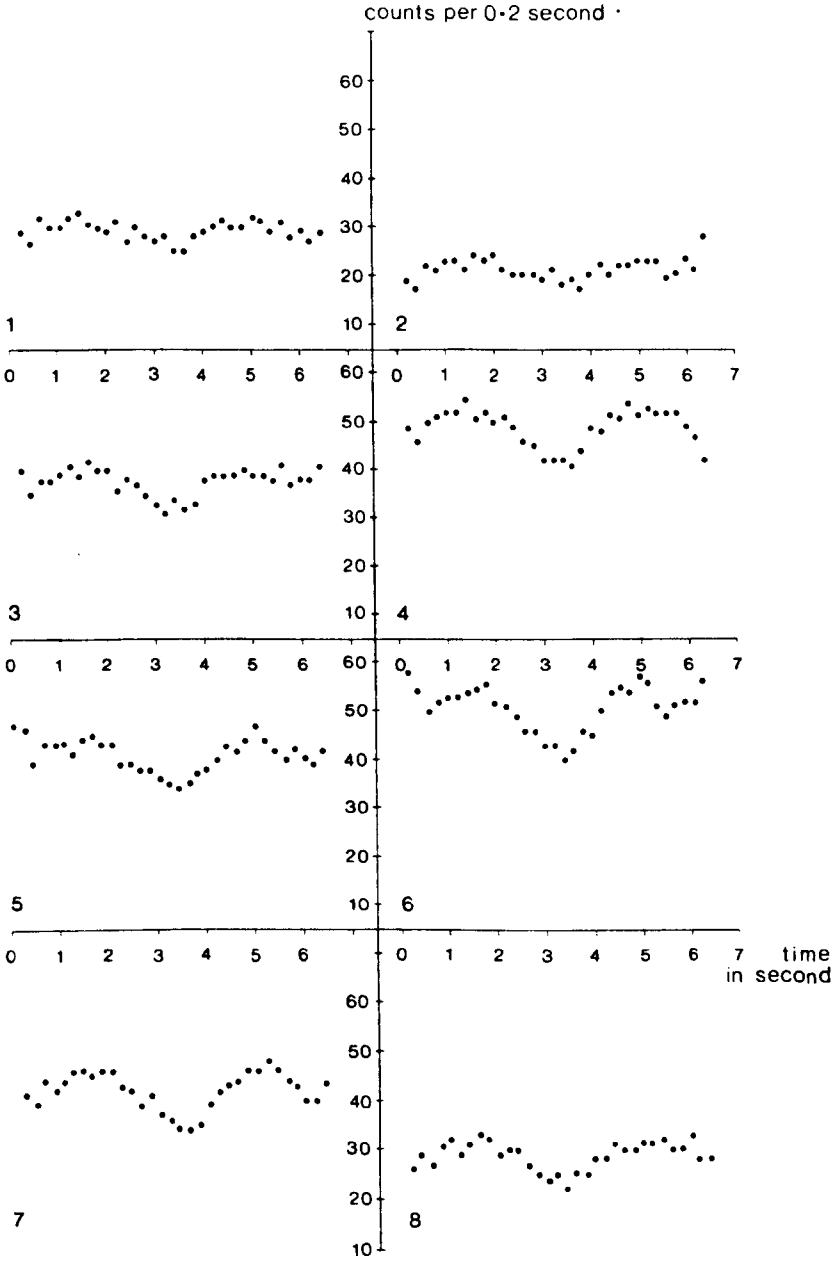

Figure 5.4. Single breath activity-time curves centred on activity minima observed in a typical patient in lung regions 9 to 15.

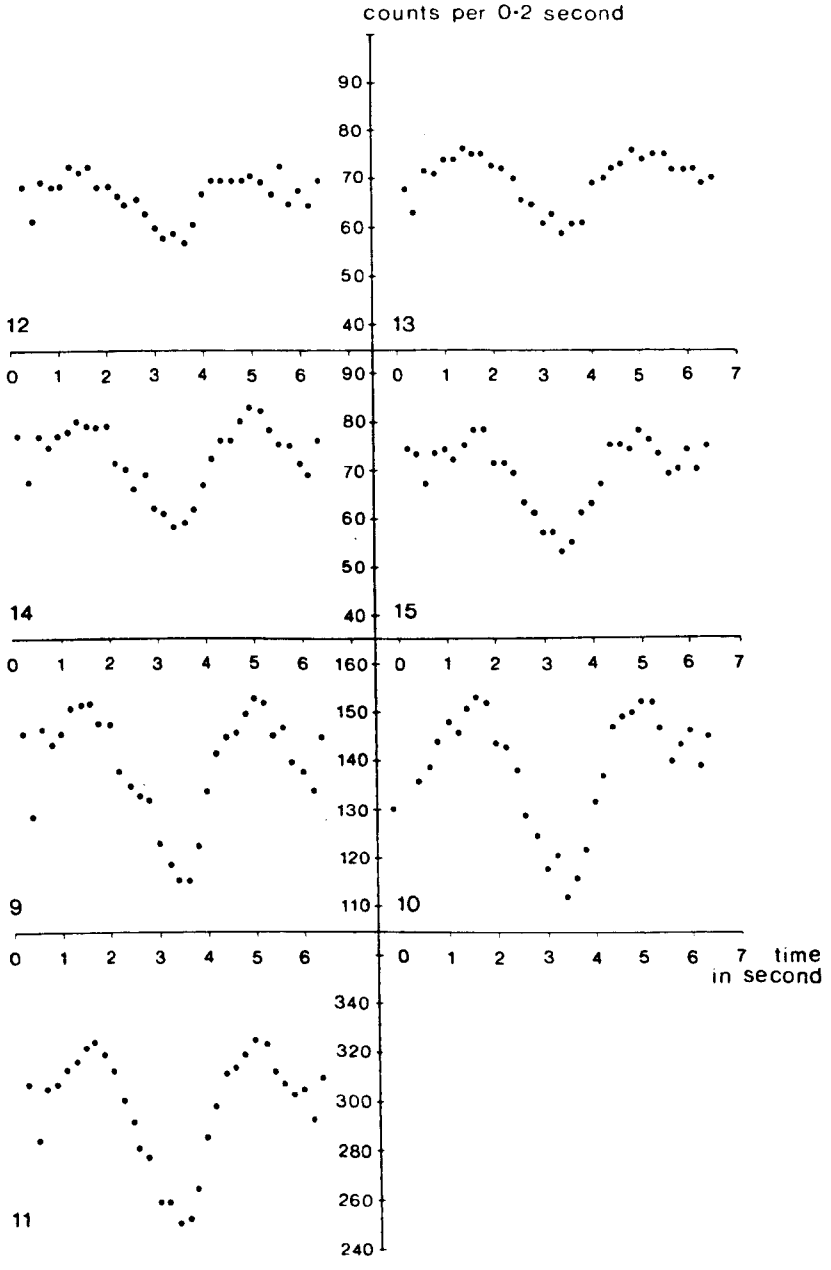

The positions of the activity maxima and minima in all 15 activity-time curves in each study were assumed to be the same as those in the multiple breath time-activity curve obtained from region 11 (both lungs taken together) in that study. This curve was chosen because, being obtained from the largest region, it had the highest signal to noise ratio.

The positions of the activity maxima and minima in activity-time curve 11 (both lungs taken together) were obtained using a series of manipulations on the curve data. In order to obtain accurate positioning, statistical fluctuations were reduced by smoothing the curve twice using a three-point linear average. The smoothed curve was then searched to find the mean durations of the inspiratory and the expiratory phases and, to exclude abberations in the breathing pattern such as sighs and coughs, only those breaths whose inspiratory and expiratory times were within 50% of the mean durations were retained for the following analysis.

5.3.2 Cross-Correlation.

The cross-correlation techniques were applied to the unprocessed multiple breath activity-time curves from the three groups of 8, 4 and 2 lung regions.

5.4 Data Analysis.

The model and the cross-correlation analyses were applied to the activity-time curves generated from the data processing described above.

5.4.1 Model.

The model analysis was applied to the expiratory phase of the single breath activity-time curves centred on activity maxima and minima. It was also applied to composite expiratory curves which were produced by combining the data points of the upper half of the curves centred on activity maxima with the data points of the lower half of the curves centred on activity minima.

5.4.2 Cross-correlation.

The multiple breath activity-time curves were cross-correlated in three groups, those from regions 1 to 8, those from regions 12 to 15 and those from regions 9 and 10. In each group, each pair of activity-time curves were cross-correlated with each other to find the time-advance or time-delay [in multiples of 0.2 second] at which they achieved maximum cross-correlation. The cross-correlogram of the regions 9 and 10 from each study showed a peak at zero time displacement. This was probably due to the large size of the lung regions masking out any changes which might be occurring in within the regions.

5.5 Studies.

A reproducibility study was undertaken involving 14 patients with various respiratory disorders who each underwent two consecutive 120 second studies, to determine the variability of the model and the cross-correlation analyses. A sensitivity study was also undertaken, involving six normal subjects and 30 patients with various respiratory disorders who each underwent one 120 second study, to determine the sensitivity of the model analysis to disease state.

The clinical details and the reports on the analogue inhalation images of the patients are listed in Appendix II Patient Details and Imaging Reports. The patient group was divided into two sub-groups, those whose inhalation image reports were normal and those whose inhalation image reports were abnormal. The patients with normal image reports were not considered with normal subjects because they had experienced symptoms of respiratory disorder.

5.6 Results of the Reproducibility Study.

The results of the reproducibility study are listed in tables (5.1) to (5.28).

5.6.1 Model.

The mean count rate in each of the lung regions for each study is shown in table (5.1). The results indicate that generally the mean count rate

increases as the size of the lung region increases but that the apical and basal regions show a decreased mean count rate because of anatomical volume variations. The mean count rate varies from 16 counts per 0.2 second in the smallest lung region to 900 counts per 0.2 second in the largest region. The lowest level approximates to the lowest level considered in the simulation studies and which returned reliable values for the model analysis.

Results are not available for four of the 14 patients who participated in the study, numbers 6, 14, 16 and 21 because the analysis was halted by computer run-time errors. These errors signal the inability of the computer program to apply the model to the single breath data and occur when the single breath activity-time curve is so noisy that it is not possible to define the limits of the expiratory phase and therefore, not possible to fit a straight line through the logarithms of the data points.

Table 5.1. The mean activity [counts per 0.2 second] of the activity-time curve obtained from each lung region of the 14 subjects who participated in the reproducibility study. Results are listed against subject number (Subj) for each of the two consecutive studies. R/T: computer run-time error.

	Lung Regions														
Subj	1	2	3	4	5	6	7	8	12	13	14	15	9	10	11
6	R/T														
10	55	40	71	91	71	109	46	58	126	130	118	167	244	297	541
	65	53	92	121	93	134	63	53	157	174	156	187	313	361	674
11	58	81	106	139	126	176	104	111	163	220	230	287	393	507	900
	43	51	77	95	88	117	77	83	121	146	165	200	286	347	633
13	25	45	53	77	45	76	16	25	78	122	61	101	139	223	362
	30	49	49	75	40	72	16	23	79	124	55	95	134	219	353
14	R/T														
15	17	29	32	37	49	60	25	32	50	66	74	92	124	158	282
	21	29	44	36	42	57	17	30	65	65	59	87	124	151	275
16	R/T														
17	26	22	33	38	32	44	24	31	59	60	55	74	115	134	249
	22	18	30	36	29	40	20	28	52	54	49	69	101	122	223
18	34	28	38	50	42	49	34	20	72	78	76	68	148	146	294
	29	20	37	48	40	49	31	18	65	68	70	67	136	135	271
20	23	50	44	61	47	64	24	33	67	111	71	97	139	208	347
	27	50	45	65	49	74	18	44	71	114	67	117	139	232	371
21	R/T														
30	39	23	73	43	66	57	43	36	112	65	109	92	221	158	379
	44	15	76	45	69	62	44	39	120	60	114	101	233	161	394
31	74	56	107	89	108	96	75	44	181	145	184	141	364	286	650
	78	61	109	89	110	97	82	49	187	150	193	146	380	296	676
32	53	32	72	49	125	51	85	53	124	81	210	104	335	184	519
	43	23	63	42	112	45	79	47	106	65	191	92	297	157	454

As shown in table (5.2), these errors correspond to more than 50% of detected breaths being excluded from the analysis because they did not fulfill the acceptance criteria. In one subject number 15, however, less than 50% of detected breaths were retained but this did not produce a computer run-time error. Results are listed for the two data reduction types of breaths centred on activity maxima and on activity minima.

The values of specific mean expiratory gas flow obtained from region 11 (both lungs taken together) for each subject in each study are shown in table (5.3). Results are listed for the two data reduction types of breaths centred on activity maxima and on activity minima and also for the composite data reduction type. The values are similar for the three types but are upto approximately six times the values of specific ventilation published in the literature. They are included for completeness because, to facilitate comparison between each study, the regional estimates of specific mean expiratory gas flow presented later were normalised to an arbitrary value of 0.1 per second in region 11 (both lungs taken together).

Table 5.2. The percentage of the breathing cycles in the multiple breath activity-time curves which fulfilled the acceptance criteria of being within ±50% of the mean duration. Results are listed against subject number (Subj) and the data reduction type (Max: single breaths centred on activity maxima and Min: single breaths centred on activity minima) for the two consecutive studies in the reproducibility study.

	Study 1		Study 2	
Subj	Max	Min	Max	Min
6	9	8	0	0
10	59	66	94	94
11	79	81	69	65
13	68	58	88	88
14	32	36	8	33
15	23	24	46	49
16	36	41	10	8
17	62	65	59	56
18	52	58	72	72
20	56	58	61	62
21	35	37	42	43
30	60	65	72	68
31	56	61	81	80
32	68	71	66	67

Table 5.3. The values of specific mean expiratory gas flow [per second] for region 11 (both lungs taken together). Results are listed against subject number (Subj) and data reduction type (Max: single breaths centred on activity maxima, Min: single breaths centred on activity minima amd Com: the combined expiratory phase which is calculated from half the data point in the Max single breaths and half the data points in the Min single breaths) for the two consecutive studies in the reproducibility study. R/T: computer run-time error.

	Study 1			Study 2		
Subj	Max	Min	Com	Max	Min	Com
6	R/T					
10	0.17	0.14	0.16	0.16	0.16	0.16
11	0.09	0.08	0.09	0.08	0.10	0.06
13	0.08	0.09	0.08	0.12	0.07	0.05
14	R/T					
15	0.03	0.06	0.06	0.08	0.05	0.19
16	R/T					
17	0.12	0.14	0.12	0.09	0.12	0.11
18	0.11	0.15	0.12	0.11	0.10	0.11
20	0.10	0.11	0.10	0.09	0.10	0.10
21	R/T					
30	0.15	0.18	0.18	0.16	0.16	0.15
31	0.16	0.07	0.06	0.16	0.11	0.09
32	0.10	0.08	0.08	0.14	0.07	0.07

The regional values of specific mean expiratory gas flow normalised to a value of 0.1 [per second] in region 11 (both lungs taken together) are shown in tables (5.4) to (5.13). Results for the regional estimates of specific mean expiratory gas flow, 95% confidence intervals and coefficients of determination are listed for the three data reduction types. Values are shown for 8, 4 and 2 lung regions and for region 11 (both lungs taken together). They generally show an apical to basal increase in specific mean expiratory gas flow. There is generally no difference between regions at the same horizontal level in each study, which is indicated by the overlap of the values for the regions on the left and right at the 95% level. The larger regions generally exhibit values which are mean values of those in the smaller regions from which they are constructed.

Justification of the choice of exponential variation in lung volume substituted into the mathematical lung model was provided by estimating how well the model fitted the clinical data from an observation of the coefficients of determination. Most of the coefficients were very near the maximum value of 1.0, those which were not tended to be obtained from the apical or the smallest lung regions where the counting statistics were poorer.

An estimate of the variability of the model

analysis was obtained by observing whether the 95% confidence intervals for corresponding estimates of specific mean expiratory gas flow, from consecutive investigations in each patient, overlapped. Those that did not are shown in bold type.

The regional estimates of specific mean expiratory gas flow from the 15 regions in each patient were analysed by paired t-test for any consistent change in magnitude between consecutive studies because of the possibility that the distribution might change between investigations. One patient, number 31, showed such a consistent change significant at the 95% confidence level. The results of this patient were excluded from the analysis. The results of the remaining nine patients indicated that the three data reduction types achieved different levels of reproducibility. The type with breaths centred on activity maxima and the composite type achieved a similar standard of 11 and 10 regions of 135 regions which failed to overlap but the type with breaths centred on activity minima produced only two regions of 135 regions which failed to overlap. This latter type was used in the following analyses. The improvement was probably due to the identification of end expiration being easier than end inspiration.

If the results are considered as percentages

of the total number of regions, there was no difference among the four groups of different region sizes as to the number of regions which failed to overlap.

Tables 5.4 to 5.13. The values of mean specific expiratory gas flow [per second], normalised to a value of 0.1 [per second] in region 11 (both lungs), 95% confidence limits and coefficients of determination for the 10 subjects on whom analysis was completed. Results are listed against the data reduction type (Max: single breaths centred on activity maxima, Min: single breaths centred on activity minima amd Com: the combined expiratory phase which is calculated from half the data point in the Max single breaths and half the data points in the Min single breaths) for the two consecutive studies of the reproducibility study. They are displayed for 8, 4 and 2 lung regions and for region 11 (both lungs taken together) numbered as shown in figure (5.2) and displayed here in the following format:

Lung regions

1 3 5 7	2 4 6 8
13 15	14 16
9	10
11	

Shown in bold type are the regions which do not overlap their estimates of specific mean expiratory gas flow at the 95% confidence level in the two consecutive studies.

Table 5.4. Subject: 10

Study 1

Max:

.06	.03	.87	.05	.02	.84
.08	.03	.90	.07	.02	.94
.11	.02	.95	.08	.02	.95
.12	.02	.95	.19	.03	.96
.07	.03	.90	.06	.02	.94
.12	.02	.95	.12	.02	.98
.10	.02	.96	.10	.02	.97
.10	.02	.97			

Min:

.07	.02	.90	.05	.02	.88
.09	.02	.95	.08	.01	.97
.10	.02	.97	.08	.02	.95
.14	.03	.95	.21	.03	.96
.08	.02	.94	.07	.01	.96
.11	.02	.97	.13	.02	.96
.10	.02	.97	.10	.02	.97
.10	.02	.97			

Com:

.07	.02	.91	.06	.01	.95
.08	.02	.96	.08	.01	.99
.10	.01	.98	.08	.02	.96
.12	.02	.97	.17	.03	.97
.08	.01	.97	.07	.01	.99
.10	.01	.99	.12	.02	.98
.10	.01	.99	.10	.01	.99
.10	.01	.99			

Study 2

Max:

.07	.02	.94	.06	.02	.92
.08	.02	.95	.07	.01	.98
.09	.02	.95	.10	.02	.95
.13	.02	.97	.26	.04	.97
.08	.02	.96	.07	.01	.97
.11	.02	.97	.13	.03	.96
.10	.02	.98	.10	.02	.97
.10	.02	.97			

Min:

.08	.02	.94	.07	.02	.95
.09	.02	.97	.07	.01	.98
.10	.02	.97	.09	.01	.98
.13	.02	.98	.24	.04	.96
.08	.01	.97	.07	.01	.98
.12	.01	.99	.13	.02	.98
.10	.01	.99	.10	.01	.99
.10	.01	.99			

Com:

.07	.02	.93	.05	.02	.93
.07	.01	.97	.07	.01	.98
.08	.01	.98	.10	.02	.96
.13	.02	.97	.22	.03	.98
.07	.01	.97	.07	.01	.98
.11	.01	.99	.13	.03	.96
.10	.01	.99	.10	.01	.98
.10	.01	.99			

Table 5.5. Subject: 11

Study 1

Max:

.09	.02	.95	.07	.02	.95
.09	.02	.95	.05	.02	.91
.08	.02	.94	.07	.02	.93
.13	.03	.91	.22	.02	.99
.09	.01	.98	.06	.02	.95
.10	.02	.94	.14	.01	.99
.10	.02	.96	.11	.01	.99
.10	.01	.97			

Min:

.09	.02	.95	.06	.02	.93
.08	.01	.97	.05	.01	.97
.08	.02	.95	.08	.01	.97
.16	.02	.96	.19	.03	.97
.08	.01	.97	.06	.01	.98
.12	.02	.97	.13	.01	.98
.11	.01	.98	.09	.01	.98
.10	.01	.98			

Com:

.08	.02	.96	.05	.02	.91
.07	.02	.96	.04	.02	.90
.07	.02	.96	.07	.01	.98
.14	.02	.97	.19	.02	.98
.07	.01	.96	.05	.01	.95
.10	.01	.98	.12	.01	.99
.11	.01	.99	.09	.01	.98
.10	.01	.99			

Study 2

Max:

.09	.04	.86	.08	.03	.87
.11	.03	.94	.06	.02	.90
.09	.03	.91	.07	.03	.88
.18	.04	.93	.25	.03	.99
.10	.02	.95	.10	.02	.97
.13	.03	.94	.12	.03	.91
.11	.02	.95	.14	.01	.99
.10	.04	.90			

Min:

.06	.03	.83	.04	.02	.89
.10	.02	.98	.04	.02	.90
.07	.03	.89	.07	.02	.91
.16	.03	.96	.18	.03	.96
.09	.01	.98	.06	.02	.96
.12	.03	.95	.10	.03	.93
.10	.02	.98	.08	.02	.93
.10	.02	.98			

Com:

.05	.06	.62	.04	.04	.76
.09	.04	.86	.05	.03	.88
.08	.05	.80	.06	.04	.80
.21	.05	.93	.33	.05	.97
.08	.04	.84	.11	.03	.94
.15	.04	.91	.13	.04	.89
.10	.04	.88	.12	.03	.95
.10	.04	.90			

Table 5.6. Subject: 13

Study 1

Max:

.09	.03	.90	.07	.03	.86
.13	.07	.85	.07	.03	.91
.10	.03	.92	**.19**	**.03**	**.97**
.27	**.07**	**.95**	.18	.09	.72
.10	.03	.92	**.09**	**.02**	**.96**
.09	.03	.87	.12	.05	.82
.07	.03	.86	**.13**	**.03**	**.96**
.10	.04	.89			

Min:

.13	.06	.88	**.03**	**.03**	**.69**
.09	.02	.94	.08	.04	.85
.11	.03	.93	.14	.05	.86
.13	.08	.71	.32	.10	.91
.08	.02	.92	.06	.03	.83
.12	.04	.89	.20	.05	.93
.09	.03	.93	.12	.04	.91
.10	.03	.90			

Com:

.04	**.06**	**.54**	.03	.04	.64
.09	.03	.94	.06	.05	.74
.06	.05	.72	.16	.05	.91
.13	.09	.67	.14	.12	.49
.08	.03	.89	.05	.04	.73
.07	.06	.67	.11	.07	.66
.05	.05	.70	.14	.05	.90
.10	.04	.87			

Study 2

Max:

.11	.05	.88	.04	.03	.81
.08	.03	.92	.02	.02	.74
.14	.02	.98	**.10**	**.04**	**.89**
.07	**.06**	**.61**	.09	.06	.67
.09	.03	.94	**.03**	**.02**	**.81**
.13	.04	.95	.12	.04	.90
.11	.03	.96	**.04**	**.03**	**.79**
.10	.03	.96			

Min:

.22	.13	.79	**.15**	**.06**	**.92**
.04	.06	.63	.08	.05	.84
.14	.05	.88	.12	.05	.87
.12	.07	.72	.31	.11	.87
.12	.06	.86	.09	.04	.87
.13	.05	.87	.16	.06	.87
.09	.05	.83	.10	.04	.86
.10	.05	.85			

Com:

.34	**.14**	**.88**	.07	.09	.63
.05	.07	.61	.05	.07	.69
.12	.08	.73	.12	.08	.71
.10	.11	.54	.21	.16	.59
.13	.08	.79	.06	.07	.68
.12	.08	.72	.15	.10	.72
.09	.07	.70	.07	.09	.60
.10	.08	.72			

Table 5.7. Subject: 15

Study 1

Max:

.23	.18	.77	.05	.17	.37
.11	.44	.27	.27	.17	.82
.34	**.29**	**.70**	.07	.07	.75
.45	**.21**	**.81**	.18	.27	.47
.29	.28	.66	.11	.10	.75
.12	.13	.64	.19	.10	.86
.11	.10	.74	.07	.08	.75
.10	.08	.82			

Min:

.07	.08	.51	.02	.05	.56
.21	.12	.86	.06	.05	.80
.10	.06	.79	.07	.07	.76
.25	.09	.88	.12	.07	.76
.19	.17	.71	.02	.03	.81
.17	.05	.94	.10	.05	.87
.08	.05	.81	.07	.03	.92
.10	.04	.93			

Com:

.04	.08	.44	.02	.06	.46
.19	.12	.83	.14	.05	.89
.15	.07	.84	.02	.04	.66
.26	.09	.89	.13	.08	.76
.27	.16	.79	**.06**	**.03**	**.85**
.10	**.06**	**.76**	.18	.05	.94
.10	.04	.87	.08	.03	.92
.10	.03	.92			

Study 2

Max:

.11	.05	.90	.05	.06	.67
.05	.03	.83	.11	.07	.78
.74	**.06**	**.75**	.02	.05	.58
.07	**.10**	**.42**	.22	.11	.83
.04	.03	.81	.07	.05	.85
.14	.07	.86	.12	.06	.86
.09	.04	.90	.10	.05	.87
.10	.04	.92			

Min:

.12	.16	.60	.05	.08	.69
.10	.05	.91	.10	.05	.83
.11	.28	.35	.12	.05	.90
.42	.14	.89	.19	.08	.83
.17	.10	.91	.12	.09	.86
.22	.23	.65	.12	.04	.92
.17	.13	.79	.11	.03	.94
.10	.03	.94			

Com:

.23	.32	.59	.02	.24	.44
.04	.13	.69	.13	.18	.62
.24	.38	.49	.11	.22	.54
.43	.43	.48	.29	.26	.59
.11	.15	.72	**.30**	**.16**	**.89**
.60	**.43**	**.72**	.16	.17	.68
.34	.22	.81	.10	.15	.66
.10	.15	.67			

Table 5.8. Subject: 17

Study 1

Max:

.08	.05	.84	-.29	.19	.85
.08	.04	.87	.11	.04	.91
.07	.04	.86	.07	.03	.88
.07	.05	.73	.13	.05	.87
.23	.21	.73	.10	.04	.92
.10	.05	.87	.11	.02	.97
.09	.03	.92	.11	.02	.97
.10	.02	.97			

Min:

.06	.03	.91	.09	.04	.92
.07	.04	.85	.08	.03	.90
.07	.03	.89	.06	.05	.75
.10	.05	.87	.15	.05	.93
.07	.03	.90	.10	.03	.96
.08	.03	.92	.10	.04	.88
.08	.02	.94	.11	.03	.95
.10	.02	.98			

Com:

.07	.05	.82	.02	.10	.24
.08	.04	.87	.07	.04	.87
.06	.04	.84	.06	.06	.73
.08	.05	.76	.15	.05	.91
.02	.08	.29	.10	.04	.90
.09	.05	.84	.11	.05	.89
.09	.04	.91	.11	.04	.93
.10	.03	.95			

Study 2

Max:

-.28	.24	.63	.05	.06	.60
.18	.11	.82	-.21	.39	.34
.10	.08	.75	.07	.04	.87
.09	.06	.74	.24	.11	.88
.15	.08	.88	.03	.04	.67
.10	.04	.94	.13	.06	.89
.13	.04	.95	.10	.05	.87
.10	.05	.88			

Min:

.09	.09	.69	.10	.03	.93
.10	.05	.85	.03	.04	.64
.07	.04	.83	.04	.02	.89
.13	.10	.81	.14	.07	.80
.11	.05	.91	.08	.03	.94
.08	.04	.86	.09	.04	.89
.10	.04	.93	.10	.03	.95
.10	.02	.98			

Com:

.03	.15	.20	.05	.04	.73
.11	.07	.82	-.00	.05	.27
.08	.05	.86	.05	.04	.82
.06	.06	.66	.17	.07	.85
.13	.05	.92	.03	.03	.74
.09	.05	.86	.12	.05	.91
.13	.04	.96	.10	.04	.92
.10	.03	.96			

Table 5.9. Subject: 18

Max:

Study 1						Study 2					
.08	.04	.84	.11	.04	.88	.03	.03	.78	.04	.04	.64
.07	.03	.86	.09	.08	.73	.09	.07	.74	.05	.05	.69
.05	.03	.86	.13	.06	.86	.10	.04	.85	.09	.03	.93
.16	.07	.81	.22	.06	.91	.18	.02	.98	.19	.10	.75
.08	.04	.85	.09	.05	.82	.07	.03	.87	.05	.04	.76
.09	.03	.87	.16	.04	.96	.13	.02	.98	.14	.03	.96
.08	.02	.93	.12	.02	.97	.10	.02	.96	.10	.03	.95
.10	.02	.96				.10	.02	.97			

Min:

.06	.04	.76	.06	.02	.94	.05	.04	.75	.04	.05	.61
.07	.05	.76	.04	.03	.79	.09	.05	.84	.07	.03	.89
.03	.02	.79	.11	.03	.94	.09	.02	.95	.11	.03	.94
.11	.05	.79	.21	.04	.97	.15	.05	.89	.24	.08	.87
.07	.04	.84	.05	.02	.92	.06	.02	.95	.07	.03	.90
.13	.04	.94	.14	.02	.99	.13	.04	.94	.15	.04	.94
.09	.02	.95	.10	.02	.98	.09	.02	.96	.11	.03	.95
.10	.01	.99				.10	.02	.97			

Com:

.05	.04	.71	.09	.03	.89	.02	.03	.68	.02	.05	.44
.07	.04	.82	.05	.04	.80	.09	.07	.74	.07	.03	.88
.04	.03	.76	.13	.04	.92	.09	.03	.92	.09	.03	.94
.16	.05	.89	.20	.04	.95	.16	.04	.95	.22	.09	.84
.07	.03	.85	.06	.03	.85	.05	.03	.82	.06	.03	.87
.07	.04	.77	.16	.02	.98	.12	.03	.96	.14	.03	.96
.07	.03	.90	.11	.02	.98	.09	.02	.95	.11	.02	.97
.10	.02	.98				.10	.02	.98			

Table 5.10. Subject: 20

Study 1

Max:

.08	.04	.83	.07	.03	.88
.07	.03	.83	.08	.03	.89
.07	.03	.85	.13	.03	.94
.18	.04	.91	.20	.04	.94
.08	.03	.90	.08	.02	.93
.11	.03	.92	.15	.03	.95
.10	.02	.95	.13	.02	.98
.10	.02	.97			

Min:

.06	.05	.72	.05	.03	.83
.07	.02	.90	.07	.02	.96
.05	.03	.82	.13	.03	.95
.18	.05	.88	.17	.03	.97
.06	.03	.90	.08	.02	.96
.11	.03	.94	.15	.02	.98
.08	.02	.96	.11	.01	.99
.10	.01	.99			

Com:

.09	.05	.81	.06	.03	.86
.06	.03	.83	.09	.02	.95
.06	.03	.87	.15	.03	.97
.18	.03	.95	**.18**	**.03**	**.97**
.07	.03	.89	.08	.02	.95
.11	.02	.96	**.17**	**.02**	**.99**
.09	.01	.97	.13	.01	.99
.10	.01	.99			

Study 2

Max:

.05	.03	.75	.11	.03	.93
.06	.03	.88	.09	.03	.92
.05	.03	.81	.11	.04	.90
.20	.09	.80	.12	.05	.85
.04	.02	.82	.09	.02	.96
.10	.04	.89	.12	.04	.92
.09	.02	.96	.10	.03	.95
.10	.02	.98			

Min:

.09	.04	.85	.08	.04	.87
.09	.02	.97	.09	.02	.96
.07	.02	.92	.10	.03	.91
.20	.04	.95	.20	.02	.97
.08	.02	.96	.09	.02	.97
.11	.02	.96	.11	.02	.96
.09	.02	.97	.11	.01	.99
.10	.02	.99			

Com:

.02	.04	.57	.09	.03	.91
.05	.02	.93	.08	.02	.92
.03	.03	.77	.10	.04	.88
.16	.04	.92	**.10**	**.03**	**.91**
.02	.02	.70	.09	.01	.98
.08	.03	.88	**.10**	**.03**	**.93**
.09	.02	.96	.11	.02	.97
.10	.01	.99			

Table 5.11. Subject: 30

Study 1

Max:

.08	.03	.86	.05	.02	.83
.09	.02	.93	.15	.05	.91
.08	.02	.91	.11	.02	.96
.12	.02	.95	.12	.02	.95
.09	.02	.91	.08	.03	.89
.10	.02	.96	.11	.02	.96
.10	.02	.96	.09	.02	.95
.10	.02	.96			

Min:

.10	.02	.94	.07	.02	.92
.09	.01	.97	.09	.02	.95
.10	.01	.98	.11	.02	.96
.11	.01	.99	.10	.02	.95
.10	.01	.99	.08	.01	.98
.10	.01	.99	.11	.01	.99
.10	.01	.99	.10	.01	.99
.10	.01	.99			

Com:

.08	.02	.91	.03	.02	.76
.09	.02	.95	.09	.02	.94
.07	.01	.96	.10	.02	.95
.10	.01	.99	.10	.01	.97
.09	.01	.97	.07	.01	.95
.10	.01	.99	.11	.01	.99
.10	.01	.99	.09	.01	.98
.10	.01	.99			

Study 2

Max:

.11	.03	.91	.08	.03	.85
.10	.02	.97	.07	.02	.88
.10	.02	.96	.10	.02	.96
.09	.03	.86	.09	.02	.93
.10	.02	.94	.08	.02	.91
.10	.02	.95	.10	.02	.96
.10	.02	.96	.09	.02	.95
.10	.02	.96			

Min:

.11	.01	.97	.09	.02	.90
.11	.01	.98	.09	.02	.95
.08	.01	.95	.11	.01	.97
.11	.02	.96	.10	.02	.96
.11	.01	.99	.09	.01	.97
.10	.01	.99	.10	.01	.98
.11	.01	.99	.10	.01	.98
.10	.01	.99			

Com:

.11	.02	.92	.09	.03	.84
.11	.01	.97	.08	.02	.92
.08	.01	.96	.10	.02	.96
.10	.02	.95	.10	.02	.92
.10	.01	.97	.08	.02	.92
.11	.01	.98	.10	.02	.95
.12	.01	.98	.10	.02	.96
.10	.01	.98			

Table 5.12. Subject: 31

Study 1

Max:

.08	.02	.97	.06	.04	.83
.11	.05	.93	.09	.02	.98
.09	.04	.93	.08	.04	.86
.16	.05	.95	.18	.05	.97
.10	.04	.95	.09	.02	.98
.12	.04	.94	.10	.05	.90
.12	.03	.99	.10	.03	.96
.10	.03	.96			

Min:

.09	.03	.93	.09	.09	.72
.12	.05	.89	.21	.08	.95
.21	.09	.95	.21	.17	.84
.43	.09	.97	.43	.13	.95
.10	.04	.91	.21	.05	.98
.15	.07	.83	.25	.09	.94
.12	.06	.87	.26	.08	.97
.10	.06	.83			

Com:

.06	.05	.80	.16	.10	.82
.10	.06	.85	.24	.06	.97
.24	.06	.98	.17	.11	.84
.47	.07	.99	.45	.07	.99
.09	.05	.87	.25	.04	.99
.10	.08	.70	.29	.08	.96
.11	.07	.83	.28	.06	.98
.10	.07	.80			

Study 2

Max:

.09	.03	.95	.06	.03	.85
.10	.06	.86	.05	.02	.96
.05	.04	.83	.07	.02	.94
.17	.05	.95	.15	.07	.84
.10	.04	.92	.06	.02	.97
.13	.05	.93	.10	.04	.91
.11	.05	.93	.08	.02	.96
.10	.04	.94			

Min:

.08	.03	.93	.13	.06	.94
.09	.02	.96	.08	.05	.93
.09	.02	.96	.05	.02	.93
.20	.05	.95	.19	.06	.91
.09	.02	.98	.05	.02	.90
.14	.03	.97	.10	.03	.95
.12	.02	.98	.08	.03	.94
.10	.02	.97			

Com:

.06	.04	.82	.10	.05	.90
.09	.04	.92	.09	.02	.97
.07	.03	.90	.05	.03	.87
.21	.07	.92	.22	.10	.83
.09	.03	.93	.04	.03	.87
.13	.04	.93	.12	.05	.90
.11	.04	.93	.09	.03	.92
.10	.04	.93			

Table 5.13. Subject: 32

Study 1

Max:

.09	.03	.92	.08	.04	.85
.09	.03	.92	.10	.04	.85
.07	.02	.93	.11	.03	.95
.14	.03	.95	.11	.03	.90
.09	.02	.95	.10	.03	.90
.09	.02	.93	.11	.03	.94
.10	.02	.96	.11	.02	.95
.10	.02	.96			

Min:

.08	.02	.93	.10	.04	.86
.09	.02	.94	.11	.02	.96
.10	.02	.98	.11	.03	.92
.15	.03	.96	.11	.03	.92
.08	.02	.96	.10	.02	.94
.13	.02	.99	.11	.03	.94
.11	.01	.98	.11	.02	.95
.10	.02	.97			

Com:

.06	.03	.89	.10	.05	.81
.07	.03	.88	.10	.04	.87
.09	**.02**	**.96**	.10	.02	.94
.15	.03	.95	.11	.03	.93
.07	.02	.94	.09	.04	.87
.11	**.02**	**.97**	.10	.03	.95
.12	.01	.99	.10	.02	.95
.10	.02	.98			

Study 2

Max:

.07	.04	.80	.11	.03	.92
.09	.02	.96	.10	.02	.96
.06	.02	.93	.10	.02	.97
.12	.03	.93	.09	.04	.86
.09	.03	.93	.10	.02	.96
.09	.02	.95	.09	.03	.93
.09	.02	.96	.10	.02	.97
.10	.02	.98			

Min:

.10	.04	.90	.18	.08	.84
.09	.05	.83	.07	.05	.74
.12	.05	.91	.09	.03	.89
.19	.04	.95	.15	.04	.93
.11	.03	.92	.08	.04	.82
.17	.04	.97	.13	.03	.94
.10	.04	.89	.10	.03	.91
.10	.03	.91			

Com:

.08	.05	.77	.17	.07	.88
.08	.04	.81	.08	.04	.81
.14	**.02**	**.98**	.08	.03	.88
.19	.04	.97	.14	.03	.95
.10	.03	.91	.08	.04	.85
.19	**.04**	**.96**	.12	.03	.96
.10	.03	.91	.10	.03	.92
.10	.03	.92			

5.6.2 Cross-Correlation.

The results of the cross-correlation analysis are shown in tables (5.14) to (5.27), indicated as the time displacement [in multiples of 0.2 second] at which activity-time curves from two lung regions achieve maximum cross-correlation.

Results are listed for eight and for four lung regions. At both levels of spatial resolution the technique is shown to not be reproducible. This is indicated by the time of maximum cross-correlation in the first study not corresponding with that in the second study. In an attempt to improve the reproducibility, smoothing of the activity-time curves prior to cross-correlation was attempted. Both a linear and a weighted three-point average, in which the middle point was given twice the weight of the outer points, were used. The results for a typical patient are shown in table (5.28). They indicate that there was no improvement with any of the smoothing techniques tried. The cross-correlation analysis was, therefore, not applied in the sensitivity study.

Tables 5.14 to 5.27. Time displacements [in multiples of 0.2 per second] at which maximum cross-correlation occurs when an activity-time curve from one lung region (tabulated as columns) is moved against an activity-time curve from another lung region (tabulated as rows). Results are listed for the two consecutive studies of the reproducibility study. They are shown for both eight (1-8) and for four (12-15) lung regions numbered as shown in figure (5.2).

Study 1

Table 5.14. Subject: 6

	2	3	4	5	6	7	8
1	0	2	2	0	0	0	1
2		0	0	-2	-1	0	-1
3			-1	0	0	-1	-1
4				-2	0	-1	0
5					0	0	0
6						0	0
7							1

	13	14	15
12	0	0	0
13		-1	-1
14			0

Study 2

	2	3	4	5	6	7	8
1	-2	0	2	0	1	-1	0
2		0	0	-1	1	1	2
3			1	-1	-1	0	0
4				-2	0	-2	1
5					0	1	0
6						0	0
7							0

	13	14	15
12	1	-1	1
13		1	0
14			0

Table 5.15. Subject: 10

	2	3	4	5	6	7	8
1	-1	0	0	0	0	1	0
2		0	0	0	0	0	0
3			0	0	0	0	1
4				0	0	0	1
5					0	0	1
6						0	0
7							0

	13	14	15
12	0	0	0
13		0	0
14			0

	2	3	4	5	6	7	8
1	0	0	0	0	0	0	0
2		0	0	0	0	0	0
3			0	0	0	0	0
4				0	0	0	1
5					0	0	0
6						0	0
7							0

	13	14	15
12	0	0	0
13		0	0
14			0

Table 5.16. Subject: 11

	2	3	4	5	6	7	8
1	1	1	0	-1	0	0	-1
2		0	0	0	0	-1	0
3			0	0	0	-1	0
4				0	0	0	0
5					0	0	0
6						0	0
7							0

	13	14	15
12	0	0	0
13		0	0
14			0

	2	3	4	5	6	7	8
1	0	0	0	0	0	0	0
2		0	0	0	0	0	0
3			0	0	0	0	0
4				0	0	0	0
5					0	0	0
6						0	0
7							0

	13	14	15
12	0	0	0
13		0	0
14			0

Study 1

Table 5.17. Subject: 13

	2	3	4	5	6	7	8
1	1	-1	0	0	0	-1	1
2		1	0	0	-1	0	-1
3			0	0	0	-1	-1
4				-1	0	0	-1
5					0	1	0
6						-1	0
7							0

	13	14	15
12	0	-1	0
13		-1	-1
14			0

Table 5.18. Subject: 14

	2	3	4	5	6	7	8
1	1	1	0	0	0	0	-1
2		0	0	0	0	1	0
3			-1	0	0	-1	0
4				0	0	0	-1
5					-1	-1	0
6						0	0
7							0

	13	14	15
12	0	0	0
13		0	0
14			0

Table 5.19. Subject: 15

	2	3	4	5	6	7	8
1	0	2	-1	1	1	0	1
2		0	0	0	0	-1	-1
3			0	-1	0	1	-1
4				0	-1	-1	0
5					1	0	1
6						0	-1
7							0

	13	14	15
12	0	1	0
13		0	-1
14			0

Study 2

	2	3	4	5	6	7	8
1	-1	0	-1	0	0	0	0
2		1	0	0	0	0	0
3			-1	0	0	0	0
4				0	0	0	0
5					0	0	0
6						0	0
7							0

	13	14	15
12	-1	0	0
13		0	0
14			0

	2	3	4	5	6	7	8
1	-1	0	0	-2	-1	-1	-1
2		0	0	-1	-1	0	-1
3			1	0	0	-1	-1
4				0	0	0	-1
5					0	0	-1
6						0	-1
7							0

	13	14	15
12	0	0	-1
13		0	-1
14			0

	2	3	4	5	6	7	8
1	-1	0	2	1	2	2	2
2		0	-1	-1	-1	0	-1
3			0	1	0	0	1
4				0	0	0	0
5					-1	-1	-1
6						-1	1
7							0

	13	14	15
12	0	1	0
13		0	-1
14			-1

Study 1

Table 5.20. Subject: 16

	2	3	4	5	6	7	8
1	-1	0	-1	0	-1	0	0
2		-1	0	0	-1	-1	-1
3			0	-1	-1	0	1
4				-1	0	-1	0
5					1	-1	0
6						0	1
7							0

	13	14	15
12	0	0	-1
13		0	0
14			0

Table 5.21. Subject: 17

	2	3	4	5	6	7	8
1	0	0	-1	1	0	0	1
2		0	-1	0	0	0	1
3			1	0	1	2	1
4				0	1	1	0
5					0	-1	0
6						0	1
7							1

	13	14	15
12	0	0	1
13		1	0
14			0

Table 5.22. Subject: 18

	2	3	4	5	6	7	8
1	2	1	1	-1	0	-1	2
2		0	0	-1	-1	-2	1
3			0	1	-1	-1	1
4				-1	-1	0	1
5					-1	0	1
6						0	0
7							0

	13	14	15
12	0	-1	0
13		-1	0
14			0

Study 2

	2	3	4	5	6	7	8
1	-1	3	0	-1	-1	0	-1
2		0	-1	2	-1	2	-1
3			0	1	0	-1	-1
4				0	-1	1	0
5					1	0	-2
6						-1	-1
7							0

	13	14	15
12	0	1	-1
13		0	-1
14			1

	2	3	4	5	6	7	8
1	1	2	1	0	2	1	0
2		0	-1	0	0	-1	1
3			-1	0	-1	-1	-1
4				0	1	1	0
5					-1	-1	0
6						1	0
7							0

	13	14	15
12	0	0	1
13		0	0
14			0

	2	3	4	5	6	7	8
1	1	2	-1	0	1	0	1
2		1	0	0	0	0	0
3			1	-1	1	0	1
4				0	1	0	0
5					0	-1	-1
6						0	0
7							0

	13	14	15
12	1	0	1
13		0	1
14			0

Study 1

Table 5.23. Subject: 20

	2	3	4	5	6	7	8
1	0	0	0	0	1	0	0
2		0	0	-1	-1	0	0
3			1	1	0	1	1
4				0	1	-1	0
5					-1	0	0
6						0	0
7							0

	13	14	15
12	0	1	0
13		0	0
14			0

Study 2

	2	3	4	5	6	7	8
1	0	1	1	0	1	1	-1
2		1	0	0	1	1	0
3			2	-1	0	1	-1
4				-1	-1	-1	0
5					1	0	1
6						0	0
7							0

	13	14	15
12	1	0	0
13		-1	0
14			1

Table 5.24. Subject: 21

	2	3	4	5	6	7	8
1	0	0	0	1	-1	-1	1
2		0	0	0	0	0	0
3			1	0	0	0	0
4				0	0	0	1
5					0	-1	0
6						0	0
7							-1

	13	14	15
12	0	0	0
13		0	0
14			0

	2	3	4	5	6	7	8
1	0	1	-1	0	0	0	0
2		0	1	1	0	0	0
3			0	-1	0	1	-1
4				-1	0	0	-1
5					-1	-1	-1
6						1	0
7							0

	13	14	15
12	0	0	0
13		1	0
14			-1

Table 5.25. Subject: 30

	2	3	4	5	6	7	8
1	0	0	0	0	0	0	-1
2		0	-1	0	0	0	-1
3			0	0	-1	0	-1
4				0	0	0	0
5					0	0	0
6						0	0
7							-1

	13	14	15
12	0	0	-1
13		0	0
14			0

	2	3	4	5	6	7	8
1	-1	0	0	0	0	0	-1
2		1	0	0	0	0	0
3			0	0	0	0	-1
4				0	0	0	0
5					0	0	0
6						0	0
7							0

	13	14	15
12	0	0	0
13		0	0
14			0

Study 1

Table 5.26. Subject: 31

	2	3	4	5	6	7	8
1	0	0	0	0	-1	0	0
2		1	1	0	0	0	0
3			0	0	0	0	0
4				0	0	0	0
5					0	0	0
6						1	0
7							0

	13	14	15
12	0	0	0
13		0	0
14			0

Study 2

	2	3	4	5	6	7	8
1	-1	0	-1	0	0	0	0
2		0	0	1	0	1	0
3			0	0	0	0	0
4				0	0	0	1
5					0	0	0
6						0	0
7							0

	13	14	15
12	0	0	0
13		0	0
14			0

Table 5.27. Subject: 32

	2	3	4	5	6	7	8
1	0	1	0	0	0	0	-1
2		0	0	0	0	0	-1
3			0	-1	0	-1	-1
4				-1	0	-1	0
5					1	0	0
6						-1	0
7							0

	13	14	15
12	0	0	0
13		-1	0
14			0

	2	3	4	5	6	7	8
1	0	1	1	-1	0	0	0
2		-1	-2	-1	1	0	-1
3			0	0	0	0	0
4				-1	1	0	0
5					1	-1	1
6						0	0
7							0

	13	14	15
12	0	0	0
13		-1	0
14			0

Table 5.28. Time displacements [in multiples of 0.2 per second] at which maximum cross-correlation occurs when a smoothed activity-time curve from one lung region (tabulated in columns) is moved against a smoothed activity-time curve from another lung region (tabulated in rows). Results are listed for the two consecutive studies from the reproducibility study. Results are shown for eight (1-8) lung regions numbered as in figure (5.2). Subject: 10.

Both activity-time curves smoothed once:

	Study 1								Study 2						
	2	3	4	5	6	7	8		2	3	4	5	6	7	8
1	0	0	0	0	0	0	1	1	0	0	0	0	0	0	0
2		0	0	0	0	1	1	2		0	0	0	0	0	0
3			0	0	0	0	1	3			0	0	0	0	0
4				0	0	0	0	4				0	0	0	1
5					0	0	0	5					0	0	0
6						0	1	6						0	0
7							0	7							0

Both activity-time curves smoothed twice

1	0	0	0	0	0	0	1	1	0	0	0	0	0	0	0
2		0	0	0	0	1	1	2		0	0	0	0	0	1
3			0	0	0	0	1	3			0	0	0	0	0
4				0	0	0	0	4				0	0	0	1
5					0	0	0	5					0	0	0
6						0	1	6						0	0
7							0	7							0

Both activity-time curves weighted smoothed once:

1	0	0	0	0	0	0	1	1	0	0	0	0	0	0	0
2		0	0	0	0	1	1	2		0	0	0	0	0	0
3			0	0	0	0	1	3			0	0	0	0	0
4				0	0	0	0	4				0	0	0	1
5					0	0	0	5					0	0	0
6						0	1	6						0	0
7							0	7							0

Both activity-time curves weighted smoothed twice

1	0	0	0	0	0	0	1	1	0	0	0	0	0	0	0
2		0	0	0	0	1	1	2		0	0	0	0	0	1
3			0	0	0	0	1	3			0	0	0	0	0
4				0	0	0	0	4				0	0	0	1
5					0	0	0	5					0	0	0
6						0	1	6						0	0
7							0	7							0

5.7 Results of the Sensitivity Study.

The results of the sensitivity study are listed in tables (5.29) to (5.32).

The percentage of detected breaths which fulfilled the acceptance criteria are listed in table (5.29). Of the seven subjects where this number was less than 50%, five displayed run-time errors. The error occurrence was not related to disease state in that they occurred in all three subject groups. They were probably caused by an irregular breathing pattern which was produced by the anxiety of the patient. Results were not obtained for these seven subjects.

Tables (5.30) to (5.32) list the regional values of specific mean expiratory gas flow, 95% confidence limits and coefficients of determination.

All three groups, normal subjects, patients with a normal inhalation image report and patients with an abnormal image report generally exhibit an apical to basal increase in specific mean expiratory gas flow. Also, in all the groups, the values obtained from the larger regions are generally the mean value of those in the smaller regions from which they are constructed. The normal subject group and the patients with normal image reports show a consistency in the apical to basal variation but the patients with abnormal image

reports, show a variable pattern.

Differences in specific mean expiratory gas flow between lung regions at the same horizontal level occurred only in the group of eight lung regions. The percentage of regions which did not overlap at the 95% level were 19% in normals, 13% in patients with normal image reports and 2% in patients with abnormal image reports.

Differences in specific mean expiratory gas flow between vertical regions occurred between the basal regions in the group of eight lung regions. The percentage of regions which did not overlap at the 95% level were 88% in normals, 58% in patients with normal image reports and 46% in patients with abnormal image reports. Differences also occurred in the group of four lung regions. The percentage of regions which did not overlap at the 95% level were 75% in normals, 62% in patients with normal image reports and 46% in patients with abnormal image reports.

Table 5.29. The percentage of the breathing cycles (%) in the multiple breath activity-time curves which fulfilled the acceptance criteria. Results are listed against subject number (#). R/T: computer run-time error.

#	%	
Normal subjects:		
1	80	
2	100	
3	74	
4	73	
5	44	
6	8	R/T
Patients with a normal image report:		
7	69	
8	89	
9	85	
10	94	
11	81	
12	71	
13	88	
14	36	R/T
15	49	
16	41	R/T
17	65	
18	72	
19	57	
20	62	
21	43	R/T
22	67	
23	75	
Patients with an abnormal image report:		
24	73	
25	63	
26	34	R/T
27	80	
28	79	
29	86	
30	68	
31	80	
32	71	
33	84	
34	63	
35	89	
36	93	

Tables 5.30 to 5.32. Values of specific mean expiratory gas flow [per second], 95% confidence limits and coefficients of determination for the 29 subjects on whom analysis was completed. Results are displayed for 8, 4 and 2 lung regions and for region 11 (both lungs taken together) number as shown in figure (5.2) and displayed here in the following format:

Lung regions

1 3 5 7	2 4 6 8
13 15	14 16
9	10
11	

Table 5.30. Normal subjects.

Subject: 1

.05	.03	.94	.05	.02	.94
.02	.02	.83	.06	.02	.92
.09	.03	.92	.06	.02	.91
.12	.03	.93	.23	.04	.96
.07	.02	.97	.05	.02	.96
.10	.02	.95	.12	.03	.96
.08	.02	.96	.10	.02	.98
.08	.02	.97			

Subject: 2

.10	.03	.93	.02	.03	.69
.04	.03	.88	.05	.03	.86
.06	.02	.94	.06	.04	.86
.16	.05	.92	.21	.03	.98
.08	.03	.94	.03	.02	.87
.09	.03	.95	.11	.02	.98
.08	.02	.95	.07	.01	.98
.07	.02	.97			

Subject: 3

.07	.01	.97	.03	.01	.94
.02	.01	.93	.04	.01	.95
.05	.01	.96	.04	.01	.97
.12	.02	.97	.13	.01	.99
.05	.01	.98	.04	.01	.96
.08	.01	.98	.08	.01	.99
.06	.01	.99	.06	.01	.99
.06	.01	.99			

Subject: 4

.08	.03	.90	.09	.03	.93
.16	.03	.96	.13	.02	.98
.17	.03	.97	.16	.02	.98
.35	.08	.94	.48	.06	.98
.13	.02	.98	.11	.02	.99
.24	.04	.96	.28	.04	.98
.19	.03	.97	.21	.02	.99
.19	.03	.97			

Table 5.31. Patients with a normal image report.

Subject: 7

.19	.05	.95	.09	.04	.89
.13	.05	.94	.12	.05	.92
.12	.04	.94	.13	.04	.96
.20	.04	.97	.14	.04	.96
.16	.04	.96	.12	.04	.95
.15	.03	.98	.14	.03	.98
.15	.02	.99	.13	.03	.98
.14	.01	.99			

Subject: 8

.08	.02	.94	.08	.04	.90
.10	.02	.98	.05	.02	.93
.10	.03	.94	.08	.03	.92
.14	.03	.97	.20	.02	.99
.08	.02	.97	.06	.02	.92
.11	.03	.96	.13	.02	.98
.11	.02	.98	.10	.02	.98
.10	.01	.99			

Subject: 9

.13	.03	.98	.08	.05	.88
.11	.04	.93	.10	.04	.93
.18	.05	.96	.15	.04	.95
.32	.07	.95	.39	.04	.99
.11	.02	.97	.08	.03	.95
.22	.05	.96	.23	.05	.97
.16	.03	.97	.18	.02	.99
.16	.03	.98			

Subject: 10

.13	.03	.94	.12	.03	.95
.14	.03	.97	.11	.02	.98
.16	.03	.97	.14	.02	.98
.21	.03	.98	.37	.06	.96
.13	.02	.97	.11	.02	.98
.18	.02	.99	.21	.03	.98
.16	.02	.99	.16	.01	.99
.16	.01	.99			

Subject: 11

.07	.02	.95	.05	.02	.93
.07	.01	.97	.04	.01	.97
.07	.01	.95	.07	.01	.97
.13	.02	.96	.16	.02	.97
.07	.01	.97	.05	.01	.98
.10	.01	.97	.11	.01	.98
.09	.01	.98	.08	.01	.98
.08	.01	.98			

Subject: 12

.12	.09	.86	.10	.10	.74
.23	.07	.97	.08	.04	.91
.22	.11	.93	.11	.11	.68
.33	.09	.96	.20	.08	.93
.19	.06	.96	.11	.05	.92
.29	.11	.95	.22	.05	.99
.23	.07	.97	.15	.02	.99
.21	.04	.99			

Subject: 13

.14	.09	.79	.10	.04	.92
.03	.04	.63	.05	.03	.84
.09	.03	.88	.08	.03	.87
.08	.05	.72	.21	.07	.87
.08	.04	.86	.06	.03	.87
.09	.03	.87	.10	.04	.87
.06	.03	.83	.07	.03	.86
.07	.03	.85			

Subject: 17

.09	.04	.91	.13	.05	.92
.10	.06	.85	.11	.04	.90
.09	.04	.89	.09	.07	.75
.14	.07	.87	.21	.07	.93
.10	.05	.90	.14	.04	.96
.11	.04	.92	.14	.06	.88
.11	.03	.94	.15	.05	.95
.14	.03	.98			

Table 5.31 (cont). Patients with a normal image report.

Subject: 18

.05	.04	.75	.04	.05	.61
.09	.05	.84	.08	.03	.89
.09	.02	.95	.12	.03	.94
.16	.05	.89	.25	.09	.87
.06	.02	.95	.07	.03	.90
.13	.04	.94	.15	.04	.94
.09	.02	.96	.11	.03	.95
.10	.02	.97			

Subject: 19

.06	.01	.98	.06	.01	.94
.05	.01	.98	.06	.01	.97
.07	.02	.95	.07	.01	.97
.13	.02	.96	.20	.02	.98
.06	.01	.99	.06	.01	.97
.09	.01	.98	.12	.02	.97
.07	.01	.99	.09	.01	.98
.09	.01	.99			

Subject: 20

.08	.04	.85	.08	.04	.87
.08	.02	.97	.08	.02	.96
.07	.02	.92	.10	.03	.91
.19	.04	.95	.13	.02	.97
.07	.02	.96	.08	.02	.97
.10	.02	.96	.11	.02	.96
.09	.02	.97	.10	.01	.99
.10	.01	.99			

Subject: 22

.05	.05	.70	.06	.08	.57
.07	.03	.88	.03	.05	.68
.08	.04	.86	.06	.04	.88
.32	.08	.94	.40	.08	.96
.07	.03	.91	.04	.01	.98
.19	.05	.94	.23	.03	.98
.15	.02	.98	.16	.01	.99
.15	.02	.99			

Subject: 23

.07	.02	.94	.12	.04	.91
.07	.02	.94	.09	.02	.94
.13	.03	.95	.10	.03	.93
.32	.06	.95	.40	.07	.96
.08	.02	.96	.09	.02	.95
.22	.04	.96	.23	.04	.97
.16	.02	.98	.18	.03	.97
.17	.02	.98			

Table 5.32. Patients with an abnormal image report.

Subject: 24

.16	.03	.96	.12	.03	.94
.18	.04	.96	.19	.04	.96
.28	.04	.97	.24	.05	.95
.35	.04	.99	.30	.04	.98
.18	.03	.98	.17	.04	.96
.30	.04	.98	.28	.04	.98
.24	.03	.99	.23	.03	.98
.24	.03	.99			

Subject: 25

.07	.05	.73	.07	.13	.41
.11	.05	.92	.12	.20	.43
.13	.03	.96	.04	.11	.36
.15	.08	.78	.10	.12	.53
.07	.04	.80	.10	.15	.55
.19	.05	.96	.06	.09	.53
.15	.05	.95	.07	.07	.77
.15	.05	.95			

Subject: 27

.12	.03	.90	.07	.02	.93
.15	.02	.97	.13	.01	.99
.13	.02	.95	.17	.01	.99
.19	.03	.96	.25	.03	.98
.14	.02	.97	.11	.01	.98
.16	.03	.96	.19	.02	.99
.15	.02	.98	.15	.01	.99
.15	.01	.99			

Subject: 28

.12	.02	.98	.07	.03	.82
.10	.02	.97	.10	.02	.96
.11	.02	.97	.13	.02	.97
.14	.03	.98	.13	.03	.93
.11	.01	.99	.09	.02	.96
.17	.02	.98	.13	.02	.98
.14	.02	.98	.11	.02	.98
.13	.02	.98			

Subject: 29

.09	.02	.93	.08	.02	.93
.11	.02	.97	.10	.02	.95
.12	.03	.94	.10	.02	.96
.25	.03	.98	.27	.04	.96
.10	.01	.98	.09	.02	.96
.15	.03	.95	.16	.02	.97
.12	.02	.98	.14	.02	.97
.13	.02	.98			

Subject: 30

.18	.02	.97	.15	.04	.90
.17	.02	.98	.15	.03	.95
.13	.02	.95	.17	.02	.97
.17	.03	.96	.17	.03	.96
.18	.01	.99	.15	.02	.97
.16	.01	.99	.17	.02	.98
.17	.01	.99	.16	.01	.98
.16	.01	.99			

Subject: 31

.08	.03	.93	.14	.07	.94
.10	.03	.96	.09	.05	.93
.10	.02	.96	.06	.02	.93
.22	.05	.95	.20	.06	.91
.10	.02	.98	.05	.03	.90
.15	.03	.97	.11	.03	.95
.13	.02	.98	.09	.03	.94
.11	.02	.97			

Subject: 32

.07	.02	.93	.08	.03	.86
.07	.02	.94	.09	.02	.96
.08	.01	.98	.09	.03	.92
.12	.02	.96	.09	.03	.92
.07	.01	.96	.08	.02	.94
.11	.01	.99	.09	.02	.94
.09	.01	.98	.09	.02	.95
.08	.02	.97			

Table 5.32 (cont). Patients with an abnormal image report.

Subject: 33

.09	.06	.81	.16	.07	.93
.14	.07	.90	.19	.08	.93
.17	.07	.95	.12	.10	.75
.23	.07	.96	.12	.13	.64
.18	.05	.98	.17	.06	.95
.16	.09	.88	.16	.12	.81
.20	.02	.99	.17	.06	.94
.21	.03	.99			

Subject: 34

.23	.06	.97	.33	.09	.96
.33	.11	.96	.27	.05	.99
.15	.04	.98	.14	.07	.92
.23	.15	.86	.26	.09	.96
.28	.08	.97	.29	.04	.99
.17	.06	.95	.16	.07	.92
.25	.05	.98	.21	.04	.98
.21	.03	.99			

Subject: 35

.06	.03	.88	.09	.03	.96
.06	.03	.93	.07	.03	.91
.08	.02	.96	.07	.03	.91
.28	.05	.97	.22	.02	.99
.08	.02	.97	.09	.03	.96
.16	.03	.98	.13	.03	.98
.11	.02	.99	.11	.02	.98
.11	.01	.99			

Subject: 36

.10	.03	.90	.09	.02	.97
.11	.02	.95	.10	.01	.98
.13	.01	.99	.13	.02	.98
.23	.03	.97	.29	.04	.97
.11	.02	.96	.10	.01	.98
.15	.02	.98	.19	.02	.99
.13	.02	.98	.14	.01	.99
.19	.01	.99			

CHAPTER 6 Discussion.

Previously reported methods of using poorly soluble radioactive gases to study regional lung ventilation have involved inhalation data acquired over a number of breathing cycles and have often involved consideration of washout curves.

When the behaviour of gas in the lungs as a whole is being considered the fact that data is acquired over a number of breathing cycles is unimportant. This is not true when regional measurements are required, however. Inter-regional communication via the dead space during a series of breathing cycles means that the behaviour of radioactive tracer gas in each region will influence the behaviour in all other regions.

Specific mean expiratory gas flow is calculated, in this work, from the activity variation occuring during expiration only, and as such will not be affected by the behaviour of radioactive gas in other regions. It is therefore a measure of the behaviour of radioactive tracer gas in the lung region under consideration only.

Consideration of expiration only also avoids the problems associated with non-uniform radioactive tracer gas concentration during inspiration because the calculation is based only on the activity variation as the radioactive gas is expired and does not consider the absolute activity

levels.

These statements will not be true, however, if the distribution of inspired gas in the region under consideration is inhomogeneous since, in this situation, there will be neither a constant expired concentration nor a mono-exponential concentration-time relationship, both of which are implicit in the model.

Phase differences in the motion of lung regions have previously been detected only using physiological triggering of transmission data rather than using inhalation techniques. The post-acquisition techniques described here offer the possibility of the measurement of phase differences in gas flow between lung regions without requiring any extra patient connected equipment.

6.1 Analysis Techniques.

To obtain indices of the behaviour of lung regions, which were independent of the behaviour of other regions, it was necessary to consider the behaviour of radioactive gas over a single breathing cycle. Problems of counting statistics, however, made this difficult to achieve but by collecting equilibrium data over a number of breathing cycles and considering the activity-time curves generated, as a sequential series of individual breaths it was possible to overcome the

problems of counting statistics sufficiently to obtain reliable results. A mathematical model of the behaviour of radioactive tracer gas was proposed and used to provide estimates of specific mean expiratory gas flow. Cross-correlation techniques were used to provide estimates of the phase differences in gas flow between different lung regions.

6.1.1 Model.

A mathematical model was proposed which described the activity variation of radioactive tracer gas in the lung during a single breath. Sufficiently small lung regions were considered in order to assume an homogeneous concentration of radioactive gas in the region at end expiration. The model required a definition of the variation in regional lung volume for which an exponential pattern was assumed. For comparison, however, a sinusoidal variation was also considered.

6.1.2 Cross-correlation.

Cross-correlation techniques were used to obtain the time displacement at which activity-time curves from two lung regions achieved maximim cross-correlation.

6.2 Simulation studies.

The adequacy of the model analysis and the susceptibility of both the model and the cross-correlation analyses to the effects of Poisson

noise were assessed in simulation studies.

6.2.1 Model.

The adequacy of the model was established by the similarity in the variation of the equilibrium activity levels predicted by the model and a previously published equilibrium model. It was also established by the similarity of the values of specific ventilation calculated from washout curves simulated by the model and the equations which define specific ventilation.

Multiple activity levels for the same value of specific ventilation occurred, however. This revealed a difficulty inherent in the interpretation of equilibrium $^{81}Kr^{m}$ inhalation images. It is possible to envisage a situation in which functional residual capacity increases in a lung region as the result of disease such as asthma, bronchitis or emphysema, thus reducing the specific ventilation. If this region is compared with an identical region on the image which is healthy and where functional residual capacity remains normal, both tidal volumes remaining equal, the diseased region will exhibit a higher activity and it will appear that the diseased region is the better ventilated. Two volume effects are involved in the measurement of activity, one the anatomical variation and the other the increase, as a result

of disease, in functional residual capacity which provides a larger reservoir for the radioactive gas. Although the concentration of radioactive gas in the lung region decreases when specific ventilation decreases, it is integrated over the regional volume to produce the activity as measured by the external detector and functional residual capacity is a component of this volume.

The equilibrium activity levels predicted by the model also suggest that the exponential or sinusoidal breathing pattern plays little part in determining the equilibrium activity level. They do not, however, indicate which pattern best fits the single breath data. Justification of the choice of exponential variation in lung volume was obtained by the results of the washin simulation study, in which the model with substituted exponential variation in lung volume produced activity-time curves similar to those observed in the clinical study.

The results of the analysis of washout activity-time curves simulated using the model were similar to the values calculated from the equations which define specific ventilation. The equation developed to describe radioisotope washout curves fitted the results better than the classical definition of specific ventilation.

The assessment of the effects of Poisson noise

indicated that at the activities encountered in the clinical studies the model analysis would be reliable.

6.2.2 Cross-Correlation.

The assessment of the effects of Poisson noise indicated that at the higher activities observed in the clinical studies which were usually encountered in the larger lung regions the results would be reliable. At the activities which were usually encountered in the smaller lung regions, however, indications were that the results would be unreliable.

6.3 Clinical Studies.

The reproducibility of the model and the cross-correlation analyses and the sensitivity of the model analysis were assessed in clinical studies.

6.4 Reproducibility Study.

The reproducibility study involved 14 patients with a variety of respiratory disorders who each underwent two consecutive investigations.

6.4.1 Model.

The results obtained from the model analysis showed that analysis was not possible in four out of 14 subjects. This corresponded to an activity-time curve in which less than 50% of detected breaths fulfilled certain acceptance criteria. In

only one of the 14 subjects in whom less than 50% of detected breaths fulfilled the acceptance criteria could the analysis be completed. In the rest the method was reproducible especially when the results of one subject whose values of specific mean expiratory gas flow changed from one investigation to the next were excluded. Only two regions of 135 failed to overlap its 95% confidence intervals for corresponding estimates in consecutive studies.

6.4.2 Cross-Correlation.

The results of the cross-correlation analysis were shown to not be reproducible in the same subject. Smoothing of the equilibrium activity-time curves before they were cross-correlated was tried but even so the method proved unreliable. It was therefore not included in the following sensitivity study.

6.5 Sensitivity Study.

The sensitivity of the model analysis to disease state was assessed in a sensitivity study involving six normal subjects and 30 patients with a variety of respiratory disorders. The patients were divided into two sub-groups, those whose inhalation images were reported as normal and those whose images were reported as abnormal. Each participant underwent only one investigation.

The adequacy of the model analysis was

confirmed by the similarity of the apical to basal variation in regional specific mean expiratory gas flow obtained in the normal subjects and the variation in regional specific ventilation previously published and shown in table (2.1). The normal subjects showed a similar but more consistent apical to basal variation in specific mean expiratory gas flow than the patients. The latter, however, was still similar to the variation in regional specific ventilation previously published and shown in table (2.2).

Although the three groups of normal subjects, patients with normal inhalation image reports and patients with abnormal inhalation image reports were fairly general there were some differences in the results of the model analysis apparent among them.

There was a reduction in the percentage of the estimates of specific mean expiratory gas flow which overlapped at the 95% level from the normal subject group to the patient with normal inhalation image report group and to the patient with abnormal image report group.

This occurred between regions at the same horizontal level, between the basal regions on the same side of the lung in the group of eight lung regions and between regions on the same side of the

lung in the group of four lung regions.

These results would seem to indicate that as the respiratory disease progressed in severity the regional variations within the lung reduce. This is consistent with previously published work (Miller J.M., et. al., 1970 and Secker-Walker R.H., et. al., 1975) and with the theory that patients with respiratory disorders breathe at higher values of functional residual capacity (Touya J.J., et. al., 1981) in order to overcome the deficiencies in their respiratory system.

The absolute values of total specific mean expiratory gas flow, from the normal subjects, are approximately three times the absolute values of total specific ventilation reported by Rosenzweig D.Y., et. al., 1969, Ciofetta G., et. al., 1980 and Bajzer Z., and Nosil J., 1980, of approximately 0.03 per second.

Table 6.1. Specific mean expiratory gas flow (f) ± 95% confidence intervals [per second] and coefficients of determination (cd) calculated by the application of the mathematical model to the first eight breaths of $^{81}Kr^{m}$ equilibrium and washout data published by Bajzer Z., and Nosil J., 1980 and reproduced in figure (2.1).

#	f	cd
1	.14±.05	.97
2	.14±.04	.98
3	.13±.09	.94
4	.20±.23	.92
5	.05±.02	.96
6	.12±.08	.85
7	.06±.03	.84
8	.11±.06	.91

This is a relationship which is demonstrated in $^{81}Kr^{m}$ equilibrium and washout data published by Bajzer Z., and Nosil J., 1980 and reproduced in figure (2.1). The total specific ventilation calculated by these authors from the washout part of their data is approximately 0.03 per second. The first 8 breaths of this data have been analysed using the mathematical model developed in this thesis and the results for total specific mean expiratory gas flow vary between .05+.02 and .20+.23, with the coefficient of determination varying between .84 and .98, as shown in table (6.1). These values are similar to the values obtained from the clinical data presented earlier.

The difference of three between specific mean expiratory gas flow and specific ventilation can be explained on the following theoretical grounds.

Specific mean expiratory gas flow, defined by:

$$\frac{V_T}{(V_T+V_R)T_e}$$

is the ratio of the change in lung volume during the expiratory phase of the breathing cycle to total lung capacity.

Specific ventilation, defined by:

$$\frac{V_T}{(V_T+V_R)T}$$

is the ratio of the change in lung volume during the whole breathing cycle to total lung capacity.

The two indices are therefore related by the ratio T/T_e which is approximately 1.8. When they are measured by external detection of radioactivity over the thorax, however, the value of specific ventilation decreases by approximately 30% (depending on the tidal volume) because of re-inspiration of the radioactive gas in the dead space and by a further 20% to 30%, in normal lungs, because of the inefficiency of gas mixing in the lung due chiefly to an uneven distribution of V_T/V_R. Thus specific mean expiratory gas flow will be expected to exceed specific ventilation by a factor of at least three which will vary over the lung field because of the uneven distribution of V_T/V_R.

Also if xenon is used for the calculation of specific ventilation by the washout technique, the ratio of specific mean expiratory gas flow to specific ventilation will increase still further because of the release of xenon from the tissues into the airways during the washout.

Confirmation of the adequacy of the exponential description of regional lung volume was provided by the consistently high regional coefficients of determination obtained in all the studies.

6.6 Conclusions.

The analysis techniques discussed offer the only methods presently available, without using physiological triggering of the data collection, of obtaining regional inhalation information, with poorly soluble radioactive gases, which reflects the behaviour of individual lung regions and which is unaffected by the behaviour of other lung regions. It has been shown to be possible to use the model analysis, but not the cross-correlation analysis, with clinical data presently available. The problems involved in the latter are associated with poor counting statistics caused by the activity available from the $^{81}Kr^{m}$ generator and could be overcome with higher activity generators.

6.7 Suggestions for Further Work.

To reduce the noise generated during the application of the mathematical model to the single breath activity-time data, different techniques of fitting the equation to the expiratory curve should be investigated. The necessity for this will be reduced as better counting statistics are achieved but an improvement in the present performance should be possible.

When higher activity $^{81}Kr^{m}$ generators become available, refinements to the data reduction in the model analysis should be investigated. For example, the inclusion of cross-correlation techniques in

the multiple breath to single breath activity-time curve reduction, possible with good counting statistics, should improve the reproducibility of the results.

The two suggestions given should improve the quality of the single breath activity-time data and the application of the mathematical model to the expiratory phase. They should enable more reproducible results, which are more sensitive to changes provoked by disease, to be obtained than are presently possible.

A similar improvement should be possible in the performance of the phase analysis by cross-correlation of activity-time curves from different lung regions. If the counting statistics were improved, not only could the analysis be applied reliably to the regions considered in this thesis but also to smaller regions and it is probable that there are phase changes between smaller regions which are averaged out between larger ones.

Both the model and the cross-correlation analysis techniques should be applied to data collected from a number of disease groups to assess their sensitivity to the detection of small airways disease in comparison with other techniques such as radioactive tracer gas washout or conventional lung function tests.

The results of the analyses developed in this thesis depend a great deal on the performance of the data reduction methods in improving the counting statistics. Physiological gating of data acquisiton during a period longer than the two minutes used in this thesis might provide a single breath activity-time curve with better definition. The model analysis could be applied to this data and any phase differences in gas flow between lung regions could be assessed using the Fourier technique reviewed in section (2.5). A comparison of this pre-acquisition method of data reduction should be made with the post-acquisition method used in this thesis.

APPENDIX I **Simulation Programming.**

The simulation program constructed activity-time curves by simulating data points every 0.2 second, chosen to be consistent with data acquisition in clinical studies. Data was simulated by substituting values for the variables in equations (3.22), (3.24), (3.32) and (3.33). The values to be specified were:

$D=\frac{\dot{V}}{V}+\lambda$.

The exponent of the expiration exponential (usually 0.2 per second).

λ.

The decay constant of the radioisotope (usually 0.05 per second).

C_i.

The concentration of the radioactive gas breathed into the lungs (usually 3000 counts per 0.2 second per litre of inspired air).

A_{ei}.

The activity at end inspiration (usually 3000 counts per 0.2 second).

T_i.

The duration of inspiration (usually 1.2 second).

T_e.

The duration of expiration (usually 1.6 second).

I.1 **Washin.**

The initial activity in the lungs was assumed

to be 0. The first inspiration was simulated according to the formula for exponential, equation (3.22) or sinusoidal, equation (3.32) lung volume change. At end-inspiration, the activity maximum was recorded and passed to the equations of expiration. The expiration was simulated according to exponential, equation (3.24) or sinusoidal, equation (3.33) lung volume change. At end-expiration, the new activity minimum was recorded and passed to the equations of inspiration. This cycling was continued until 600 data points had been simulated.

The simulated array was searched to find the avarage count at equilibrium. This was done by searching backwards from the last data point in the simulated array until the first inspiration was detected. The first point encountered on an inspiration was labelled A. From A backwards, the array was searched until the first minimum was encountered. This minimum was labelled B. One point further back was labelled C. From B backwards, the array was searched until the next maximum was detected. This maximum was called A. From A backwards, the array was searched until the next minimum was detected. This minimum was called B. From B to C all the counts were summed and divided by the total number of points to calculate the average count at equilibrium.

I.2 **Washout.**

A washout curve was generated by simulating a washin to equilibrium curve and the making C_i zero and continuing the simulation until the activity was zero.

I.3 **Equilibrium.**

The initial activity in the lungs was assumed to be A_{ei} counts per 0.2 second. The first expiration was simulated according to the formula assuming an exponential variation in lung volume,

$$N_e(t)=A_{ei}e^{-Dt_e} \qquad (I.1)$$

At end expiration, the activity minimum was recorded and passed to the equation of inspiration,

$$N_i(t)=C_1\left[1-C_2e^{-\lambda t_i}\right] \qquad (I.2)$$

The constants,

$$C_1=\frac{A_{ei}}{1-C_2e^{-\lambda T_i}} \qquad (I.3)$$

and,

$$C_2=\frac{1-e^{-DT_e}}{1-e^{-\lambda T_i-DT_eT}} \qquad (I.4)$$

were chosen so that the new activity maximum was exactly the same as the original value, A_{ei}.

I.4 Cross-correlation.

The activity-time curves for lung regions 2,4,6 and 8 in the right lung were moved forward one data point and the first data point was moved to position 600 in the array.

I.5 Poisson Noise.

Poisson noise was superimposed on the curves by adding to each data point a number obtained from its square root, which is its standard deviation, multiplied by a normally distributed random number obtained using the method of Organick E.I., and Meissener L.P., 1974. This method uses a standard random number generator to produce uniformly distributed random numbers in the range 0.0 to 1.0. A Gaussian distribution with standard deviation 1.0 and mean 6.0 is obtained by summing 12 of these random numbers. Poisson noise is obtained by taking 6.0 away from each generated number and multiplying the result by the square root of the data point and adding this to the data point.

APPENDIX II **Patient Details and Imaging Reports.**

II.1 **Normal subjects.**

Subj

1 Clinical details: Normal subject.

2 Clinical details: Normal subject.

3 Clinical details: Normal subject.

4 Clinical details: Normal subject.

5 Clinical details: Normal subject.

6 Clinical details: Normal subject, but a known Asthmatic.

II.2 Patients with a normal image report.

Subj

7 Clinical details: Progressive dyspnoea since January 1979. Night sweats. Hepatomegaly. Query Multiple Pulmonary Emboli. Image report: Bilateral isotope distribution satisfactory and no localised abnormal uptake shown.

8 Clinical details: Previous V/Q scan suggested P.E. Resp. Function tests suggest Emphysema. Image report: Bilateral isotope distribution fairly satisfactory. No localised cold areas shown to suggest localised Emphysema.

9 Clinical details: Pleuritic type of chest pain - since 2/7. O/E: basal creps (bel). Pleuritic rub R base. X-Ray opacities R base and small opacities L base. To rule out Pulmonary Embolism. Image report: Bilateral isotope distribution satisfactory. No localised defect shown.

10 Clinical details: Sero +ve rheumatoid arthritis. Knee joint replacement this year. Bilateral swollen and tender legs. Increasing shortness of breath and repeated pleuritic chest pain. ? Pulmonary Embolus. ? Rheumatoid Arthritic lung disease. Image report: Bilateral isotope distribution fairly uniform. No localised defects shown.

Subj

11 Clinical details: 2 years H/O occasional tightness of the chest and sweating and cramps in legs. Last episode 2/7 ago was worse. Known angina (MI, PE, DVT - 1977). Image report: Slight uniform reduction in the isotope uptake on the left side compared with the opposite side. There is, however, no evidence of a localised ventilation defect to suggest a segmental or a regional obstructive airways disease. The heart is not enlarged.

12 Clinical details: Myocardial Infarct. Arrested. Query Pulmonary Embolus. Image report: Bilateral isotope distribution fairly uniform but is a little less so on the right side. No definite localised defects shown.

13 Clinical details: Admitted as a case of myocardial infarction. Developed shortness of breath. ? P.E. Image report: Bilateral isotope distribution satisfactory. No localised areas of reduced activity shown.

14 Clinical details: Left chest pain + dyspnoea. Pleuritic x 2/12. No cough, wheezing. Oedema of ankles. Some slight oedema of ankles. CXR-NAD, ECG-NAD, FEV/VC=2.2/2.3 ? P.E. Image report: Bilateral isotope distribution fairly uniform. Left sided cardiac enlargement noted.

Subj

15 Clinical details: ? multiple P.E. Old colon Ca. Image report: Bilateral isotope distribution fairly uniform and satisfactory.

16 Clinical details: Chest pain. ? Pulmonary Embolism. Image report: Bilateral isotope distribution satisfactory.

17 Clinical details: Known case of Hypertrophic Obstructive Cardiomyopathy. Right chest pain since 2.8.80 for 3 days before admission. Pleuritic in nature. Possible Pulmonary Embolism. CXR clear. On anticoagulants - Warfarin. Image report: NAD.

18 Clinical details: Haemoptysis ++. Lung scan suggestive of Pulmonary Embolism Rt upper lung. Image report: Bilateral isotope distribution fairly satisfactory. No evidence of Obstructive Airways Disease shown.

19 Clinical details: Sarcoidosis affecting: nose, larynx and L main bronchus. Query any Ventilation/Perfusion defect on the L side. Very poor transfer factor. Image report: Bilateral isotope distribution satisfactory. No localised cold areas detected.

Subj

20 Clinical details: Long history Bronchitis - moderate exercise dyspnoea 2-3 years. Noted to be Erythrocythaemic (associated thumping headaches and giddiness). Blood gases and level of Erythrocythaemia worse than limit of exercise dyspnoea would suggest. ? nature of primary lung disease. Image report: Bilateral isotope distribution fairly satisfactory and there is no definite scan evidence to suggest obstructive airways disease, although the radiograph appearance is in keeping with Chronic Bronchitis with Emphysema.

21 Clinical details: Right posterior chest pain with initial chest X-ray changes of small abcess. ? changes. Image report: Bilateral isotope distribution uniform and satisfactory.

22 Clinical details: Chronic cough. Crep left base. Query bronchiectasis left base. Image report: Bilateral isotope distribution fairly uniform and satisfactory.

23 Clinical details: Massive L pleural effusion developed suddenly 3/52 ago. Previous CXR 30.12.78 more or less NAD other than slight pleural thickening. Effusion aspirated - high protein content. No malignant cells seen. Query cause. Image report: Bilateral isotope distribution satisfactory.

II.3 Patients with an abnormal image report.

Subj

24 Clinical details: Has had swollen left calf since May. Morning of 14.8.79 sudden onset pleuritic L chest pain. Now has small effusion and reduced breath sound L lower chest antero-laterally. Plain CXR unhelpful in diagnosis. Scan and P.E. in 1973. Image report: The L side appears normal but there is diminished activity seen at the R base on this scan also. The scan suggests that there has been a recent embolus at the L lung base but that the changes at the R lung base are more likely to be due to localised Emphysema.

25 Clinical details: Diffuse shadow R.U.Z. To exclude Pulmonary Emboli - Pulmonary Hypertension. Image report: Isotope activity is almost absent in the R lower lung, this would be compatible with involvement of R lower lobe.

26 Clinical details: Kr studies suggested after lung scan which showed multiple perfusion defects. Image report: Isotope distribution is fairly satisfactory. Therefore this would exclude significant obstructive airways disease and the perfusion defect shown at earlier lung scan of 9.6.80, would be due to Pulmonary Embolism.

Subj

27 Clinical details: Cor Pulmonale. Query cause. R ventricular failure. Image report: Poor krypton uptake in some areas, especially R base consistent with Emphysema or Fibrosis.

28 Clinical details: For investigation of non-perfused right lung. Image report: Despite absent perfusion of R lung in the conventional lung scan, there is evidence of isotope activity in the ventilation scanμ particularly in the upper and part of the mid zones. This would favour the diagnosis of a hilar neoplasm probably involving the lower main bronchus. Left lung is clear.

29 Clinical details: CXR and lung scan in April this year suggested multiple Pulmonary Emboli. However, she has been a heavy smoker and I am sure there must be some Emphysema as well. Image report: There is absence of isotope activity in the R mid zone at the periphery corresponding to the defect in the perfusion scan. This suggests another possibility that this could be due to a localised Emphysema at this site. There is no definite suggestion of multiple Pulmonary Embolism, at this examination.

Subj

30 Clinical details: Increasing dyspnoea. X-Ray: upper zone Emphysema with increased markings in lower zones. Also some linear basal opacities. Has varicose veins. ? Recurrent Emboli. Image report: Markedly reduced isotope uptake in the R lung especially in the upper and mid zones and the left upper zone. Appearances again in keeping with Emphysema espacially in upper lobesμ more marked on the right side.

31 Clinical details: Chronic obstructive lung disease. Multiple apical bullae. Image report: There is no isotope uptake in the R upper zone and this would be in keeping with Emphysematous bulla, which is present in the chest radiograph. The rest of the lung fields show uniform isotope distribution.

32 Clinical details: ? P.E. Clinically perfusion deficit on scan but identical to scan in 1978. CXR unhelpfull. Image report: Multiple areas of reduced ventilation in both lung fields indicative of bilateral obstructive airways disease.

33 Clinical details: C.O.A.D. for comparison with radioaerosols. Image report: Areas of reduced perfusion in both lung fields more so in the R side consistent with obstructive airways disease.

34 Clinical details: C.O.A.D. for comparison with radioaerosols. Image report: There are areas of reduced perfusion and the isotope distribution is pathy. Appearance compatible with obstructive airways disease.

35 Clinical details: Acute onset of L side pleuritic chest pain and night sweats. Had similar episode 4 weeks previously. CXR and lung scan compatible with patchy consolidation. Query any change in lung scan consistent with Pulmonary Emboli. Image report: There are areas of reduced perfusion in both mid zones and these areas also show reduced krypton activity in the inhalation scan indicating lung Fibrosis and obstructive airways disease. No definite evidence of Pulmonary Embolus shown.

36 Clinical details: Query recurrent Pulmonary Emboli. Lung scan inconclusive as patient has widespread Emphysema. Image report: Multiple areas of reduced isotope activity in both scans in keeping with widespread bilateral obstructive airways disease.

References.

Alderson P.O., Line B.R.,1980,
'Scintigraphic Evaluation of Regional Pulmonary Ventilation' Semin. Nucl. Med. 10:218-242.

Alpert N.M., McKusick K.A., Correia J.A., Shea W., Brownell G.L., and Potsaid M.S.,1975,
'Initial Assessment of a Simple Functional Image of Ventilation' J. Nucl. Med. 17,2:88-92.

Amis T.C., Ciofetta G., Clark J.C, Hughes J.M.B., Jones H.A., and Pratt T.A.,1978,
'Use of Krypton 81m and 85m for Measurement of Ventilation and Perfusion Distribution Within the Lungs' In: 'Clinical and Experimental Applications of Krypton 81m' Lavender J.P., ed. Br. J. Radiol. Special Report 15:52-59.

Amis T.C.,1979,
'Regional Lung Function in Man and the Dog' Ph.D. Thesis, University of London.

Anger H.O.,1958,
'The Scintillation Camera' Rev. Scient. Instrum. 29:27.

Anger H.O.,1963,
'Gamma-ray and Positron Scintillation Camera' Nucleonics 21, UCLA 56-65.

Anger H.O., Gottschalk D.C., Yano Y., and Schaer L.R.,1965,
'Scintillation Camera in Diagnosis and Research' Nucleonics 23,1:57.

Anger H.O.,1967,
'Radioisotope Cameras' in 'Instrumentaion in Nuclear Medicine' (G.J. Hine - ed.) Academic Press, New York 1:486.

Arnot R.N., Sykes M.K., Clark J.C., Herring A.N., Chakrabarti K., and Buranapong P.,1978,
'Measurement of Total Lung Ventilation in Anaesthetized Dogs using Krypton 81m and Nitrogen 13' In: 'Clinical and Experimental Applications of Krypton 81m' Lavender J.P., ed. Br. J. Radiol. 15:69-82.

Arnot R.N., Clark J.C., Herring A.N., Chakrabarti M.K., and Sykes M.K.,1981,
'Measurements of Regional Ventilation Using Nitrogen-13 and Krypton-81m in Mechanically Ventilated Dogs' Clin. Phys. Physiol. Meas. 2,3:183-197.

Bajzer Z., and Nosil J.,1977,
'A Simple Mathematical Lung Model for Quantitative Regional Ventilation Measurement using Kr-81m' Phys. Med. Biol. 22,5:975-980.

Bajzer Z., Nosil J., and Spaventi S.,1977,
'A Mathematical Lung Model for Ventilation Studies with Radioactive Tracers' First Mediterranean Conference on Medical and Biological Engineering, Digest of Papers, Vol. 1,6-17 to 6-19.

Bajzer Z., and Nosil J.,1980,
'Lung Ventilation Model for Radioactive Tracer Tidal Breathing' Phys. Med. Biol. 25,2:293-307.

Ball W.C.Jr., Stewart P.B., Newsham L.G.S., and Bates D.V.,1962,
'Regional Pulmonary Function Studied with Xenon' J. Clin. Invest. 41,3:519-531.

Bassingthwaighte J.B., Knopp T.J., and Anderson D.U.,1970,
'Flow Estimation by Indicator Dilution (Bolus Injection). Reduction of Errors due to Time-Average Sampling during Unsteady Flow' Circ. Res. 27:277-291.

Bossuyt A., Vincken W., and Deconinck F.,1981,
'Patterns of Regional Lung Expansion Studied by Dynamic Transmission Scintigraphy and the Temporal Fourier Transform' In: 'Functional Mapping of Organ Systems and Other Computer Topics' Esser P.D., ed., The Society of Nuclear Medicine, New York. p57-64.

Brigham E.O.,1974,

'The Fast Fourier Transform' Prentice-Hall.

Bunow B., Line B.R., Horton M.R., and Weiss G.H.,1979,

'Regional Ventilatory Clearance by Xenon Scintigraphy: a Critical Evaluation of Two Estimation Procedures' J. Nucl. Med. 20,7:703-710.

Chackett K.F.,1980,

'The Application of Laguerre Functions to Washout Curves' (letter) Phys. Med. Biol. 25:570-573.

Chatfield C.,1975,

'Statistics for Technology' Chapman and Hall.

Ciofetta G., Silverman M., and Hughes J.M.B.,1980,

'Quantitative Approach to the Study of Regional Lung Function in Children Using Krypton-81m' Br. J. Radiol. 53:950-959.

Cooper G.R., and McGillem C.D.,1967,

'Methods of Signal and System Analysis' Holt, Rinehart and Winston.

Cotes J.E.,1975,

'Lung Function - Assessment and Application in Medicine' 3rd. edition, Blackwell, London.

Devos P., Demedets M., Vandecruys A., Cosemans J., and DeRoo M.,1978,
'Comparison of ^{133}Xe Washout Curves after Bolus Inhalation, Perfusion and Equilibration' Respiration 35:115-121.

Douce J.L.,1963,
'The Mathematics of Servo-Mechanisms' English Universities Press.

Fazio F., and Jones T.,1975,
'Assessment of Regional Ventilation by Continuous Inhalation of Radioactive Krypton-81m' Br. Med. J. 3:673-676.

Fazio F., Palla A., Santolicandro A., Solfanelli S., Fornai E., and Giuntini C.,1979,
'Studies of Regional Ventilation in Asthma Using ^{81m}Kr' Lung 156:185-194.

Fowler W.S.,1952,
'Intrapulmonary Distribution of Inspired Gas' Physiol. Rev. 32,1:1-20.

Goris M., Daspit S.,1978,
'Krypton-81m. In: Guter M (ed) Progress in Nuclear Medicine, Vol 5. Newer Radiogases in Practice' S. Karger, Basel, pp 69-92.

Grant J.B., Jones H.A., and Hughes J.M.B.,1974,
'Sequence of Regional Filling during a Tidal Breath in Man' J. Appl. Physiol. 2:158-165.

Grenvik A., Hedstrand U., and Sjogren H.,1966,
'Problems in Pneumotachography' Acta. Anaesth. Scandinav. 10:147-155.

Ham H.R., Vandevivere J., Dab I., Baran D., and Piepsz A.,1981,
'Limitations of Steady State Krypton-81m Ventilation Study in Children' Nucl. Med. Comm. 2:43-48.

Harf A., Pratt T., and Hughes J.M.B.,1978,
'Regional Distribution of $\dot{V}_A/\dot{Q}$ in Man at Rest and with Excercise Measured with Krypton-81m' J. Appl. Physiol.:Respirat. Environ. Exercise Physiol. 44,1:115-123.

Henriksen O., Lonborg-Jensen H., and Vejlo Rasmussen F.,1980,
'Evaluation of a Method for Determination of Mean Transit Time of Xenon-133 in the Lungs' J. Nucl. Med. 21:333-341.

Higenbottam T., and Maisey M.N.,1979,
'Ventilation Perfusion Lung Scanning' Hospital Update 23-41.

Hughes J.M.B.,1979,
'Short-life Radionuclides and Regional Lung Function' Br. J. Radiol. 52:353-370.

Jones R.H., Goodrich J.K., and Sabistan D.C.,1974,
'Evaluation of Xe-133 Techniques for Measurement of Regional Ventilation' J. Nucl. Med. 15,7:598-604.

Jones T.,1978a,

'Introduction' In: 'Clinical and Experimental Applications of Krypton-81m' Lavender J.P., ed. Br. J. Radiol. Special Report 15:1-6.

Jones T.,1978b,

'Theoretical Aspects of the Use of Krypton-81m' In:'Clinical and Experimental Applications of Krypton-81m' Lavender J.P., ed. Br. J. Radiol. Special Report 15:33-37.

Jones T., Clark J.C., Rhodes C.G., Heather J., and Tofts P.,1978,

'Combined Use of Krypton 81m and 85m in Ventilation Studies' In: 'Clinical and Experimental Applications of Krypton 81m' Lavender J.P., ed. Br. J. Radiol. Special Report 15:46-51.

Kety S.S.,1949,

'Measurement of Regional Circulation by the Local Clearance of Radioactive Sodium' Am. Heart J. 38:321

Khalil Ali M., Mountain C., Miller J.M., Johnston D.A., and Shullenberger C.C.,1975,

'Regional Pulmonary Function before and after Pneumonectomy using ^{133}Xenon' Chest 68,3:288-296.

Konietzko N., Ruhle K.H., Sigmund E., Overrath G., Spilker D., Matthys H., and Adam W.E.,1970, 'Investigation of the Lung Function using Inert Radioactive Gases' Int. At. Energ. Agen. Symp., Vienna:799-807.

Lamb J.F., Baker G.A., Goris M.L., Khentigan A., Moore H.A., Neesan W.C., and Winchell H.S.,1978, 'Production and Clinical Evaluation of a Commercial Krypton 81m Gas Generator and its Delivery System' In: 'Clinical and Experimental Applications of Krypton 81m' Lavender J.P., ed. Br. J. Radiol. Special Report 15:22-32.

Leeman S., and Orr J.S.,1979, 'Mean Transit Time Measurement from General Washout Curve'(letter) Phys. Med. Biol. 24,6:1295-1297.

Loken M.K., Medina J.R., Lillehei J.P.,1969, 'Regional Pulmonary Function Evaluation using Xenon 133, a Scintillation Camera, and Computer' Radiol. 93:1261-1266.

Mannell T.J., Prime F.J., and Smith D.W.,1966, 'A Practical Method of Using Radioactive Xenon for Investigating Regional Lung Function' Scand. J. Resp. Dis. Suppl. 62:41-57.

Matthews C.M.E., and Dollery C.T.,1965,
'Interpretation Of Xe-133 Lung Wash-in and Wash-out Curves Using an Analogue Computer' Clin. Sci. 28,573-590.

McKenzie S.A., and Fitzpatrick M.L.,1981,
'Regional Lung Function in Children: the Accuracy of Nitrogen-13 Inhalation and Infusion Studies' Clin. Phys. Physiol. Meas. 2,3:223-235.

Meier P., and Zierler K.L.,1954,
'On the Theory of the Indicator-Dilution Method for Measurement of Blood Flow and Volume' J. Appl. Physiol. 6,12:731-744.

Miller J.M., Khalil Ali M., and Howe C.D.,1970,
'Clinical Determination of Regional Pulmonary Function During Normal Breathing Using Xenon-133' Am. Rev. Resp. Dis. 101,2:218-229.

Miller T.R., Biello D.R., Lee J.I., Davis H.H., Mattar A.G., Ehrhardt G.J., and Siegel B.A.,1981,
'Ventilation Imaging with Kr-81m. A Comparison with Xe-133' Eur. J. Nucl. Med. 6:11-16.

Modell H.I., and Graham M.M.,1982,
'Limitations of Kr-81m for Quantitation of Ventilation Scans' J. Nucl. Med. 23:301-305.

Mostafa A.B., Childs P.O., and Causer D.A.,1983,
'A Quantitative Evaluation of Breathing Systems Used with Kr-81m Generators' J. Nucl. Med. 24,2:157-159.

Nosil J., Hughes J.M.B., Hudson F.R., Myers M.J., and Ewan P.W.,1976,
'Functional Imaging of Lung Ventilation using the Concept of Mean Transit Time' Phys. Med. Biol. 21,2:251-262.

Nosil J., Bajzer Z., and Spaventi S.,1977,
'The Use of Kr-81m Gas for the Measurement of Absolute Regional Lung Ventilation' Nuklearmedizin XVI,1:13-17.

Orr J.S., Myers M.J., Leeman S., and Hughes J.M.B.,1978,
'Transit Time and Ratio of Moments' (letter) Phys. Med. Biol. 23:998.

Orr J.S.,1979,
'Continuous Administration of Short-Lived Radioisotope Tracers and the Analagous Laplace Transform' J. Theor. Biol. 78:101-111.

Organick E.I., and Meissener L.P.,1974,
'Fortran IV: 2nd Edition' Addison-Wesley.

Overton T.R., Friedenberg L.W., and Sproule B.J.,1973,
'Multidetector Instrumentation and Data Analysis for Regional Pulmonary Function Studies Using Xenon-133' Phys. Med. Biol. 18,2:246-255.

Parkin A., Robinson P.J., and Hickling P.,1982,
'Regional Lung Ventilation in Ankylosing Spondylitis' Br. J. Radiol. 55:833-836.

Ram G.,1979,
'A General Purpose Computerized Display and Analysis System for Image Processing in Nuclear Medicine' Comp. Prog. Biomed. 10:245-260.

Ronchetti R., Benci S., Federici M., Ciofetta L., and Gentili G.,1974,
'Theoretical Bases for the Calculation of the Regional Ventilation/Perfusion Ratio ($\dot{V}/\dot{Q}$) of the Lung in the Newborn' J. Nucl. Biol. Med. 18,3:123-135.

Rosenzweig D.Y., Hughes J.M.B., and Jones T.,1969,
'Uneven Ventilation Within and Between Regions of the Normal Lung Measured with Nitrogen-13' Resp. Phys. 8:86-97.

Schor R.A., Shames D.M., Weber P.M., Dos Remedios L.V.,1978,
'Regional Ventilation Studies with Kr-81m and Xe-133: A Comparative Analysis' J. Nucl. Med. 19:348-353.

Secker-Walker R.H., Hill R.L., Markham J., Baker J., Wilhelm J., Alderson P.O., and Potchen E.J.,1973,
'The Measurement of Regional Ventilation in Man: A New Method of Quantitation' J. Nucl. Med. 14:725-732.

Secker-Walker R.H., Alderson P.O., Wilhelm J., Hill R.L., Markham J., Baker J., and Potchen E.J.,1975,
'The Measurement of Regional Ventilation During Tidal Breathing: a Comparison of Two Methods in Healthy Subjects, and Patients with Chronic Obstructive Lung Disease' Br. J. Radiol. 48:181-189.

Secker-Walker R.H.,1978,
'Pulmonary Physiology, Pathology and Ventilation-Perfusion Studies' J. Nucl. Med. 19:961-968.

Simpson A.E., Elliott J.A., Horton P.W., and Adams F.G.,1980,
'Dynamic Xe-133 Lung Scans for Monitoring Treatment Response in Bronchial Carcinoma' Clin. Phys. Physiol. Meas. 1,4:275-285.

Spaventi S., Nosil J., Bajzer Z., and Pardon R.,1978,
'Clinical and Experimental Applications of a New Mathematical Lung Model for Krypton-81m Inhalation' In:'Clinical and Experimental Applications of Krypton-81m' Lavender J.P., ed. Br. J. Radiol. Special Report 15:60-68.

Tofts P.S., and Linney A.D.,1978,
'Transit Time and Ratio of Moments' (letter) Phys. Med. Biol. :455.

Touya J.J., Price R.R., Patton J.A., et. al.,1979,
'Gated Regional Spirometry' J. Nucl. Med. 20:620 (abstract).

Touya J.J., Jones J.P., Patton J.J., Erickson J.J., Rollo F.D., and Price R.R.,1981,
'Ventilation/Perfusion Ratio Images by Gated Regional Spirometry' In: 'Functional Mapping of Organ Systems and Other Computer Topics' Esser P.D., ed., The Society of Nuclear Medicine, New York. p31-37.

Ullmann V., and Kuba J.,1978,

'Dynamic Scintigraphy: Calculation and Imaging of Regional Distribution of Quantitative Parameters' Eur. J. Nucl. Med. 3:153-160.

Van der Mark Th. W., Peset R., Beekhuis H., Kiers A., Rookmaker A.E.C., and Woldring M.G.,1980,

'An Improved Method for the Analysis of Xenon-133 Washin and Washout Curves' J. Nucl. Med. 21,11:1029-1034.

Vos P.H.,1981,

'Fourier Amplitude and Phase Images of the Heart' MDS Systems.

Wagner H.N. Jr. -ed.,1975,

'Nuclear Medicine' H.P. Publishing, New York.

Wainwright R.J., and Maisey M.N.,1978,

'Cardiac Imaging. Part 2, Radionuclide Angiography' November Hospital Update.

Wendt R.E., Murphy P.H., Clark J.W., and Burdine J.A.,1982,

'Interpretation of Multigated Fourier Functional Images' J. Nucl. Med. 23:715-724.

West J.B.,1966,

'Distribution of Blood and Gas in Lungs' Phys. Med. Biol. 11,3:357-370.

West J.B.,1977,

'Regional Differences in the Lung' Academic Press, New York pp 33-84.

Williams L.E.,1981,

'On the Improvement of Analyses of Xenon-133 Lung Washin and Washout Curves' (letter) J. Nucl. Med. 22,8:744-745.

Winlove C.P., Freedman N., and Godfrey S.,1976,

'The Quantitation of Regional Lung Function in Infants and Young Children' Hammersmith Hospital, London:Preprint.

Yano Y., McRae J., and Anger H.O.,1970,

'Lung Function Studies using Short Lived Kr-81m and the Scintillation Camera' J. Nucl. Med. 11:674-679.

Zadro M., Nosil J., Bajzer Z., and Svarc A.,1981,

'Mean Transit Time Measurement from Wash-in and Wash-out Curves' (letter) Phys. Med. Biol. 26,6:1171-1172.

Zierler K.L.,1965,

'Equations for Measuring Blood Flow by External Monitoring of Radioisotopes' Circ. Res. XVI,4:309-321.